

Electronic Supplementary Information for

Ni(0)-Promoted Activation of C_{sp2}-H and C_{sp2}-O Bonds

Sehye Min,^a Jonghoon Choi,^b Changho Yoo,^c Peter M. Graham*^d and Yunho Lee*^b

a. Department of Chemistry, Korea Advanced Institute of Science and Technology (KAIST), Daejeon 34141, Republic of Korea

b. Department of Chemistry, Seoul National University, Seoul 08826, Republic of Korea. E-mail: yunhochem@snu.ac.kr; Tel: +82 2 880 6653

c. Korea Research Institute of Chemical Technology, Daejeon, Republic of Korea

d. Department of Chemistry, Saint Joseph's University, 5600 City Avenue, Philadelphia, PA 19131

Contents

Experimental Section	S4
Figure S1. ¹ H NMR spectrum of {(^{acri} PNP)Ni-(N ₂)-Na(THF) ₂ } ₂ (2).....	S22
Figure S2. ¹³ C NMR spectrum of {(^{acri} PNP)Ni-(N ₂)-Na(THF) ₂ } ₂ (2).....	S22
Figure S3. ³¹ P NMR spectrum of {(^{acri} PNP)Ni-(N ₂)-Na(THF) ₂ } ₂ (2).....	S22
Figure S4. ³¹ P NMR spectrum of (^{acri} PNP)NiH (3) with triphenylphosphine oxide (OPPh ₃).....	S23
Figure S5. ³¹ P NMR spectra of the reaction of 2 with benzene.....	S23
Figure S6. ³¹ P NMR spectra of the reaction of 2 with benzene in the presence of OPPh ₃	S24
Figure S7. ³¹ P NMR spectrum of the reaction of 2 with benzene in pentane.....	S24
Figure S8. ¹ H NMR spectra of the mixture of 3 and (^{acri} PNP)NiPh (4-Ph) and OPPh ₃	S25
Figure S9. ³¹ P NMR spectra of the mixture of 3 and (^{acri} PNP)NiPh (4-Ph) and OPPh ₃	S25
Figure S10. ¹ H NMR spectra of the mixture of 3 and (^{acri} PNP)NiPh (4-Ph) and OPPh ₃ at 60 °C.....	S26
Figure S11. ³¹ P NMR spectra of the mixture of 3 and (^{acri} PNP)NiPh (4-Ph) and OPPh ₃ at 60 °C.....	S26
Figure S12. ¹ H NMR spectrum of (^{acri} PNP)NiPh (4-Ph).....	S27
Figure S13. ¹³ C NMR spectrum of (^{acri} PNP)NiPh (4-Ph).....	S27
Figure S14. ³¹ P NMR spectrum of (^{acri} PNP)NiPh (4-Ph).....	S27
Figure S15. ¹ H NMR spectrum of sodium phenoxide.....	S28
Figure S16. ¹ H NMR spectrum of sodium anilide.....	S28
Figure S17. ¹ H NMR spectrum of the reaction of 2 with triphenylmethane.....	S29
Figure S18. ³¹ P NMR spectrum of the reaction of 2 with triphenylmethane.....	S30
Figure S19. ¹ H NMR spectrum of (^{acri} PNP)NiPh- <i>d</i> ₅ (4-C₆D₅).....	S31
Figure S20. ³¹ P NMR spectrum of (^{acri} PNP)NiPh- <i>d</i> ₅ (4-C₆D₅).....	S31
Figure S21. ¹ H NMR spectrum of (^{acri} PNP)NiD (3-D).....	S31
Figure S22. ³¹ P NMR spectrum of (^{acri} PNP)NiD (3-D).....	S32
Figure S23. ³¹ P NMR spectrum of the reaction of 2 with naphthalene.....	S32
Figure S24. ³¹ P NMR spectrum of the reaction of 2 with naphthalene in the presence of OPPh ₃	S32
Figure S25. ¹ H NMR spectrum of (^{acri} PNP)Ni(2-naphthyl) (4-Naph).....	S33
Figure S26. ¹³ C NMR spectrum of (^{acri} PNP)Ni(2-naphthyl) (4-Naph).....	S33
Figure S27. ³¹ P NMR spectrum of (^{acri} PNP)Ni(2-naphthyl) (4-Naph).....	S33
Figure S28. ³¹ P NMR spectrum of the reaction of 2 with anthracene.....	S34
Figure S29. ³¹ P NMR spectrum of the reaction of 2 with anthracene in the presence of OPPh ₃	S34
Figure S30. ¹ H NMR spectrum of (^{acri} PNP)Ni(2-anthracenyl) (4-Anth).....	S34
Figure S31. ¹³ C NMR spectrum of (^{acri} PNP)Ni(2-anthracenyl) (4-Anth).....	S35
Figure S32. ³¹ P NMR spectrum of (^{acri} PNP)Ni(2-anthracenyl) (4-Anth).....	S35
Figure S33. ³¹ P NMR spectra of the reaction of 2 with toluene.....	S36
Figure S34. ³¹ P NMR spectra of the reaction of 2 with toluene in the presence of OPPh ₃	S36

Figure S35.	^{31}P NMR spectrum of the reaction of 2 with toluene in pentane.....	S37
Figure S36.	^1H NMR spectrum of $(^{\text{acri}}\text{PNP})\text{Ni}(o\text{-tolyl})$ (4-<i>o</i>Tol).....	S37
Figure S37.	^{13}C NMR spectrum of $(^{\text{acri}}\text{PNP})\text{Ni}(o\text{-tolyl})$ (4-<i>o</i>Tol).....	S37
Figure S38.	^{31}P NMR spectrum of $(^{\text{acri}}\text{PNP})\text{Ni}(o\text{-tolyl})$ (4-<i>o</i>Tol).....	S38
Figure S39.	^1H NMR spectrum of $(^{\text{acri}}\text{PNP})\text{Ni}(m\text{-tolyl})$ (4-<i>m</i>Tol).....	S38
Figure S40.	^{13}C NMR spectrum of $(^{\text{acri}}\text{PNP})\text{Ni}(m\text{-tolyl})$ (4-<i>m</i>Tol).....	S38
Figure S41.	^{31}P NMR spectrum of $(^{\text{acri}}\text{PNP})\text{Ni}(m\text{-tolyl})$ (4-<i>m</i>Tol).....	S39
Figure S42.	^1H NMR spectrum of $(^{\text{acri}}\text{PNP})\text{Ni}(p\text{-tolyl})$ (4-<i>p</i>Tol).....	S39
Figure S43.	^{13}C NMR spectrum of $(^{\text{acri}}\text{PNP})\text{Ni}(p\text{-tolyl})$ (4-<i>p</i>Tol).....	S39
Figure S44.	^{31}P NMR spectrum of $(^{\text{acri}}\text{PNP})\text{Ni}(p\text{-tolyl})$ (4-<i>p</i>Tol).....	S40
Figure S45.	^1H NMR spectrum of $(^{\text{acri}}\text{PNP})\text{Ni}(\text{benzyl})$	S40
Figure S46.	^{13}C NMR spectrum of $(^{\text{acri}}\text{PNP})\text{Ni}(\text{benzyl})$	S40
Figure S47.	^{31}P NMR spectrum of $(^{\text{acri}}\text{PNP})\text{Ni}(\text{benzyl})$	S41
Figure S48.	^1H NMR spectrum of the reaction of triethyl phosphonoacetate with NaH.....	S41
Figure S49.	^1H NMR spectrum of $\{(^{\text{acri}}\text{PNP})\text{Ni}-(\text{N}_2)-\text{K}(\text{THF})_2\}_2$ (2-K).....	S41
Figure S50.	^{13}C NMR spectrum of $\{(^{\text{acri}}\text{PNP})\text{Ni}-(\text{N}_2)-\text{K}(\text{THF})_2\}_2$ (2-K).....	S42
Figure S51.	^{31}P NMR spectrum of $\{(^{\text{acri}}\text{PNP})\text{Ni}-(\text{N}_2)-\text{K}(\text{THF})_2\}_2$ (2-K).....	S42
Figure S52.	^{31}P NMR spectrum of the reaction of 2-K with benzene.....	S43
Figure S53.	^1H NMR spectrum of $\{(^{\text{acri}}\text{PNP})\text{Ni}-(\text{N}_2)-\text{Li}(\text{THF})_2\}_2$ (2-Li).....	S44
Figure S54.	^{13}C NMR spectrum of $\{(^{\text{acri}}\text{PNP})\text{Ni}-(\text{N}_2)-\text{Li}(\text{THF})_2\}_2$ (2-Li).....	S44
Figure S55.	^{31}P NMR spectrum of $\{(^{\text{acri}}\text{PNP})\text{Ni}-(\text{N}_2)-\text{Li}(\text{THF})_2\}_2$ (2-Li).....	S44
Figure S56.	^{31}P NMR spectrum of the reaction of 2-Li with benzene.....	S45
Figure S57.	^{31}P NMR spectra of generation of 4-Ph from $(^{\text{acri}}\text{PNP})\text{NiCl}$ and 3	S46
Figure S58.	^{31}P NMR spectra of the reaction of 2 with C_6H_6 and C_6D_6	S47
Figure S59.	^1H NMR spectra of the reaction of 2 with $\text{C}_6\text{H}_6/\text{C}_6\text{D}_6$ (1:1).....	S48
Figure S60.	^{31}P NMR spectra of the reaction of 2 with $\text{C}_6\text{H}_6/\text{C}_6\text{D}_6$ (1:1).....	S48
Figure S61.	^1H NMR spectrum of $(^{\text{acri}}\text{PNP})\text{Ni}(\text{CH}=\text{CH}_2)$ (5) in C_6D_6	S48
Figure S62.	^1H NMR spectrum of $(^{\text{acri}}\text{PNP})\text{Ni}(\text{CH}=\text{CH}_2)$ (5) in acetonitrile- d_3	S49
Figure S63.	^{13}C NMR spectrum of $(^{\text{acri}}\text{PNP})\text{Ni}(\text{CH}=\text{CH}_2)$ (5).....	S49
Figure S64.	^{31}P NMR spectrum of $(^{\text{acri}}\text{PNP})\text{Ni}(\text{CH}=\text{CH}_2)$ (5).....	S49
Figure S65.	COSY NMR spectrum of $(^{\text{acri}}\text{PNP})\text{Ni}(\text{CH}=\text{CH}_2)$ (5).....	S50
Figure S66.	HSQC NMR spectrum of $(^{\text{acri}}\text{PNP})\text{Ni}(\text{CH}=\text{CH}_2)$ (5).....	S50
Figure S67.	Crude ^{31}P NMR spectrum of the reduction of 4-Ph in the presence of 15-C-5.....	S51
Figure S68.	Crude ^{31}P NMR spectra of the reduction of 4-Ph in the presence of glyme.....	S51
Figure S69.	Crude ^1H NMR spectrum of the reaction of glyme, C_6D_6 and PhLi.....	S51
Figure S70.	Crude ^1H NMR spectrum of the reaction of 15-C-5, C_6D_6 and PhLi.....	S52
Figure S71.	Crude ^1H NMR spectra of $\text{Na}\{\text{O}(\text{C}_2\text{H}_4\text{O})_4\}$ from the reaction of 5 and 15-C-5 and that of Na and tetraethyleneglycol.....	S52
Figure S72.	Crude ^{31}P NMR spectrum of the reaction of 2 with 15-C-5 and PhLi.....	S53
Figure S73.	^1H NMR spectra of 1 at room temperature.....	S53
Figure S74.	^1H NMR spectra of 1 at 60 °C.....	S54
Figure S75.	^1H NMR spectra of 1 in the presence of $\text{NaBAr}^{\text{F}_4}$ at room temperature.....	S54
Figure S76.	^1H NMR spectra of 1 in the presence of $\text{NaBAr}^{\text{F}_4}$ at 60 °C.....	S55
Figure S77.	MAS ^{23}Na NMR spectra of NaH and NaOH and NaCl.....	S55
Figure S78.	^{31}P NMR and X-band EPR spectroscopy of the reaction of 2 with toluene.....	S56
Figure S79.	Solid-state structure of 2	S57
Table S1.	Selected bond distances and angles of 2	S57
Figure S80.	Solid-state structure of 4-Ph	S58
Table S2.	Selected bond distances and angles of 4-Ph	S58
Figure S81.	Solid-state structure of 4-Naph	S59
Table S3.	Selected bond distances and angles of 4-Naph	S59

Figure S82. Solid-state structure of 4-Anth	S60
Table S4. Selected bond distances and angles of 4-Anth	S60
Figure S83. Solid-state structure of 4-oTol	S61
Table S5. Selected bond distances and angles of 4-oTol	S61
Figure S84. Solid-state structure of 4-mTol	S62
Table S6. Selected bond distances and angles of 4-mTol	S62
Figure S85. Solid-state structure of 4-pTol	S63
Figure S7. Selected bond distances and angles of 4-pTol	S63
Figure S86. Solid-state structure of $(^{acri}PNP)Ni(benzyl)$	S64
Table S8. Selected bond distances and angles of $(^{acri}PNP)Ni(benzyl)$	S64
Figure S87. Solid-state structure of 5	S65
Table S9. Selected bond distances and angles of 5	S65
Figure S88. Core structures of 2 , $\{Na\} \{ (^{acri}PNP)Ni(CO) \}$, $\{Na(12-crown-4)_2\} \{ (^{acri}PNP)Ni(CO) \}$ and $(^{acri}PNP)NiCl$	S66
Figure S89. XRD structural data comparisons of 1 •C ₁₀ H ₈ , 2 , and 4-Ph	S66
Figure S90. UV-Vis spectra of 2 , 4-Ph , 4-Naph and 4-Anth	S67
Figure S91. UV-Vis spectra of 4-oTol , 4-mTol , 4-pTol and $(^{acri}PNP)Ni(benzyl)$	S67
Figure S92. Calibration curve of the benzophenone radical in THF at room temperature.....	S68
Figure S93. UV-Vis spectra of benzophenone radical with various concentrations.....	S68
Figure S94. UV-Vis spectrum of $[Na(18-crown-6)DME][C_{10}H_8]$	S69
Figure S95. Photo images of NH ₃ (<i>l</i>), the solution of a black powder isolated from the reaction of 2 in benzene and an authentic sample of Na(0) in NH ₃ (<i>l</i>).....	S69
Figure S96. Plots of the normalized signal intensities (<i>I</i> / <i>I</i> ₀) versus gradient strength (<i>G</i>) and plots of ln(<i>I</i> / <i>I</i> ₀) versus <i>G</i> ² for 2 , 4-Ph , 4-Naph and $\{ (^{acri}PNP)Ni \}_2-\mu-CO_2-\kappa^2C, O$	S70
Table S10. Diffusion constants and R _{solution} for 2 , 4-Ph , 4-Naph and $\{ (^{acri}PNP)Ni \}_2-\mu-CO_2-\kappa^2C, O$	S70
Figure S97. IR spectra of 2 , 2-K and 2-Li	S71
Figure S98. IR spectra of 3-D , 4-Ph and 4-C₆D₅	S71
Figure S99. IR spectra of 4-Naph and 4-Anth	S72
Figure S100. IR spectra of 4-oTol , 4-mTol , 4-pTol and $(^{acri}PNP)Ni(benzyl)$	S72
Figure S101. IR spectra of 5 and 4-Ph	S73
Figure S102. ESI MS of 5	S74
Figure S103. Cyclic voltammogram of 1 •C ₁₀ H ₈	S75
Figure S104. Cyclic voltammogram of 3	S75
Figure S105. Cyclic voltammogram of 4-Ph	S76
Figure S106. Optimized structure of $(^{acri}PNP)NiCl$	S77
Table S11. Selected bond distances and angles of $(^{acri}PNP)NiCl$	S77
Figure S107. Optimized structures of 4-Naph and $(^{acri}PNP)Ni(1-naphthyl)$	S78
Table S12. Selected bond distances and angles of 4-Naph and $(^{acri}PNP)Ni(1-naphthyl)$	S78
Figure S108. Optimized structures of 4-Anth , $(^{acri}PNP)Ni(1-anthracenyl)$ and $(^{acri}PNP)Ni(9-anthracenyl)$	S79
Table S13. Selected bond distances and angles of 4-Anth , $(^{acri}PNP)Ni(1-anthracenyl)$ and $(^{acri}PNP)Ni(9-anthracenyl)$	S79
Figure S109. Optimized structures of 4-oTol , 4-mTol , 4-pTol and $(^{acri}PNP)Ni(benzyl)$	S80
Table S14. Selected bond distances and angles of 4-oTol , 4-mTol , 4-pTol and $(^{acri}PNP)Ni(benzyl)$	S81
Figure S110. Electronic structures for 5	S82
References	S83

EXPERIMENTAL SECTION

General Considerations. All manipulations were carried out using standard Schlenk or glovebox techniques under a N₂ or Ar atmosphere. Unless otherwise noted, solvents were deoxygenated and dried by thoroughly sparging with Ar gas, followed by passage through an activated alumina column. Nonhalogenated solvents were tested with a standard purple solution of sodium benzophenone ketyl in THF in order to confirm effective oxygen and moisture removal. All reagents were purchased from commercial vendors and used without further purification unless otherwise stated. (^{acri}PNP)Ni•C₁₀H₈ (**1**•C₁₀H₈), (^{acri}PNP)NiH (**3**) and NaBAr^F₄ were prepared according to the literature procedures.¹ Elemental analyses of **2-Na**, **4-Ph**, **4-Naph**, **4-Anth**, **4-oTol**, **4-mTol**, **4-pTol** and (^{acri}PNP)Ni(benzyl) were carried out at KAIST Analysis Center for Research Advancement on a Thermo Scientific FLASH 2000 series or Flash EA 1112 instrument and **2-K**, **2-Li** and **5** at the Organic Chemistry Research Center in Sogang University on a Thermo Scientific Flash EA 1112 instrument. Deuterated solvents were purchased from Euriso-top or Deutero, degassed, and dried over activated 4 Å molecular sieves prior to use.

X-ray Crystallography. The diffraction data of **4-Naph** was collected on ADSC Quantum-210 detector at 2D SMC at the Pohang Accelerator Laboratory, Korea. A suitable size and quality of crystal was coated with Paratone-Noil and mounted on a Dual-Thickness MicroLoops LD purchased from MiTeGen. The data was collected with Si(111) double crystal monochromated synchrotron radiation ($\lambda = 0.70000$ Å) at 100 K. The ADSC Q210 ADX program was used for data collection and HKL3000sm (Ver. 703r) was used for cell refinement, reduction and absorption correction. The diffraction data of **2**, **4-Ph**, **4-Anth**, **4-oTol**, **4-mTol**, **4-pTol**, and (^{acri}PNP)Ni(benzyl) were collected on a Bruker SMART 1000. The data were collected with graphite-monochromated MoK α radiation ($\lambda = 0.71073$ Å) under a stream of N₂ (g) at 120 K. Cell parameters were determined and refined by SMART program.² Data reduction was performed using SAINT software.³ An empirical absorption correction was applied using the SADABS program⁴. The structures were solved by direct methods, and all non-hydrogen atoms were subjected to anisotropic refinement by full-matrix least squares on F^2 by using the SHELXTL/PC package.⁵ Unless otherwise noted, hydrogen atoms were placed at their geometrically calculated positions and refined riding on the corresponding carbon atoms with isotropic thermal parameters. The diffraction data of **5** was collected on a Rigaku XtaLAB PRO at National Center for Inter-University Research Facilities. The data was collected with Cu K α radiation ($\lambda = 1.54184$ Å) at –180 °C. CrysAlisPro was used for cell refinement, reduction and absorption correction. Full crystallographic details can be obtained free of charge from the Cambridge Crystallographic Data Center via www.ccdc.cam.ac.uk/data_request/cif (CCDC 1968048-1968055 for **2**, **4-Ph**, **4-Naph**, **4-Anth**, **4-oTol**, **4-mTol**, **4-pTol** and (^{acri}PNP)Ni(benzyl) and 2078589 for **5**).

Spectroscopic Measurements. A Bruker AVHD-400 and a Varian-400 spectrometer were used to measure ¹H, ¹³C and ³¹P NMR spectra. The chemical shifts for ¹H NMR spectra were quoted in part per million (ppm) referenced to residual solvent peaks. ¹³C NMR chemical shifts were quoted in part per million (ppm) referenced to internal solvent peaks. The chemical shifts for ³¹P NMR spectra were quoted in parts per million (ppm) referenced to external phosphoric acid. Coupling constants, J , were reported in hertz unit (Hz). The following abbreviations were used to describe peak splitting patterns when appropriate: s = singlet, d = doublet, t = triplet, q = quartet, m = multiplet. Diffusion NMR experiments for **2**, **4-Ph**, **4-Naph** and $\{(\text{acriPNP})\text{Ni}\}_2\text{-}\mu\text{-CO}_2\text{-}\kappa^2\text{C, O}^6$ were conducted using a Bruker AVANCE III HD 850 spectrometer at National Center for Inter-

University Research Facilities. The data were collected in THF-*d*₈ at 298 K with the bipolar pulse pairs stimulated echo pulse sequence (ledbpgp2s). Solid-state ²³Na magic angle spinning (MAS) NMR experiments were acquired at Bruker AVANCE II⁺ 400 MHz NMR system (in KBSI Seoul Western Center). The chemical shifts for ²³Na NMR spectra were quoted in part per million (ppm) referenced to external NaCl. The pulse field gradient was incremented from 0 to 48 G cm⁻¹ with 24 steps. UV-vis spectra were measured by an Agilent Cary 60 UV-vis spectrophotometer using a 1 cm two-window quartz spectrophotometer cell sealed with a screw-cap purchased from Hellma Analytics (117.100-QS). Infrared spectra were recorded in KBr pellets by Bruker VECTOR 33 and PerkinElmer Spectrum Two FT-IR Spectrometer. Frequencies are given in reciprocal centimeters (cm⁻¹) and only selected absorbances were reported. All EPR measurements were carried out at Korea Basic Science Institute (KBSI) in Seoul, Korea. CW X-band EPR spectra were collected on a Bruker EMX plus 6/1 spectrometer equipped with an Oxford Instrument ESR900 liquid He cryostat using an Oxford ITC 503 temperature controller. Spectra were collected with the following experimental parameters: microwave frequency, 9.6 GHz; microwave power, 0.93 mW; modulation amplitude, 10 G; modulation frequency, 100 kHz; temperature, 10 K.

Electrochemistry. Electrochemical measurements were carried out in a glovebox under a N₂ atmosphere using an Autolab PGSTAT12 potentiostat. A glassy carbon electrode was used as the working electrode and a platinum wire was used as the auxiliary electrode. The reference electrode was Ag/AgNO₃ in an electrolyte solution. Solution of 0.3 M tetra-*n*-butylammonium hexafluorophosphate in THF was used as an electrolyte solution. The solutions of reference electrode, electrolyte and analyte were also prepared under an inert atmosphere. The ferrocene couple FeCp₂/FeCp₂⁺ was used as an external reference.

Computational Details. Single point calculations, geometry optimizations and frequency calculations were performed with the Gaussian09⁷ with the B3LYP functional⁸⁻¹⁰ theory. The 6-311+g** basis set was used for all other atoms. The initial geometries for computational models of (acriPNP)NiCl,¹ **4-Naph**, **4-Anth**, **4-*o*Tol**, **4-*m*Tol**, **4-*p*Tol**, (acriPNP)Ni(benzyl) and **5** were obtained from its corresponding X-ray crystal structure. The initial geometries for computational models of (acriPNP)Ni(1-naphthyl), (acriPNP)Ni(1-anthracenyl) and (acriPNP)Ni(9-anthracenyl) were obtained from X-ray crystal structure of those analogous compounds. Optimized structures were verified using frequency calculations to confirm the absence of any imaginary frequency.

Synthesis of $\{(\text{acriPNP})\text{Ni}-(\text{N}_2)-\text{Na}(\text{THF})_2\}_2$ (2**).** After sodium (106 mg, 4.61 mmol) was added to a solution of naphthalene (118 mg, 0.918 mmol) in 5 mL of THF, the reaction mixture was stirred for 3 hrs at room temperature. The resulting sodium naphthalide solution was filtered away from remaining sodium and added dropwise to a solution of $(\text{acriPNP})\text{Ni}\cdot\text{C}_{10}\text{H}_8$ (599 mg, 0.914 mmol) in 10 mL of THF at -35°C with stirring. The reaction mixture was gradually warmed to room temperature resulting in a color change from reddish brown to red. After stirring for additional 30 min, the reaction mixture was filter through Celite, and the volatiles were removed under vacuum. The resulting residue was dissolved in 50 mL of pentane/THF (5:1), and the solution was cooled to -35°C . A red crystalline solid was precipitated out after two days. An resulting product $\{(\text{acriPNP})\text{Ni}-(\text{N}_2)-\text{Na}(\text{THF})_2\}_2$ (**2**, 475 mg, 0.358 mmol, 78.3%) was obtained after washing with cold pentane and drying under vacuum. ^1H NMR (400 MHz, THF- d_8) δ 7.02 (s, 4H, Ar-*H*), 6.86 (t, $J = 7.2$ Hz, 4H, Ar-*H*), 2.39 – 2.34 (m, 8H, $\text{CH}(\text{CH}_3)_2$), 2.20 (s, 12H, Ar- CH_3), 1.45 (s, 12H, $\text{Ar}_2\text{C}(\text{CH}_3)_2$), 1.25 (q, $J = 7.2$ Hz, 24H, $\text{CH}(\text{CH}_3)_2$), 1.09 (q, $J = 7.2$ Hz, 24H, $\text{CH}(\text{CH}_3)_2$). ^{13}C NMR (101 MHz, THF- d_8) δ 156.76 (t, $J = 14.1$ Hz, Ar-*C*), 130.50 (t, $J = 5.1$ Hz, Ar-*C*), 130.26 (s, Ar-*C*), 129.78 (s, Ar-*C*), 124.96 (t, $J = 3.0$ Hz, Ar-*C*), 119.01 (t, $J = 16.2$ Hz, Ar-*C*), 36.84 (s, $\text{Ar}_2\text{C}(\text{CH}_3)_2$), 32.94 (s, $\text{Ar}_2\text{C}(\text{CH}_3)_2$), 26.37 (s, $\text{CH}(\text{CH}_3)_2$), 20.84 (s, Ar- CH_3), 20.00 (t, $J = 3.0$ Hz, $\text{CH}(\text{CH}_3)_2$), 18.83 (s, $\text{CH}(\text{CH}_3)_2$). ^{31}P NMR (162 MHz, THF- d_8) δ 48.1 (s). Anal. Calcd. for $\text{C}_{74}\text{H}_{120}\text{N}_6\text{Na}_2\text{Ni}_2\text{O}_4\text{P}_4$: C, 61.51; H, 8.37; N, 5.82. Found: C, 61.35; H, 8.57; N, 4.56. Elemental analysis data were reproducibly low in nitrogen, due to modest lability of the N_2 ligand of **2** under strong vacuum. UV-vis [THF, nm ($\text{L mol}^{-1} \text{cm}^{-1}$): 354 (21,000), 390 (sh, 6,600), 480 (sh, 780). IR (KBr Pellet, cm^{-1}): $\nu_{\text{NN}} = 1944$. X-ray quality crystals were grown by slow evaporation of pentane to a saturated THF solution of **2** at -35°C .

Reaction of **2 with benzene.** After **2** (20 mg, 0.014 mmol) was dissolved in 5 mL of benzene, the reaction mixture was stirred at room temperature. The red color of **2** was immediately disappeared and the reaction mixture was turned to yellow. The reaction mixture was stirred for 15 min, resulting in a conversion of **2** to **3** (51%) and **4-Ph** (49%). The reaction mixture was further stirred for 24 hrs, and the product ratio changes to give lower concentration of **3** (5%) and higher concentration of **4-Ph** (95%). The identity of the products was confirmed by a comparison of its ^1H and ^{31}P NMR data with those of an authentic sample of **3** and **4-Ph**.

Single-pulse ^{31}P NMR experiment for the quantification. To a solution of **3** (11 mg, 0.021 mmol) in 0.2 mL of C_6D_6 , a solution of triphenylphosphine oxide (12 mg, 0.042 mmol) in 0.2 mL of C_6D_6 . Single-pulse ^{31}P NMR spectra was obtained, as shown in Figure S4.

Quantification of nickel complexes from the reaction of **2 with benzene-15 min.** After **2** (21 mg, 0.014 mmol) was dissolved in 5 mL of benzene, the reaction mixture was stirred at room temperature. The red color of **2** immediately disappeared and the reaction mixture turned to brown. The reaction mixture was stirred for 15 min and the reaction mixture was filtered through Celite and dried under vacuum. To the reaction mixture, a triphenylphosphine oxide (16 mg, 0.057 mmol) solution in C_6D_6 was added and the yield of **3** (43%) and **4-Ph** (57%) in the solution was confirmed by integration versus triphenylphosphine oxide in the single-pulse ^{31}P NMR data.

Quantification of nickel complexes from the reaction of **2 with benzene-24 hrs.** After **2** (21 mg, 0.014 mmol) was dissolved in 5 mL of benzene, the reaction mixture was stirred at room temperature. The red color of **2** immediately disappeared and the reaction mixture turned to yellow. The reaction mixture was stirred for 24 hrs and the reaction mixture was filtered through Celite and dried under vacuum. To the reaction mixture, a triphenylphosphine oxide (16 mg, 0.057 mmol)

solution in C₆D₆ was added and the yield of **3** (8%) and **4-Ph** (91%) in the solution was confirmed by integration versus triphenylphosphine oxide in the single-pulse ³¹P NMR data.

The reaction of 2 with benzene in pentane. A solution of **2** (22 mg, 0.016 mmol) and benzene (31 μL, 0.31 mmol) in 10 mL of pentane was stirred at room temperature for 48 hrs. After the solution was dried under vacuum, the remaining residue was dissolved in benzene. The solution was filtered through Celite and the filtrate was dried under vacuum. To the reaction mixture, a solution of triphenylphosphine oxide (18 mg, 0.061 mmol) in C₆D₆ was added and the yield of **3** (48%) and **4-Ph** (51%) in the solution was confirmed by a comparison of triphenylphosphine oxide in the single-pulse ³¹P NMR data.

Synthesis of (^{acri}PNP)NiPh (4-Ph**).** A solution of PhMgBr (180 μL, 1.0 M in THF, 180 μmol) was added dropwise to a solution of (^{acri}PNP)NiCl (99 mg, 176 μmol) in 5 mL of benzene at room temperature. The reaction mixture was stirred for 12 hrs resulting in a color change from green to yellow. After adding 1,4-dioxane the reaction mixture was stirred for 15 min, and volatiles were removed under vacuum. After the remained residue was dissolved in benzene the solution was filtered through Celite. The filtrate was dried under vacuum. The resulting product (^{acri}PNP)NiPh (**4-Ph**, 98 mg, 163 μmol, 92.6%) was isolated as a yellow solid after washing with pentane and drying under vacuum. ¹H NMR (400 MHz, C₆D₆) δ 7.70 (m, 2H, Ar-H), 7.12 (t, *J* = 7.2 Hz, 2H, Ar-H), 6.96 (tt, *J* = 7.2, 1.2 Hz, 1H, Ar-H), 6.84 (t, *J* = 4.4 Hz, 2H, Ar-H), 2.31 – 2.22 (m, 4H, CH(CH₃)₂), 2.27 (s, 6H, Ar-CH₃), 1.63 (s, 6H, Ar₂C(CH₃)₂), 1.09 (q, *J* = 7.3 Hz, 12H, CH(CH₃)₂), 0.98 (q, *J* = 7.2 Hz, 12H, CH(CH₃)₂). ¹³C NMR (101 MHz, C₆D₆) δ 156.10 (t, *J* = 13.8 Hz, Ar-C), 151.62 (t, *J* = 30.5 Hz, Ar-C), 139.12 (t, *J* = 3.2 Hz, Ar-C), 130.86 (t, *J* = 5.4 Hz, Ar-C), 130.55 (Ar-C), 129.63 (s, Ar-C), 126.55 (t, *J* = 2.0 Hz, Ar-C), 124.72 (t, *J* = 3.3 Hz, Ar-C), 121.71 (t, *J* = 2.2 Hz, Ar-C), 117.00 (t, *J* = 17.1 Hz, Ar-C), 36.40 (s, Ar₂C(CH₃)₂), 34.50 (s, Ar₂C(CH₃)₂), 22.64 (t, *J* = 12.6 Hz, CH(CH₃)₂), 20.97 (s, Ar-CH₃), 17.73 (t, *J* = 2.1 Hz, CH(CH₃)₂), 17.31 (CH(CH₃)₂). ³¹P NMR (162 MHz, C₆D₆) δ 39.3 (s). Anal. Calcd. for C₃₅H₄₉NNiP₂: C, 69.55; H, 8.17; N, 2.32. Found: C, 69.85; H, 8.27; N, 2.28. UV-vis [THF, nm (L mol⁻¹ cm⁻¹): 344 (20,000), 352 (20,000), 400 (sh, 3,000), 503 (sh, 300). IR (KBr Pellet, cm⁻¹): ν_{Ar} = 1604, 1593, 1564. X-ray quality crystals were grown by slow evaporation of a saturated diethyl ether solution of **4-Ph** at room temperature.

Synthesis of (^{acri}PNP)NiPh-*d*₅ (4-C₆D₅**).** After **2** (156 mg, 0.107 mmol) was dissolved in 15 mL of benzene-*d*₆, the reaction mixture was stirred for 1 day at room temperature resulting in a color change from red to yellow. After the volatiles were removed under vacuum, the remaining yellow solid was dissolved in pentane. The solution was filtered through Celite, and the filtrate was dried under vacuum. The resulting product (^{acri}PNP)NiPh-*d*₅ (**4-C₆D₅**, 120 mg, 197 μmol, 92.1%) was isolated as a yellow solid after washing with pentane and drying under vacuum. ¹H NMR (400 MHz, C₆D₆) δ 6.83 (t, *J* = 4.4 Hz, 2H, Ar-H), 2.31 – 2.22 (m, 4H, CH(CH₃)₂), 2.27 (s, 6H, Ar-CH₃), 1.62 (s, 6H, Ar₂C(CH₃)₂), 1.09 (q, *J* = 7.3 Hz, 12H, CH(CH₃)₂), 0.98 (q, *J* = 7.2 Hz, 12H, CH(CH₃)₂). ³¹P NMR (162 MHz, C₆D₆) δ 39.4 (s). IR (KBr Pellet, cm⁻¹): no ν_{C-H} signal at 3043, ν_{C-D} = 2254 (Δ(CD) = 789), ν_{Ar} = 1604, 1593, 1564.

Synthesis of (^{acri}PNP)NiD (3-D**).** To a solution of **2** (212 mg, 0.146 mmol) in 15 mL of THF, methanol-*d*₄ (6 μL, 0.148 mmol) was added dropwise at -35°C with stirring. The reaction mixture was gradually warmed to room temperature resulting in a color change from red to yellow. After stirring for 5 min the volatiles were removed under vacuum. The resulting residue was dissolved in pentane, and the solution was filtered through Celite. The filtrate was dried under vacuum to remove the volatiles. The resulting product (^{acri}PNP)NiD (**3-D**, 136 mg, 0.257 mmol, 88.0%) was

isolated as a yellow solid after washing with pentane and drying under vacuum. ^1H NMR (400 MHz, C_6D_6) δ 7.18 (d, $J = 4.0$ Hz, 2H, Ar-*H*), 6.91 (t, $J = 4.2$ Hz, 2H, Ar-*H*), 2.31 (s, 6H, Ar- CH_3), 2.17 – 2.12 (m, 4H, $\text{CH}(\text{CH}_3)_2$), 1.64 (s, 6H, $\text{Ar}_2\text{C}(\text{CH}_3)_2$), 1.26 (q, $J = 7.9$ Hz, 12H, $\text{CH}(\text{CH}_3)_2$), 1.08 (q, $J = 7.1$ Hz, 12H, $\text{CH}(\text{CH}_3)_2$). ^{31}P NMR (162 MHz, C_6D_6) δ 61.4 (t, $J = 9.7$ Hz). IR (KBr pellet, cm^{-1}): no $\nu_{\text{Ni-H}}$ signal at 1842, $\nu_{\text{Ar}} = 1589$.

Stability of 3 and 4-Ph. A solution of **3** (12 mg, 0.022 mmol), **4-Ph** (11 mg, 0.019 mmol), naphthalene (12 mg, 0.096 mmol) and triphenylphosphine oxide (11 mg, 0.038 mmol) in C_6D_6 was shaken at room temperature for 24 hrs. The reaction mixture was heated at 60 °C for 24 hrs and the solution was monitored by both ^1H and ^{31}P NMR spectroscopy.

Reaction of 2 with phenol. To a solution of **2** (57 mg, 0.039 mmol) in 5 mL of THF, a solution of phenol (7.5 mg, 0.080 mmol) in 5 mL of THF was added dropwise at -35°C resulting in an immediate color change from red to yellow. The reaction mixture was stirred for 10 min at room temperature resulting in conversion of **2** to **3**. The identity of the product was confirmed by a comparison of its ^1H and ^{31}P NMR data with those of an authentic sample of **3**. After **3** was washed out with pentane (3×5 mL), a white solid was isolated. The formation of sodium phenoxide was confirmed by its ^1H NMR data.

Reaction of 2 with aniline. To a solution of **2** (52 mg, 36 μmol) in 5 mL of THF, aniline (7 μL , 77 μmol) was added at -35°C resulting in an immediate color change from red to yellow. The reaction mixture was stirred for 10 min at room temperature resulting in conversion of **2** to **3**. The identity of the product was confirmed by a comparison of its ^1H and ^{31}P NMR data with those of an authentic sample of **3**. After **3** was washed out with pentane (3×5 mL), a white solid was isolated. The formation of sodium anilide was confirmed by its ^1H NMR data.

Reaction of 2 with triphenylmethane. A solution of **2** (21 mg, 15 μmol) and triphenylmethane (42 mg, 170 μmol) in 10 mL of pentane was stirred at room temperature for 2 days resulting in a color change from red to yellow. After all volatiles were removed under vacuum, the remaining residue was dissolved in benzene. The solution was filtered through Celite, and the filtrate was dried under vacuum. The formation of **3** (53%) and the corresponding ($^{\text{acri}}\text{PNP}$)NiAr species (47%) was established with the ^1H and ^{31}P NMR spectroscopic data. The ratio of the species in the product mixture was determined by integration of the corresponding signals in the ^{31}P NMR spectrum.

Reaction of 2 with 1 equiv. of triphenylmethane. A solution of **2** (38 mg, 26 μmol) and 1 equivalent of triphenylmethane (7 mg, 29 μmol) in 10 mL of pentane was stirred at room temperature for 2 days. After all volatiles were removed under vacuum, the remaining residue was dissolved in benzene- d_6 to quench the unreacted **2**. The formation of **3** and **3-D** (51%), the corresponding ($^{\text{acri}}\text{PNP}$)NiAr species (8%) and **4-C₆D₅** (41%) was established with the ^1H and ^{31}P NMR spectroscopic data. The ratio of the species in the product mixture was determined by integration of the corresponding signals in the ^{31}P NMR spectrum.

Reaction of 2 with 2 equiv. of triphenylmethane. A solution of **2** (36 mg, 25 μmol) and 2 equivalents of triphenylmethane (12 mg, 49 μmol) in 10 mL of pentane was stirred at room temperature for 2 days. After all volatiles were removed under vacuum, the remaining residue was dissolved in benzene- d_6 to quench the unreacted **2**. The formation of **3** and **3-D** (50%), the corresponding ($^{\text{acri}}\text{PNP}$)NiAr species (7%) and **4-C₆D₅** (43%) was established with the ^1H and ^{31}P

NMR spectroscopic data. The ratio of the species in the product mixture was determined by integration of the corresponding signals in the ^{31}P NMR spectrum.

Reaction of 2 with naphthalene. A solution of **2** (20 mg, 0.014 mmol) and naphthalene (35 mg, 0.27 mmol) in 10 mL of pentane was stirred at room temperature for 40 hr resulting in a color change from red to yellow. After the volatiles were removed under vacuum, the remaining residue was dissolved in benzene. The solution was filtered through Celite and the filtrate was dried under vacuum. The formation of **3** (43%) and **4-Naph** (57%) was observed. The identity of the products was confirmed by a comparison of its ^1H and ^{31}P NMR data with those of an authentic sample of **3** and **4-Naph**.

Quantification for the reaction of 2 with naphthalene. A solution of **2** (21 mg, 0.014 mmol) and naphthalene (38 mg, 0.29 mmol) in 10 mL of pentane was stirred at room temperature for 48 hrs resulting in a color change from red to yellow. After the volatiles were removed under vacuum, the remaining residue was dissolved in benzene. The solution was filtered through Celite and the filtrate was dried under vacuum. To the reaction mixture, a solution of triphenylphosphine oxide (17 mg, 0.058 mmol) in 0.6 mL of C_6D_6 was added and the yield of **3** (45%) and **4-Naph** (51%) in the solution was confirmed by a comparison of triphenylphosphine oxide in the single-pulse ^{31}P NMR data.

Reaction of 2 with anthracene. A solution of **2** (20 mg, 0.014 mmol) and anthracene (53 mg, 0.30 mmol) in 10 mL of pentane was stirred at room temperature for 40 hr resulting in a color change from red to yellow. After the volatiles were removed under vacuum, the remaining residue was dissolved in benzene. The solution was filtered through Celite and the filtrate was dried under vacuum. The formation of **3** (46%) and **4-Anth** (54%) was observed. The identity of the products was confirmed by a comparison of its ^1H and ^{31}P NMR data with those of an authentic sample of **3** and **4-Anth**.

Quantification for the reaction of 2 with anthracene. A solution of **2** (22 mg, 0.015 mmol) and anthracene (55 mg, 0.30 mmol) in 10 mL of pentane was stirred at room temperature for 48 hrs resulting in a color change from red to yellow. After the volatiles were removed under vacuum, the remaining residue was dissolved in benzene. The solution was filtered through Celite and the filtrate was dried under vacuum. To the reaction mixture, a solution of triphenylphosphine oxide (17 mg, 0.060 mmol) in 2 mL of THF was added. To a 0.4 mL of aliquots, few drops of C_6D_6 was added. The yield of **3** (56%) and **4-Anth** (43%) in the solution was confirmed by a comparison of triphenylphosphine oxide in single-pulse ^{31}P NMR data.

Reaction of ($^{\text{acri}}\text{PNP}$)NiCl with 1-naphthyl lithium. A solution of 1-naphthyl lithium (11 mg, 0.082 mmol) in 5 mL of Et_2O was added dropwise to a solution of ($^{\text{acri}}\text{PNP}$)NiCl (39 mg, 0.069 mmol) in 5 mL of Et_2O at -35°C with stirring. The reaction mixture was gradually warmed to room temperature and monitored for >12 hrs by ^{31}P NMR spectra. No product was detected from the reaction between ($^{\text{acri}}\text{PNP}$)NiCl with 1-naphthyl lithium.

Separate synthesis of ($^{\text{acri}}\text{PNP}$)Ni(2-naphthyl) (4-Naph). A solution of 2-naphthyl lithium (61 mg, 0.46 mmol) in 5 mL of Et_2O was added dropwise to a solution of ($^{\text{acri}}\text{PNP}$)NiCl (225 mg, 0.399 mmol) in 5 mL of Et_2O at -35°C with stirring. The reaction mixture was gradually warmed to room temperature resulting in a color change from green to yellow. After stirring for 30 min the volatiles were removed under vacuum. The remained residue was dissolved in benzene, and the

solution was filtered through Celite. The filtrate was dried under vacuum. The resulting product (^{acri}PNP)Ni(2-naphthyl) (**4-Naph**, 252 mg, 0.385 mmol, 96.5%) was isolated as a yellow solid after washing with pentane and drying under vacuum. ¹H NMR (400 MHz, C₆D₆) δ 8.13 (s, 1H, Ar-*H*), 7.94 (dd, *J* = 8.0, 1.2 Hz, 1H, Ar-*H*), 7.71 (t, *J* = 8.8 Hz, 2H, Ar-*H*), 7.57 (d, *J* = 8.4 Hz, 1H, Ar-*H*), 7.32 (m, 1H, Ar-*H*), 7.22 (t, *J* = 7.6 Hz, 1H, Ar-*H*), 6.82 (t, *J* = 4.7 Hz, 2H, Ar-*H*), 2.27-2.15 (m, 4H, CH₂(CH₃)₂, Ar₂C(CH₃)₂), 1.63 (d, 6H, Ar-CH₃), 1.08 (qd, *J* = 7.2, 2.8 Hz, 12H, CH(CH₃)₂), 0.93 (q, *J* = 2.8, 6H, CH(CH₃)₂), 0.86 (q, *J* = 2.8, 6H, CH(CH₃)₂). ¹³C NMR (101 MHz, C₆D₆) δ 156.14 (t, *J* = 13.8 Hz, Ar-C), 150.45 (t, *J* = 30.6 Hz, Ar-C), 137.58 (t, *J* = 2.6 Hz, Ar-C), 136.81 (t, *J* = 4.1 Hz, Ar-C), 133.72 (t, *J* = 2.7 Hz, Ar-C), 131.14 (Ar-C), 130.90 (t, *J* = 5.5 Hz, Ar-C), 130.58 (s, Ar-C), 129.63 (s, Ar-C), 125.92 (s, Ar-C), 125.47 (s, Ar-C), 124.85 (t, *J* = 3.2 Hz, Ar-C), 124.45 (s, Ar-C), 123.32 (s, Ar-C), 116.99 (t, *J* = 17.3 Hz, Ar-C), 36.40 (s, Ar₂C(CH₃)₂), 34.45 (d, *J* = 35.5 Hz, Ar₂C(CH₃)₂), 22.86 (dt, *J* = 47.2, 12.5 Hz, CH(CH₃)₂), 20.95 (s, Ar-CH₃), 17.79 (s, CH(CH₃)₂), 17.45 (s, CH(CH₃)₂), 17.26 (s, CH(CH₃)₂). ³¹P NMR (162 MHz, C₆D₆) δ 39.7 (s). Anal. Calcd. for C₃₉H₅₁NNiP₂: C, 71.57; H, 7.58; N, 2.14. Found: C, 71.28; H, 7.97; N, 2.02. UV-vis [THF, nm (L mol⁻¹ cm⁻¹): 340 (23,000), 349 (22,000), 396 (sh, 4,100), 461 (sh, 1,000). IR (KBr Pellet, cm⁻¹): ν_{Ar} = 1604, 1591, 1572, 1556. X-ray quality crystals were grown by slow evaporation of a saturated Et₂O solution of **4-Naph** at room temperature.

Synthesis of (^{acri}PNP)Ni(2-anthracenyl) (4-Anth). A solution of 2-anthracenyl lithium (121 mg, 0.657 mmol) in 5 mL of Et₂O was added dropwise to a solution of (^{acri}PNP)NiCl (365 mg, 0.640 mmol) in 5 mL of Et₂O at -35°C with stirring. The reaction mixture was gradually warmed to room temperature resulting in a color change from green to yellow. After stirring for 30 min the volatiles were removed under vacuum. The remained residue was dissolved in benzene, and the solution was filtered through Celite. The filtrate was dried under vacuum. The resulting product (^{acri}PNP)Ni(2-anthracenyl) (**4-Anth**, 416 mg, 0.590 mmol, 92.2%) was isolated as a yellow solid after washing with pentane and drying under vacuum. ¹H NMR (400 MHz, C₆D₆) δ 8.26 (s, 1H, Ar-*H*), 8.23 (s, 1H, Ar-*H*), 8.20 (s, 1H, Ar-*H*), 7.99 (d, *J* = 8 Hz, 1H, Ar-*H*), 7.90 (d, *J* = 8 Hz, 1H, Ar-*H*), 7.85 (d, *J* = 8 Hz, 1H, Ar-*H*), 7.81 (dd, *J* = 6.4, 3.2 Hz, 1H, Ar-*H*), 7.72 (d, *J* = 8 Hz, 1H, Ar-*H*), 7.25 (m, 3H, Ar-*H*), 7.18 (d, *J* = 2 Hz, 2H, Ar-*H*), 6.83 (t, *J* = 5.6 Hz, 2H, Ar-*H*), 2.33-2.21 (m, 10H, CH₂(CH₃)₂, Ar₂C(CH₃)₂), 1.66 (s, 3H, Ar-CH₃), 1.63 (s, 3H, Ar-CH₃), 1.11 (m, 12H, CH(CH₃)₂), 0.99 (q, *J* = 8 Hz, 6H, CH(CH₃)₂), 0.91 (q, *J* = 8 Hz, 6H, CH(CH₃)₂). ¹³C NMR (101 MHz, C₆D₆) δ 156.13 (t, *J* = 13.1 Hz, Ar-C), 150.99 (s, Ar-C), 137.16 (s, Ar-C), 136.21 (s, Ar-C), 132.48 (s, Ar-C), 132.31 (s, Ar-C), 130.93 (s, Ar-C), 130.63 (s, Ar-C), 129.63 (s, Ar-C), 126.73 (s, Ar-C), 126.45 (s, Ar-C), 125.58 (s, Ar-C), 125.07 (s, Ar-C), 124.92 (t, *J* = 3.0 Hz, Ar-C), 124.12 (s, Ar-C), 122.55 (s, Ar-C), 116.91 (t, *J* = 17.2, Ar-C), 36.41 (s, Ar₂C(CH₃)₂), 34.71 (s, Ar₂C(CH₃)₂), 34.20 (s, Ar₂C(CH₃)₂), 23.27 (t, *J* = 12.1, CH(CH₃)₂), 22.65 (t, *J* = 13.1, CH(CH₃)₂), 20.94 (s, Ar-CH₃), 17.82 (t, *J* = 2.0 Hz, CH(CH₃)₂), 17.50 (s, CH(CH₃)₂), 17.27 (s, CH(CH₃)₂). ³¹P NMR (162 MHz, C₆D₆) δ 40.0 (s). Anal. Calcd. for C₄₃H₅₃NNiP₂: C, 73.31; H, 7.58; N, 1.99. Found: C, 73.66; H, 7.73; N, 1.78. UV-vis [THF, nm (L mol⁻¹ cm⁻¹): 308 (sh, 4,400), 342 (24,000), 391 (6,600), 467 (sh, 930). IR (KBr Pellet, cm⁻¹): ν_{Ar} = 1604, 1591, 1560, 1550. X-ray quality crystals were grown by slow diffusion of toluene into a saturated THF solution of **4-Anth** at -35°C.

Reaction of 2 with toluene. After **2** (20 mg, 0.014 mmol) was dissolved in 5 mL of toluene, the reaction mixture was stirred at room temperature. The red color of **2** immediately disappeared and the reaction mixture turned to yellow. The reaction mixture was stirred for 15 min, resulting in a conversion of **2** to **3** (50%), **4-*m*Tol** (35%) and **4-*p*Tol** (15%). The reaction mixture was further

stirred for 24 hrs, and the product ratio changes to give lower concentration of **3** (6%) and higher concentration of **4-*m*Tol** (65%) and **4-*p*Tol** (29%). The identity of the products was confirmed by a comparison of its ^1H and ^{31}P NMR data with those of an authentic sample of **3**, **4-*m*Tol** and **4-*p*Tol**.

Quantification of nickel complexes from the reaction of 2 with toluene-15 min. After **2** (22 mg, 0.015 mmol) was dissolved in 5 mL of toluene, the reaction mixture was stirred at room temperature. The red color of **2** immediately disappeared and the reaction mixture turned to brown. The reaction mixture was stirred for 15 min and the reaction mixture was filtered through Celite and dried under vacuum. To the reaction mixture, a triphenylphosphine oxide (17 mg, 0.060 mmol) solution in 0.6 mL of C_6D_6 was added and the yield of **3** (48%), **4-*m*Tol** (38%) and **4-*p*Tol** (14%) in the solution was confirmed by a comparison of triphenylphosphine oxide in single-pulse ^{31}P NMR data.

Quantification of nickel complexes from the reaction of 2 with benzene-24 hrs. After **2** (21 mg, 0.014 mmol) was dissolved in 5 mL of toluene, the reaction mixture was stirred at room temperature. The red color of **2** immediately disappeared and the reaction mixture turned to yellow. The reaction mixture was stirred for 24 hrs and the reaction mixture was filtered through Celite and dried under vacuum. To the reaction mixture, a triphenylphosphine oxide (17 mg, 0.058 mmol) solution in 0.6 mL of C_6D_6 was added and the yield of **3** (28%), **4-*m*Tol** (50%) and **4-*p*Tol** (21%) in the solution was confirmed by a comparison of triphenylphosphine oxide in single-pulse ^{31}P NMR data.

The reaction of 2 with toluene in pentane. A solution of **2** (22 mg, 0.015 mmol) and toluene (32 μL , 0.30 mmol) in 10 mL of pentane was stirred at room temperature for 48 hrs. After the solution was dried under vacuum, the remaining residue was dissolved in benzene. The solution was filtered through Celite and the filtrate was dried under vacuum. To the reaction mixture, a solution of triphenylphosphine oxide (17 mg, 0.060 mmol) in C_6D_6 was added and the yield of **3** (45%), **4-*m*Tol** (43%) and **4-*p*Tol** (11%) in the solution was confirmed by a comparison of triphenylphosphine oxide in the single-pulse ^{31}P NMR data.

Synthesis of ($^{\text{acri}}\text{PNP}$)Ni(*o*-tolyl) (4-*o*Tol**).** A solution of *o*-tolylLi (56 mg, 0.58 mmol) in 5 mL of Et_2O was added dropwise to a solution of ($^{\text{acri}}\text{PNP}$)NiCl (320 mg, 0.568 mmol) in 5 mL of Et_2O at -35°C with stirring. The reaction mixture was gradually warmed to room temperature resulting in a color change from green to yellow. After stirring for 30 min the volatiles were removed under vacuum. The remained residue was dissolved in benzene, and the solution was filtered through Celite. The filtrate was dried under vacuum. The resulting product ($^{\text{acri}}\text{PNP}$)Ni(*o*-tolyl) (**4-*o*Tol**, 336 mg, 0.543 mmol, 95.6%) was isolated as a yellow solid after washing with pentane and drying under vacuum. ^1H NMR (400 MHz, C_6D_6) δ 7.69 (d, 1H, Ar-*H*), 7.16 (m, 2H, Ar-*H*), 6.99 (m, 3H, Ar-*H*), 6.78 (t, $J = 4$ Hz, 2H, Ar-*H*), 2.95 (s, 3H, Ar- CH_3), 2.32-2.27 (m, 8H, $\text{CH}(\text{CH}_3)_2$, Ar- CH_3), 2.20-2.15 (m, 2H, $\text{CH}(\text{CH}_3)_2$), 1.69 (d, 3H, $\text{C}(\text{CH}_3)_2$), 1.51 (d, 3H, $\text{C}(\text{CH}_3)_2$), 1.06 (m, 12H, $\text{CH}(\text{CH}_3)_2$), 1.00 (q, $J = 8$ Hz, 6H, $\text{CH}(\text{CH}_3)_2$), 0.88 (q, $J = 8$ Hz, 6H, $\text{CH}(\text{CH}_3)_2$). ^{13}C NMR (101 MHz, C_6D_6) δ 156.11 (t, $J = 14.1$ Hz, Ar-C), 151.23 (t, $J = 30.3$ Hz, Ar-C), 139.92 (t, $J = 4.1$ Hz, Ar-C), 136.06 (t, $J = 12.0$ Hz, Ar-C), 134.82 (t, $J = 2.0$ Hz, Ar-C), 130.84 (t, $J = 6.1$ Hz, Ar-C), 130.51 (s, Ar-C), 129.63 (s, Ar-C), 126.32 (t, $J = 3.0$ Hz, Ar-C), 124.68 (t, $J = 3.0$, Ar-C), 122.60 (t, $J = 3.0$, Ar-C), 117.06 (t, $J = 17.2$, Ar-C), 36.41 (s, $\text{Ar}_2\text{C}(\text{CH}_3)_2$), 34.48 (d, $J = 29.3$ Hz, $\text{Ar}_2\text{C}(\text{CH}_3)_2$), 22.69 (t, $J = 13.1$, $\text{CH}(\text{CH}_3)_2$), 21.95 (s, Ar- CH_3), 20.98 (s, Ar- CH_3), 17.75 (dt, $J = 22.2$, 2.0 Hz, $\text{CH}(\text{CH}_3)_2$), 17.33 (d, $J = 7.1$ Hz, $\text{CH}(\text{CH}_3)_2$). ^{31}P NMR (162 MHz, C_6D_6) δ 37.4 (s).

Anal. Calcd. for $C_{36}H_{51}NNiP_2$: C, 69.92; H, 8.31; N, 2.26. Found: C, 70.08; H, 8.57; N, 2.19. UV-vis [THF, nm ($L\ mol^{-1}\ cm^{-1}$)]: 339 (22,000), 350 (sh, 20,000), 393 (sh, 3,900), 436 (1,100). IR (KBr Pellet, cm^{-1}): ν_{Ar} = 1604, 1592, 1570, 1554. X-ray quality crystals were grown by slow evaporation of a saturated Et_2O solution of **4-*o*Tol** at room temperature.

Separate synthesis of (^{acri}PNP)Ni(*m*-tolyl) (4-*m*Tol). A solution of *m*-tolylLi (38 mg, 0.39 mmol) in 3 mL of Et_2O was added dropwise to a solution of (^{acri}PNP)NiCl (210 mg, 0.373 mmol) in 5 mL of Et_2O at $-35^\circ C$ with stirring. The reaction mixture was gradually warmed to room temperature resulting in a color change from green to yellow. After stirring for 30 min the volatiles were removed under vacuum. The remained residue was dissolved in benzene, and the solution was filtered through Celite. The filtrate was dried under vacuum. The resulting product (^{acri}PNP)Ni(*m*-tolyl) (**4-*m*Tol**, 215 mg, 0.348 mmol, 93.3%) was isolated as a yellow solid after washing with pentane and drying under vacuum. 1H NMR (400 MHz, C_6D_6) δ 7.59 (s, 1H, Ar-*H*), 7.51 (d, J = 7.6 Hz, 1H, Ar-*H*), 7.07 (t, J = 7.6 Hz, 1H, Ar-*H*), 6.84 (t, J = 4.4 Hz, 2H, Ar-*H*), 6.78 (d, J = 7.6 Hz, 1H, Ar-*H*), 2.32 – 2.27 (m, 13H, $CH_2(CH_3)_2$, Ar- CH_3), 1.61 (d, 6H, Ar- CH_3), 1.11 (q, J = 7.6 Hz, 12H, $CH(CH_3)_2$), 1.01 (q, J = 7.6 Hz, 12H, $CH(CH_3)_2$). ^{13}C NMR (101 MHz, C_6D_6) δ 156.11 (t, J = 14.1 Hz, Ar-*C*), 151.23 (t, J = 30.3 Hz, Ar-*C*), 139.92 (t, J = 4.1 Hz, Ar-*C*), 136.06 (t, J = 12.0 Hz, Ar-*C*), 134.82 (t, J = 2.0 Hz, Ar-*C*), 130.84 (t, J = 6.1 Hz, Ar-*C*), 130.51 (s, Ar-*C*), 129.63 (s, Ar-*C*), 126.32 (t, J = 3.0 Hz, Ar-*C*), 124.68 (t, J = 3.0, Ar-*C*), 122.60 (t, J = 3.0, Ar-*C*), 117.06 (t, J = 17.2, Ar-*C*), 36.41 (s, $Ar_2C(CH_3)_2$), 34.48 (d, J = 29.3 Hz, $Ar_2C(CH_3)_2$), 22.69 (t, J = 13.1, $CH(CH_3)_2$), 21.95 (s, Ar- CH_3), 20.98 (s, Ar- CH_3), 17.75 (dt, J = 22.2, 2.0 Hz, $CH(CH_3)_2$), 17.33 (d, J = 7.1 Hz, $CH(CH_3)_2$). ^{31}P NMR (162 MHz, C_6D_6) δ 39.0 (s). Anal. Calcd. for $C_{36}H_{51}NNiP_2$: C, 69.92; H, 8.31; N, 2.26. Found: C, 69.55; H, 8.17; N, 2.32. UV-vis [THF, nm ($L\ mol^{-1}\ cm^{-1}$)]: 344 (23,000), 352 (23,000), 396 (sh, 4,000), 466 (sh, 790). IR (KBr Pellet, cm^{-1}): ν_{Ar} = 1604, 1591, 1572, 1556. X-ray quality crystals were grown by slow evaporation of a saturated THF solution of **4-*m*Tol** at room temperature.

Separate synthesis of (^{acri}PNP)Ni(*p*-tolyl) (4-*p*Tol). A solution of *p*-tolylLi (46 mg, 0.47 mmol) in 3 mL of Et_2O was added dropwise to a solution of (^{acri}PNP)NiCl (248 mg, 0.440 mmol) in 5 mL of Et_2O at $-35^\circ C$ with stirring. The reaction mixture was gradually warmed to room temperature resulting in a color change from green to yellow. After stirring for 30 min the volatiles were removed under vacuum. The remained residue was dissolved in benzene, and the solution was filtered through Celite. The filtrate was dried under vacuum. The resulting product (^{acri}PNP)Ni(*p*-tolyl) (**4-*p*Tol**, 260 mg, 0.420 mmol, 95.5%) was isolated as a yellow solid after washing with pentane and drying under vacuum. 1H NMR (400 MHz, C_6D_6) δ 7.59 (m, 2H, Ar-*H*), 7.01 (d, J = 7.2 Hz, 2H, Ar-*H*), 6.84 (t, J = 4.4, 2H, Ar-*H*), 2.30 – 2.25 (m, 13H, $CH(CH_3)_2$, Ar- CH_3), 1.63 (s, 6H, $Ar_2C(CH_3)_2$), 1.11 (q, J = 7.6 Hz, 12H, $CH(CH_3)_2$), 1.00 (q, J = 7.6 Hz, 12H, $CH(CH_3)_2$). ^{13}C NMR (101 MHz, C_6D_6) δ 156.14 (t, J = 13.8 Hz, Ar-*C*), 145.53 (t, J = 30.8 Hz, Ar-*C*), 138.89 (t, J = 3.3 Hz, Ar-*C*), 130.84 (t, J = 3.3 Hz, Ar-*C*), 130.51 (Ar-*C*), 130.29 (t, J = 2.4 Hz, Ar-*C*), 129.64 (s, Ar-*C*), 124.68 (t, J = 3.2 Hz, Ar-*C*), 117.15 (t, J = 17.0 Hz, Ar-*C*), 36.40 (t, J = 1.7 Hz, $Ar_2C(CH_3)_2$), 34.48 (s, $Ar_2C(CH_3)_2$), 22.70 (t, J = 12.5 Hz, $CH(CH_3)_2$), 21.15 (s, Ar- CH_3), 20.96 (s, Ar- CH_3), 17.82 (t, J = 2.1 Hz, $CH(CH_3)_2$), 17.34 (s, $CH(CH_3)_2$). ^{31}P NMR (162 MHz, C_6D_6) δ 39.1 (s). Anal. Calcd. for $C_{36}H_{51}NNiP_2$: C, 69.92; H, 8.31; N, 2.26. Found: C, 69.75; H, 8.52; N, 2.31. UV-vis [THF, nm ($L\ mol^{-1}\ cm^{-1}$)]: 344 (23,000), 352 (23,000), 396 (sh, 4,000), 466 (sh, 790). IR (KBr Pellet, cm^{-1}): ν_{Ar} = 1603, 1591, 1583, 1568. X-ray quality crystals were grown by slow evaporation of a saturated Et_2O solution of **4-*p*Tol** at room temperature.

Separate synthesis of (^{acri}PNP)Ni(benzyl). To a solution of (^{acri}PNP)NiCl (305 mg, 0.542 mmol) in 5 mL of Et₂O, a solution of benzyl magnesium chloride (390 μL, 1.4 M in THF, 0.546 mmol) was added at -35°C with stirring. The reaction mixture was gradually warmed to room temperature and stirred for 1 day resulting in a color change from green to red. After adding 1,4-dioxane (92 μL, 95 mg, 0.80 mmol) the reaction mixture was stirred for 30 min, and the volatiles were removed under vacuum. After the residue was dissolved in benzene, the solution was filtered through Celite, and volatiles were removed under vacuum. The resulting product (^{acri}PNP)Ni(benzyl) (298 mg, 0.482 mmol, 88.9%) was isolated as an orange solid after washing with cold pentane and drying under vacuum. ¹H NMR (400 MHz, C₆D₆) δ 7.62 (d, *J* = 4 Hz, 2H, Ar-*H*), 7.01 (t, *J* = 8 Hz, 1H, Ar-*H*), 6.91 (t, *J* = 4 Hz, 2H, Ar-*H*), 2.29 (s, 6H, Ar-CH₃), 2.27 – 2.25 (br, 2H, PhCH₂), 2.04 – 1.99 (m, 4H, CH(CH₃)₂), 1.55 (s, 6H, Ar₂C(CH₃)₂), 1.21 (q, *J* = 8 Hz, 12H, CH(CH₃)₂), 1.14 (q, *J* = 8 Hz, 12H, CH(CH₃)₂). ¹³C NMR (101 MHz, C₆D₆) δ 156.29 (t, *J* = 13.1 Hz, Ar-C), 151.87 (t, *J* = 3.0 Hz, Ar-C), 130.81 (t, *J* = 5.1 Hz, Ar-C), 129.27 (s, Ar-C) 129.24 (s, Ar-C), 124.83 (t, *J* = 3.0 Hz, Ar-C), 123.06 (s, Ar-C), 117.52 (t, *J* = 18.2 Hz, Ar-C), 36.25 (t, *J* = 2.0 Hz, Ar₂C(CH₃)₂), 32.18 (s, Ar₂C(CH₃)₂), 24.24 (t, *J* = 11.1 Hz, CH(CH₃)₂), 21.04 (s, Ar-CH₃), 19.08 (t, *J* = 3.0 Hz, CH(CH₃)₂), 18.11 (s, CH(CH₃)₂), -0.84 (t, *J* = 22.2, Ni-C) ³¹P NMR (162 MHz, C₆D₆) δ 37.1 (s). Anal. Calcd. for C₃₆H₅₁NNiP₂: C, 69.92; H, 8.31; N, 2.26. Found: C, 70.03; H, 8.41; N, 1.89. UV-vis [THF, nm (L mol⁻¹ cm⁻¹): 317 (sh, 15,000), 346 (24,000), 382 (sh, 6,000), 434 (sh, 1,400). IR (KBr Pellet, cm⁻¹): ν_{Ar} = 1591, 1570. X-ray quality crystals were grown by slow evaporation of a saturated pentane solution of (^{acri}PNP)Ni(benzyl) at room temperature.

Reaction of 2 with toluene followed by NMR and X-band EPR experiments. **2** (18 mg, 0.012 mmol) was treated with toluene/THF-*d*₈ (25:1) to bring the final volume to 5 mL (2.5 mM of **2**). The reaction mixture was allowed to stir at room temperature. Aliquots were taken at 5 min, 25 min and 2 hrs to monitor the reaction by ³¹P NMR and X-band EPR spectroscopy.

Detection of sodium in the black solid residue with naphthalene. After **2** (366 mg, 0.253 mmol) was dissolved in 10 mL of benzene, the reaction mixture was stirred at room temperature. After stirring for 15 min, the reaction mixture was dried under vacuum. The sodium was isolated as a black solid after washing with pentane (5 × 5 mL). After a solution of naphthalene (54 mg, 0.42 mmol) and 18-crown-6 (106 mg, 0.401 mmol) in 5 mL of 1,2-dimethoxyethane (DME) was added to the isolated black powder, the color of the reaction mixture immediately turns to deep green. After stirring for additional 10 min, the reaction mixture was filter through Celite, and the volatiles were removed under vacuum. The resulting residue was dissolved in 3 mL of DME, and the solution was cooled to -35°C. A red crystalline solid was precipitated out after two days. A desired material [Na(18-crown-6)DME][C₁₀H₈] (32 mg, 0.063 mmol, 12%) was obtained after washing with cold pentane and drying under vacuum. UV-vis [THF, nm (L mol⁻¹ cm⁻¹): 322 (sh, 5,400), 327 (9,100), 327 (9,100), 409 (sh, 1,900), 442 (1,600), 455 (sh, 1,400), 469 (1,100), 695 (sh, 1,100), 789 (1,700), 875 (1,500). The UV-vis spectrum, as shown in **Figure S69** reveals the formation of the naphthalenide species as reported.¹¹

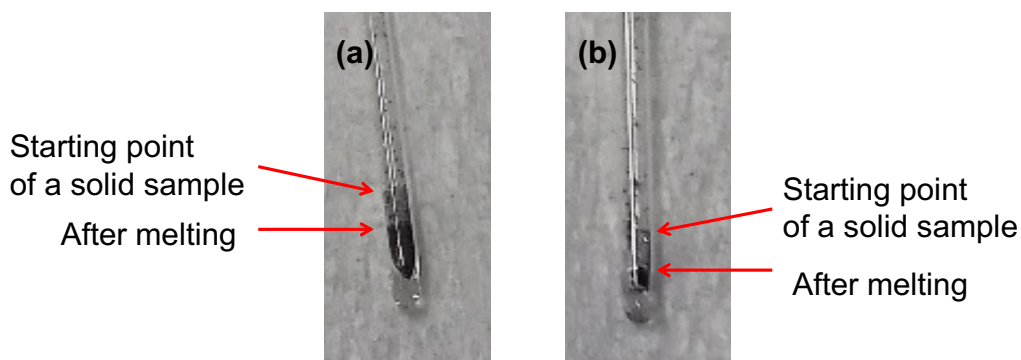
Quantification of sodium with benzophenone radical. After **2** (106 mg, 0.0734 mmol) was dissolved in 10 mL of benzene, the reaction mixture was stirred at room temperature. After stirring for 15 min, the reaction mixture was dried under vacuum. The sodium was isolated as a black solid after washing with pentane (5 × 5 mL). To the isolated sodium powder, a benzophenone solution (14 mg, 0.77 mmol in 20 mL of THF) was introduced. After 1 mL of the resulting solution was diluted to 10mL, the concentration of the resulting benzophenone radical was spectroscopically

measured from the absorption at 682 nm (1.14), and the yield was 68%. The calibration curve was derived from the absorption measurement of a 3.68 mM of stock solution (**Figure S92** and **S93**). Upon dilution of the stock solution (0.37, 0.18, 0.09 and 0.05 mM, respectively), the absorption at 628 nm was measured (1.88, 0.91, 0.47 and 0.25, respectively).

Quantification of sodium with naphthalene and 1,1-diphenylethylene. After **2** (118 mg, 0.0817 mmol) was dissolved in 10 mL of benzene, the reaction mixture was stirred at room temperature. After stirring for 15 min, the reaction mixture was dried under vacuum. The sodium was isolated as a black solid after washing with pentane (5×5 mL). The isolated sodium was titrated according to the literature procedure.¹¹ After the isolated black powder was added to a solution of naphthalene (22 mg, 0.17 mmol) in 5 mL of THF, the color of the reaction mixture immediately turns to deep green. The sodium naphthalenide solution was added dropwise to 0.5 mL of 1,1-diphenylethylene in 100 mL of round-bottom flask, and the color of the reaction mixture immediately turned to intense red indicating the formation of dianion. The dianion solution was titrated against 0.50 M of *t*-butanol solution in toluene. Upon addition of 230 μ L of *t*-butanol solution, the color of the reaction mixture changed to a pale-yellow end-point, and the yield of the sodium was calculated based on the following equation: $(0.50 \text{ M} \times 230 \mu\text{L}) / (0.0817 \text{ mmol} \times 2) = 70.4\%$.

Control experiments for detecting a naphthalenide radical from the reaction of NaH and PhLi with naphthalene. To a solution of naphthalene (11 mg, 0.086 mmol) in 5 mL of THF the reagent (0.090~0.092 mmol) was added at room temperature. The reaction mixture was stirred for 3 hrs, and THF was added to the resulting solution to give a final volume of 20 mL. UV-vis spectrum ($200 \text{ nm} < \lambda < 1100 \text{ nm}$) was measured by diluting 1 mL of the stock solution into 10 mL of THF to give final concentration of 0.43 mM of naphthalene or naphthalenide solution. The distinctive broad absorption of naphthalenide radical at 830 nm ($\epsilon = ca. 2000$) was not observed, confirming that sodium was generated from the reaction of **2** with benzene.

Determination of the melting point of sodium(0). After **2** (558 mg, 0.386 mmol) was dissolved in 20 mL of benzene, the reaction mixture was stirred at room temperature. After stirring for 15 min, the reaction mixture was dried under vacuum. The resulting solid was isolated as a black powder after washing with pentane (5×5 mL). A capillary was charged with an isolated powder, which melted at around 101 $^{\circ}\text{C}$. The reversibility of the melting point of the black powder was not determined in this experiment. The same measurement was conducted with an authentic sample of Na(0), which gave the same melting point, see Figure shown below, (a) a black powder isolated from the reaction and (b) an authentic sample of Na(0).



Purification of NH₃(g). Sodium metal in a Schlenk flask was taken out of the dry-box and connected to the Schlenk line. After the flask was connected to an oil bubbler and an ammonia gas cylinder, NH₃(g) was transferred and liquified at $-78\text{ }^{\circ}\text{C}$ by using an acetone/dry-ice bath. The resulting liquid ammonia was dried over sodium metal revealing a dark blue color solution.

Detection of sodium in the black solid residue with liquid ammonia. After **2** (310 mg, 215 mmol) was dissolved in 10 mL of benzene, the reaction mixture was stirred at room temperature for 10 min. All volatiles were removed and the solid reaction mixture was dried under vacuum. The resulting solid was isolated as a black powder after washing with pentane (5×5 mL). The isolated black powder in a Schlenk cuvette was taken out of the dry-box and connected to the Schlenk line. To the cuvette at $-80\text{ }^{\circ}\text{C}$, purified NH₃(g) stored as a blue stock solution of NH₃(l) was added, revealing the formation of a blue solution. The same procedure conducted with an authentic Na(0) showed the same blue solution (**Figure S95**).

Elemental analysis of the black solid residue. After **2** (384 mg, 0.266 mmol) was dissolved in 20 mL of benzene, the reaction mixture was stirred for 30 min at room temperature. All volatiles were removed and the solid reaction mixture was dried under vacuum. The resulting solid was isolated as a black powder after washing with pentane (5×5 mL). The procedure was repeated 5 times to collect the solid residue for EA analysis. Elemental analysis data reveals only a trace amount of C and H (C, 0.11; H, 0.05) and nitrogen was not detected.

Quantification of NaH with ethyl diethylphosphonoacetate. After **2** (209 mg, 0.144 mmol) was dissolved in 15 mL of benzene, the reaction mixture was stirred at room temperature. After stirring for 1 day, the reaction mixture was dried under vacuum. The NaH was isolated as a gray powder after washing with pentane (5×5 mL). The isolated NaH was titrated according to the literature procedure.¹² After 1 mL of THF was added to the NaH, the gray suspension was cooled to $-35\text{ }^{\circ}\text{C}$. Ethyl diethylphosphonoacetate (100 μL , 0.489 mmol) was added dropwise to the suspension, and the reaction mixture was gradually warmed to room temperature. A pale yellow, homogeneous solution was generated after 5 min of stirring. The yield of the corresponding anion generated from the hydride content of the sample was determined by comparing the integration of a peak at 3.33 ppm (those associated with the methylene proton of remaining ethyl diethylphosphonoacetate, 1.00) vs. a peak at 2.81 ppm (those associated with the vinylic methine proton of ethyl sodiodiethylphosphonoacetate, 0.46) in ¹H NMR spectrum, shown in **Figure S41**. The yield of the NaH was calculated based on the following equation: $\{0.46 \cdot 0.489\text{ mmol} / (1.0 \cdot 0.5 + 0.46)\} / (0.144\text{ mmol} \cdot 2) = 81\%$.

Magic angle spinning (MAS) Solid state ²³Na NMR spectrum of NaH. After **2** (237 mg, 0.164 mmol) was dissolved in 15 mL of benzene, the reaction mixture was stirred at room temperature. After stirring for 1 day, the reaction mixture was dried under vacuum. The NaH was isolated as a gray powder after washing with pentane (5×5 mL) (**Figure S77**).

Synthesis of $\{(\text{acriPNP})\text{Ni}-(\text{N}_2)-\text{K}(\text{THF})_2\}_2$ (2-K**).** After potassium (42 mg, 1.1 mmol) was added to a solution of naphthalene (29 mg, 0.23 mmol) in 5 mL of THF, the reaction mixture was stirred for 3 hrs at room temperature. The resulting potassium naphthalenide solution was filtered away from remaining potassium and added dropwise to a solution of (acriPNP)Ni•C₁₀H₈ (148 mg, 0.226 mmol) in 5 mL of THF at $-35\text{ }^{\circ}\text{C}$ with stirring. The reaction mixture was gradually warmed to room temperature resulting in a color change from reddish brown to red. After stirring for additional 30 min, the reaction mixture was filter through Celite, and the volatiles were removed

under vacuum. The resulting residue was dissolved in 15 mL of pentane/THF (5:1), and the solution was cooled to -35°C . A red crystalline solid was precipitated out after two days. An analytically pure material $\{(\text{acriPNP})\text{Ni}-(\text{N}_2)-\text{K}(\text{THF})_2\}_2$ (**2-K**, 112 mg, 0.0758 mmol, 67.1%) was obtained after washing with cold pentane and drying under vacuum. ^1H NMR (400 MHz, THF- d_8) δ 7.01 (s, 4H, Ar-*H*), 6.86 (t, $J = 7.2$ Hz, 4H, Ar-*H*), 2.39 – 2.32 (m, 8H, CH(CH₃)₂), 2.20 (s, 12H, Ar-CH₃), 1.45 (s, 12H, Ar₂C(CH₃)₂), 1.27 (q, $J = 7.2$ Hz, 24H, CH(CH₃)₂), 1.12 (q, $J = 7.2$ Hz, 24H, CH(CH₃)₂). ^{13}C NMR (101 MHz, THF- d_8) δ 156.58 (t, $J = 14.1$ Hz, Ar-C), 130.31 (t, $J = 5.1$ Hz, Ar-C), 130.09 (s, Ar-C), 129.61 (s, Ar-C), 124.78 (t, $J = 3.0$ Hz, Ar-C), 118.73 (t, $J = 16.2$ Hz, Ar-C), 36.84 (s, Ar₂C(CH₃)₂), 32.94 (s, Ar₂C(CH₃)₂), 26.37 (s, CH(CH₃)₂), 20.84 (s, Ar-CH₃), 20.00 (t, $J = 3.0$ Hz, CH(CH₃)₂), 18.83 (s, CH(CH₃)₂). ^{31}P NMR (162 MHz, THF- d_8) δ 47.9 (s). Anal. Calcd. for C₇₄H₁₂₀K₂N₆Ni₂O₄P₄: C, 60.17; H, 8.19; N, 5.69. Found: C, 60.22; H, 8.24; N, 5.57. IR (KBr Pellet, cm⁻¹): $\nu_{\text{NN}} = 1946$.

Reaction of 2-K with benzene. In an NMR tube equipped with a J-Young valve, a red solution of **2-K** (8.6 mg, 5.8 mmol) in 0.6 mL of benzene- d_6 was taken out of the dry-box and shaken at room temperature for 12 hrs. As monitored by ^{31}P NMR spectroscopy, no reaction occurs under ambient conditions, but new species appear when the reaction mixture was heated at 40°C for 12 hrs. The resulting mixture contains a starting material **2-K** (64%) with **3-D** (14%), **4-C₆D₅** (14%) and an unknown species (8%). The identity of the products was confirmed by a comparison of its ^1H and ^{31}P NMR data with those of an authentic sample of **3-D** and **4-C₆D₅**.

Synthesis of $\{(\text{acriPNP})\text{Ni}-(\text{N}_2)-\text{Li}(\text{THF})_2\}_2$ (2-Li**).** After lithium (11 mg, 1.6 mmol) was added to a solution of naphthalene (210 mg, 1.64 mmol) in 10 mL of THF, the reaction mixture was stirred for 3 hrs at room temperature. The resulting lithium naphthalenide solution was filtered away and added dropwise to a solution of (acriPNP)Ni•C₁₀H₈ (1056 mg, 1.611 mmol) in 20 mL of THF at -35°C with stirring. The reaction mixture was gradually warmed to room temperature resulting in a color change from reddish brown to red. After stirring for additional 30 min, the reaction mixture was filter through Celite, and the volatiles were removed under vacuum. The resulting residue was dissolved in 50 mL of pentane/THF (5:1), and the solution was cooled to -35°C . A red crystalline solid was precipitated out after two days. An analytically pure material $\{(\text{acriPNP})\text{Ni}-(\text{N}_2)-\text{Li}(\text{THF})_2\}_2$ (**2-Li**, 808 mg, 0.572 mmol, 71.0 %) was obtained after washing with cold pentane and drying under vacuum. ^1H NMR (400 MHz, THF- d_8) δ 7.01 (s, 4H, Ar-*H*), 6.86 (t, $J = 7.2$ Hz, 4H, Ar-*H*), 2.39 – 2.33 (m, 8H, CH(CH₃)₂), 2.20 (s, 12H, Ar-CH₃), 1.45 (s, 12H, Ar₂C(CH₃)₂), 1.26 (q, $J = 7.2$ Hz, 24H, CH(CH₃)₂), 1.10 (q, $J = 7.2$ Hz, 24H, CH(CH₃)₂). ^{13}C NMR (101 MHz, THF- d_8) δ 156.58 (t, $J = 14.1$ Hz, Ar-C), 130.31 (t, $J = 5.1$ Hz, Ar-C), 130.09 (s, Ar-C), 129.61 (s, Ar-C), 124.78 (t, $J = 3.0$ Hz, Ar-C), 118.79 (t, $J = 16.2$ Hz, Ar-C), 36.66 (s, Ar₂C(CH₃)₂), 32.76 (s, Ar₂C(CH₃)₂), 26.21 (s, CH(CH₃)₂), 20.67 (s, Ar-CH₃), 19.81 (t, $J = 3.0$ Hz, CH(CH₃)₂), 18.64 (s, CH(CH₃)₂). ^{31}P NMR (162 MHz, THF- d_8) δ 47.6 (s). Anal. Calcd. for C₇₄H₁₂₀Li₂N₆Ni₂O₄P₄: C, 62.90; H, 8.56; N, 5.95. Found: C, 62.95; H, 8.84; N, 5.83. IR (KBr Pellet, cm⁻¹): $\nu_{\text{NN}} = 1944$.

Reaction of 2-Li with benzene. In an NMR tube equipped with a J-Young valve, a red solution of **2-Li** (8.0 mg, 5.7 mmol) in 0.6 mL of benzene- d_6 was taken out of the dry-box and shaken at room temperature for 12 hrs. As monitored by ^{31}P NMR spectroscopy, no reaction occurs under ambient conditions, but new species appear when the reaction mixture was heated at 40°C for 12 hrs. The resulting mixture contains **3-D** (11%), **4-C₆D₅** (60%) and (acriPNP)Li(THF) (29%). The

identity of the products was confirmed by a comparison of its ^1H and ^{31}P NMR data with those of an authentic sample of **3-D** and **4-C₆D₅** and ($^{\text{acri}}\text{PNP}$)Li(THF).¹

Reaction of ($^{\text{acri}}\text{PNP}$)Ni-L (L = H, Cl or empty) with excess sodium in benzene. After sodium (85~90 mg, 3.7~3.9 mmol) was added to a solution of ($^{\text{acri}}\text{PNP}$)Ni-L (L = H, Cl or empty) (0.187~0.189 mmol) in 15 mL of benzene, the reaction mixture was stirred at room temperature. Aliquots were taken at 1.0, 1.5 and 2.0 hrs to monitor the reaction with ^{31}P NMR spectroscopy (**Figure S57**). After stirring for 2 hrs, the reaction mixture was filtered through Celite. The filtrate was dried under vacuum to remove the volatiles. The product **4-Ph** (107~111 mg, 0.178~0.184 mmol, 95.2~97.3%) was isolated as a yellow powder after drying under vacuum. The identity of the product was confirmed by a comparison of its ^1H and ^{31}P NMR data with those of an authentic sample of **4-Ph**.

Reaction of ($^{\text{acri}}\text{PNP}$)Ni-L (L = H, Cl or empty) with excess sodium in toluene. After sodium (83~90 mg, 3.6~3.9 mmol) was added to a solution of ($^{\text{acri}}\text{PNP}$)Ni-L (L = H, Cl or empty) (0.176~0.189 mmol) in 15 mL of toluene, the reaction mixture was stirred at room temperature. After stirring for 2 hrs, the reaction mixture was filtered through Celite. The filtrate was dried under vacuum to remove the volatiles. The mixture of **4-mTol** and **4-pTol** (101~112 mg, 0.164~0.181 mmol, 93.2~95.8%) was isolated as a yellow powder after drying under vacuum. The identity of the products was confirmed by a comparison of its ^1H and ^{31}P NMR data with those of an authentic sample of **4-mTol** and **4-pTol**.

Reaction of ($^{\text{acri}}\text{PNP}$)Ni-L (L = H or Cl) with sodium and excess naphthalene. After sodium (11~12 mg, 0.48~0.52 mmol) was added to a solution of ($^{\text{acri}}\text{PNP}$)Ni-L (L = H or Cl) (0.217~0.237 mmol) in 25 mL of pentane/THF (20:1), the reaction mixture was stirred at room temperature resulting in a color change to red brown. After stirring for 6 hrs naphthalene (557~609 mg, 4.35~4.75 mmol) was added, and the reaction mixture was further stirred for 2 days. After the volatiles were removed under vacuum, the remaining solid was dissolved in benzene. The solution was filtered through Celite, and the filtrate was dried under vacuum. The product **4-Naph** (101~103 mg, 0.154~0.157 mmol, 66.2~71.4%) was isolated as a yellow powder after washing with pentane and drying under vacuum. The identity of the product was confirmed by a comparison of its ^1H and ^{31}P NMR data with those of an authentic sample of **4-Naph**.

Reaction of ($^{\text{acri}}\text{PNP}$)Ni-L (L = H or Cl) with sodium and excess anthracene. After sodium (11~13 mg, 0.48~0.57 mmol) was added to a solution of ($^{\text{acri}}\text{PNP}$)Ni-L (L = H or Cl) (0.214~0.259 mmol) in 25 mL of pentane/THF (20:1), the reaction mixture was stirred at room temperature resulting in a color change to red brown. After stirring for 6 hrs anthracene (763~916 mg, 4.28~5.14 mmol) was added, and the reaction mixture was further stirred for 2 days. After the volatiles were removed under vacuum, the remaining solid was dissolved in benzene. The solution was filtered through Celite, and the filtrate was dried under vacuum. The product **4-Anth** (71~87 mg, 0.10~0.12 mmol, 47~48%) was isolated as a yellow powder after washing with pentane and drying under vacuum. The identity of the product was confirmed by a comparison of its ^1H and ^{31}P NMR data with those of an authentic sample of **4-Anth**.

Kinetic Isotope Effect Experiments

Determination of kinetic isotope effect from the parallel reactions. **2** (19 mg, 0.013 mmol) was treated with benzene or benzene-*d*₆ to bring the final volume of 2 mL (0.0065 M of **2**). Around 0.6

mL of the resulted solution was placed into the NMR tube with a J-Young valve. The solution was stored frozen in acetone/dry ice bath until retrieved to perform ^{31}P NMR kinetic studies at 298 K. After the reaction mixture was warmed to room temperature, the spectra were collected with 3 min intervals over the course of 12 min with benzene and 18 min with benzene- d_6 . Integration of the peak of the starting **2** was used for plotting the $\ln[2]$ vs. time graph (**Figure S58**). According to the kinetic study, the KIE was calculated as follows: $k_H/k_D = 0.00354 \text{ s}^{-1}/0.00101 \text{ s}^{-1} = 3.5$.

Determination of kinetic isotope effect from an intermolecular competition. After **2** (26 mg, 0.018 mmol) was dissolved in 4 mL of benzene/benzene- d_6 (1:1), the reaction mixture was stirred at room temperature. After stirring for 15 min, the resulting products were confirmed by their ^1H and ^{31}P NMR spectra (**Figure S49** and **S50**). The intermolecular KIE was derived from the relative integration of a peak at 7.70 ppm (those associated with the Ar- H proton of phenyl ligand in **4-Ph**, 2.00) vs. a peak at 6.90 ppm (those associated with the Ar- H proton of $^{\text{acri}}\text{PNP}$ ligand in **4-Ph** and **4-C $_6$ D $_5$** , 2.60) in ^1H NMR spectrum. The KIE was calculated as follows: $[\text{P}_\text{H}]/[\text{P}_\text{D}] = 2.00/(2.60-2.00) = 3.3$.

Synthesis of ($^{\text{acri}}\text{PNP}$)Ni(CH=CH $_2$) (5**) from **4-Ph** and **15-crown-5**.** Sodium metal (28.8 mg, 1.25 mmol) was added to a solution of naphthalene (28.5 mg, 0.222 mmol, 2.78 equiv) in THF (3 mL), the reaction mixture was stirred for 3 hrs at room temperature. The resulting dark green sodium naphthalenide solution was cooled to -35°C for 10 minutes. In a separate vial, a solution of **4-Ph** (22.7 mg, 0.0799 mmol) and **15-crown-5** (32.6 mg, 0.148 mmol, 1.85 equiv) in THF (3 mL) was also cooled to -35°C for 30 minutes. Next the sodium naphthalenide solution was filtered away from the remaining sodium and added dropwise over one minute to the **4-Ph** solution while stirring. The solution immediately darkened to give a dark brown solution. After 20 hrs, the solution color changed to a light yellow brown. The crude ^{31}P NMR spectrum indicated the presence of 61% **5**, 37% **3** and 2% unknown species (**Figure S51**). The volatiles were then removed under vacuum.

Isolation of tetraethylene glycol disodium salt. Pentane (2 mL) was added to the crude residue and removed under vacuum. This procedure was repeated and then pentane (10 mL) was added to the residue again. A Celite column (1 \times 0.6 cm) was prepared with pentane and the reaction mixture was added. A yellow fraction was collected and the Celite was washed with pentane (5 mL). The resulting yellow fraction was set aside (see below for isolation of **5**). Next, the column was then washed with THF (2 mL) to give a brown fraction, which was reduced to a brown residue under vacuum. The brown residue was dissolved in a 4:1 mixture of pentane:benzene (5 mL) and stored at -35°C for 16 hrs. The pale yellow solution was decanted from the resulting solid, washed three times with cold pentane (1 mL, -35°C) and dried under vacuum to give tetraethylene glycol disodium salt as an off-white residue $\text{Na}\{\text{O}(\text{C}_2\text{H}_4\text{O})_4\}\text{Na}$ (9.1 mg, 0.0382 mmol, 47.9% based on Ni). See **Figure S71** for comparison of NMR spectra to independently prepared sample.

*Isolation of **5**.* A silica column (3 \times 4 cm) was prepared in a 30 mL fritted Buchner funnel with pentane and the yellow pentane soluble fraction was added. A colorless fraction was eluted with pentane. The residue was identified as naphthalene by ^1H NMR and was discarded. Next a yellow fraction eluted with 10:1 pentane:benzene which was dried under vacuum to give **5** (12.3 mg, 0.0222 mmol, 59.0%) as a yellow-orange powder. ^1H NMR (400 MHz, C_6D_6) δ 7.15 (2 m overlap $\text{C}_6\text{D}_5\text{H}$, 3H, $^{\text{acri}}\text{PNP}$ Ar- H + Ni- CHCH_2), 6.90 (t, $J = 4.0$ Hz, 2H, $^{\text{acri}}\text{PNP}$ Ar- H), 5.89 (dtd, $J = 11.8$, 4.5, 2.5 Hz, 1H, Ni- CHCH_2), 5.49 (m, $J = 19.0$, 3.0 Hz, 1H, Ni- CHCH_2), 2.36 (sextet, $J = 2.8$ Hz, 4H, $\text{CH}(\text{CH}_3)_2$), 2.28 (s, 6H, $^{\text{acri}}\text{PNP}$ Ar- CH_3), 1.60 (s, 6H, $^{\text{acri}}\text{PNP}$ Ar $_2\text{C}(\text{CH}_3)_2$), 1.30 (q, $J = 7.4$

Hz, 12H, CH(CH₃)₂), 1.16 (q, *J* = 7.1 Hz, 12H, CH(CH₃)₂). ¹³C NMR (126 MHz, C₆D₆) δ 156.3 (t, *J* = 14.1 Hz, ^{acri}PNP Ar-C-N), 151.8 (t, *J* = 32.2 Hz, Ni-CH=CH₂), 130.7 (t, *J* = 5.4 Hz, ^{acri}PNP Ar-C), 130.2 (^{acri}PNP Ar-C), 129.8 (^{acri}PNP Ar-C), 124.8 (t, *J* = 3.4 Hz, ^{acri}PNP Ar-C), 122.0 (t, *J* = 6.0 Hz, CH=CH₂), 117.3 (t, *J* = 16.9 Hz, ^{acri}PNP Ar-C-P), 36.42 (Ar₂C(CH₃)₂), 34.00 (Ar₂C(CH₃)₂), 23.4 (t, *J* = 13.0 Hz, CH(CH₃)₂), 21.0 (Ar-CH₃), 18.6 (CH(CH₃)₂), 18.0 (CH(CH₃)₂). ³¹P NMR (162 MHz, C₆D₆) δ 40.8. UV-vis [THF, nm (L mol⁻¹ cm⁻¹)]: 348, 353, 395 (sh), 465 (sh). ESI-MS {(^{acri}PNP)Ni(CH=CH₂)}⁺: calcd: 553.25 (100.0%), 554.26 (33.5%), 555.25 (38.5%), 556.25 (12.9%), 557.25 (5.3%), 558.25 (1.8%), 559.25 (1.4%); found: 553.25 (100.0%), 554.25 (33.76%), 555.17 (42.13%), 556.17 (15.00%), 557.17 (7.18%), 558.17 (1.94%), 559.17 (1.63%). Anal. Calcd. for C₃₁H₄₇NNiP₂: C, 67.17; H, 8.55; N, 2.53; Found: C, 67.19; H, 8.56; N, 2.57. IR (KBr Pellet, cm⁻¹): ν_{Ar} = 1604, 1593, 1546. X-ray quality crystals were grown by vapor diffusion of acetonitrile into a saturated toluene solution of **5** at -35 °C.

Synthesis of (^{acri}PNP)Ni(CH=CH₂) (5**) from 4-C₆D₅ and 15-crown-5.** The reaction above was repeated under analogous reaction and workup conditions using sodium metal (64.5 mg, 2.80 mmol) and naphthalene (30.6 mg, 0.239 mmol, 2.25 equiv) in THF (3 mL), and 4-C₆D₅ (64.4 mg, 0.106 mmol) and 15-crown-5 (58.8 mg, 0.267 mmol, 2.52 equiv) in THF (3 mL) to give **5** (27.3 mg, 0.0492 mmol, 46.5%). The identity of the product was confirmed by a comparison of its ¹H and ³¹P NMR data with those of an authentic sample of **5**.

Synthesis of (^{acri}PNP)Ni(CH=CH₂) (5**) from 4-Ph and glyme.** The reaction above was repeated under analogous reaction and workup conditions using sodium metal (60.9 mg, 2.54 mmol) and naphthalene (9.1 mg, 0.071 mmol, 2.1 equiv) in glyme (3 mL), and 4-Ph (19.8 mg, 0.0328 mmol) in THF (3 mL) to give **5** (9.6 mg, 0.017 mmol, 53%). NaOMe (2.0 mg, 0.037 mmol, 1.1 eq) was also isolated from the pentane insoluble fraction.

Synthesis of (^{acri}PNP)Ni(CH=CH₂) (5**) from 4-C₆D₅ and glyme.** The reaction above was repeated under analogous reaction conditions using sodium metal (39.0 mg, 1.70 mmol) and naphthalene (27.7 mg, 0.216 mmol, 2.70 equiv) in glyme (3 mL) and 4-C₆D₅ (60.2 mg, 0.0799 mmol) in THF (4 mL). The crude residue (before chromatography) was taken in C₆D₆ and a ³¹P NMR spectrum indicated the presence of 78% **5**, 17% **3**, and 5% unknown species. The workup above conditions gave **5** (32.6 mg, 0.0588 mmol, 59.5%).

Synthesis of (^{acri}PNP)Ni(CH=CH₂) (5**) from **2**, glyme, and PhLi.** PhLi (1.8 mg, 0.021 mmol) was dissolved in glyme (1 mL), which produced *in situ* methyl vinyl ether. The resulting solution was added to crystalline **2** (14.0 mg, 0.00969 mmol) at room temperature and the reaction mixture was stirred for 18 hrs. The workup conditions above were repeated to give **5** (7.9 mg, 0.014 mmol, 73%).

Synthesis of (^{acri}PNP)Ni(CH=CH₂) (5**) from **2**, 15-crown-5, and PhLi.** After PhLi (2.4 mg, 0.029 mmol) was added to the solution of 15-crown-5 (17.7 mg, 0.0804 mmol) in THF (1 mL), the reaction mixture turned a pale violet color, resulting in the formation of *in situ* vinyl ether. The reaction mixture was added to crystalline **2** (15.0 mg, 0.0104 mmol) at room temperature and the reaction was stirred for 5 hrs. A crude ³¹P NMR spectrum was taken (0.1 mL of THF-*d*₈ was added to facilitate locking) and indicated the presence of 73% **5**, 15% **3** and 12% **2** unknown species (**Figure S72**). The workup conditions above were repeated to give **5** (6.3 mg, 0.011 mmol, 55%).

Reaction of 2 and glyme. Glyme (0.1 mL) was added to **2** (26.4 mg, 0.0183 mmol) in THF (4 mL) at room temperature and the reaction was stirred for 18 hrs. The solvent was removed under vacuum and the reaction mixture was taken in C₆D₆. The crude ³¹P NMR spectrum of the reaction mixture showed a br singlet at -3.4 ppm (75%, likely (acriPNP)Na), doublet at 61.3 ppm (14%, **3**), singlet at 40.8 ppm (4%, (acriPNP)Ni(CH=CH₂)), **5**, 48.3 ppm (3%), 30.2 ppm (2%), 48.8 ppm (2%). The workup conditions described above did not result in a measurable yield of **5**.

Synthesis of (acriPNP)Ni(CH=CH₂) (5) from 2 and ethyl vinyl ether. Ethyl vinyl ether (12.0 mg, 0.166 mmol, 11.8 eq) in THF (1 mL) was added to **2** (20.3 mg, 0.0141 mmol) in THF (4 mL) at room temperature and the reaction was stirred for 18 hrs. The workup conditions above were repeated to give **5** (7.8 mg, 0.014 mmol, 50%).

Control experiments related to the synthesis of 5:

Reduction of 4-Ph in THF. The reaction above was repeated under analogous reaction conditions using sodium metal (18.5 mg, 0.804 mmol) and naphthalene (5.3 mg, 0.041 mmol, 4.0 equiv) in THF (3 mL) and (acriPNP)NiPh (6.2 mg, 0.010 mmol) in THF (2 mL). The reaction mixture retained the dark green color of the naphthalide solution for 4 hrs but faded to a brown solution after 18 hrs. The solvent was removed under vacuum and the reaction mixture was taken in C₆D₆. No vinyl complex (**5**) was observed in the crude ³¹P NMR spectrum. The crude ³¹P NMR spectrum of the reaction mixture showed a broad peak at 48.4 ppm (80% by integration, likely a Ni(0) species, **2**) was detected along with a peak at 39.3 ppm (20%, **4-Ph**).

Reaction of 1•C₁₀H₈ with glyme. To the solution of 1•C₁₀H₈ (4.5 mg, 0.0085 mmol) dissolved in THF (1 mL), glyme (0.1 mL) was added. After 20 hrs, volatiles were removed under vacuum and the reaction mixture was taken in C₆D₆. No vinyl complex (**5**) was detected in the crude ³¹P NMR spectrum.

Reaction of 1•C₁₀H₈ with ethyl vinyl ether. To the solution of 1•C₁₀H₈ (7.0 mg, 0.013 mmol) dissolved in THF (1 mL), ethyl vinyl ether (4.0 mg, 0.055 mmol, 4.3 equiv) was added. After 20 hrs, all volatiles were removed under vacuum and the reaction mixture was taken in C₆D₆. No vinyl complex (**5**) was detected in the crude ³¹P NMR spectrum.

Reaction of 1•C₁₀H₈ with glyme and PhLi. To the solution of 1•C₁₀H₈ (8.5 mg, 0.016 mmol) dissolved in THF (1 mL), the mixture of PhLi (1.4 mg, 0.017 mmol, 1.0 equiv) and glyme (0.5 mL) was added. After 20 hrs, all volatiles were removed under vacuum and the reaction mixture was taken in C₆D₆. No vinyl complex (**5**) was detected in the crude ³¹P NMR spectrum.

Synthesis of (acriPNP)Ni(CH=CH₂) (5) from (acriPNP)NiCl and ethyl vinyl ether with magnesium powder. Ethyl vinyl ether (50.0 mg, 0.693 mmol, 3.90 equiv) was added to (acriPNP)NiCl (100.4 mg, 0.178 mmol) in THF (5 mL). Magnesium powder (112.9 mg, 4.65 mmol, 26.1 equiv) was added to reaction, which was stirred for 24 hrs at room temperature. The workup conditions above were repeated to give **5** (92.3 mg, 0.166 mmol, 93.5%). The identity of the product was confirmed by a comparison of its ¹H and ³¹P NMR data with those of an authentic sample of **5**.

Stability test of 1•C₁₀H₈ in the presence of NaBAr^F₄. To a solution of 1•C₁₀H₈ (18 mg, 0.027 mmol) in C₆D₆, a solution of NaBAr^F₄ (23 mg, 0.027 mmol) in THF-*d*₈ was added and the reaction

mixture was monitored by ^1H NMR spectroscopy resulting that 1 is stable in the C_6D_6 at room temperature as well as elevated temperature at $60\text{ }^\circ\text{C}$ for over 24 hrs.

Figure S1. ^1H NMR spectrum of $\{(\text{acriPnP})\text{Ni}-(\text{N}_2)\text{-Na}(\text{THF})_2\}_2$ (**2**) in $\text{THF-}d_8$ at room temperature (●: THF, ●: pentane).

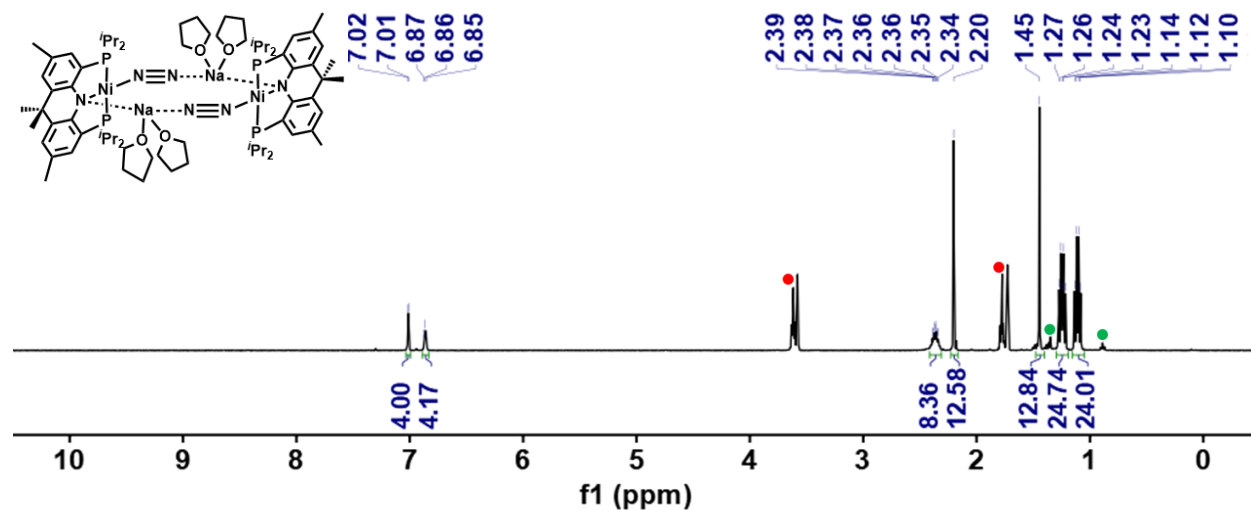


Figure S2. ^{13}C NMR spectrum of $\{(\text{acriPnP})\text{Ni}-(\text{N}_2)\text{-Na}(\text{THF})_2\}_2$ (**2**) in $\text{THF-}d_8$ at room temperature.

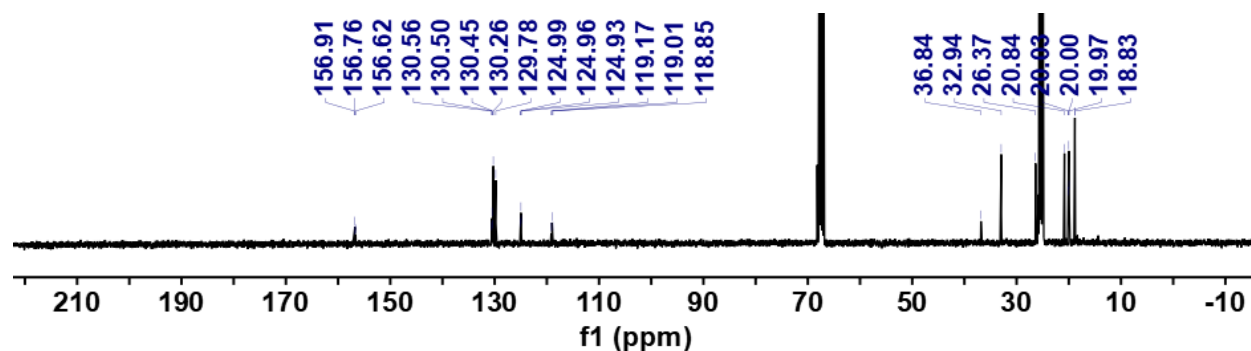


Figure S3. ^{31}P NMR spectrum of $\{(\text{acriPnP})\text{Ni}-(\text{N}_2)\text{-Na}(\text{THF})_2\}_2$ (**2**) in $\text{THF-}d_8$ at room temperature.

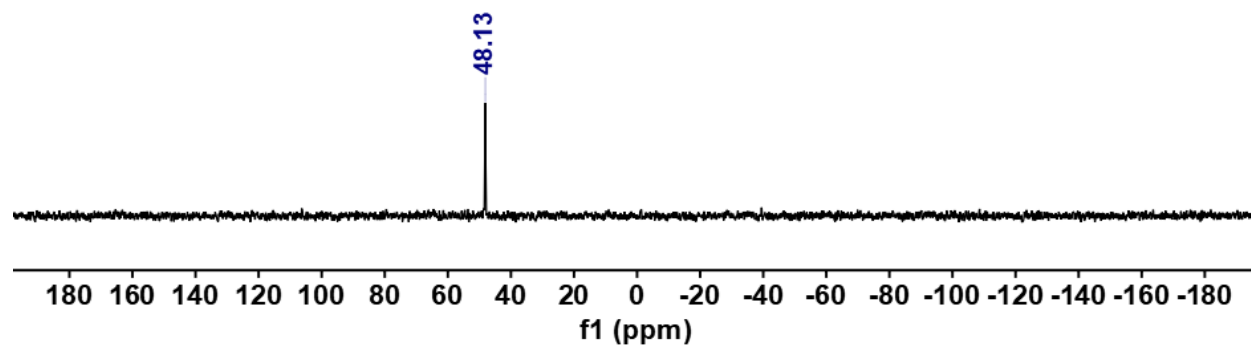


Figure S4. Single-pulse ^{31}P NMR spectrum of $(^{\text{acri}}\text{PNP})\text{NiH}$ (**3**) in C_6D_6 at room temperature. 2 equivalents of triphenylphosphine oxide was added as an internal standard (●: **3**, ●: triphenylphosphine oxide).

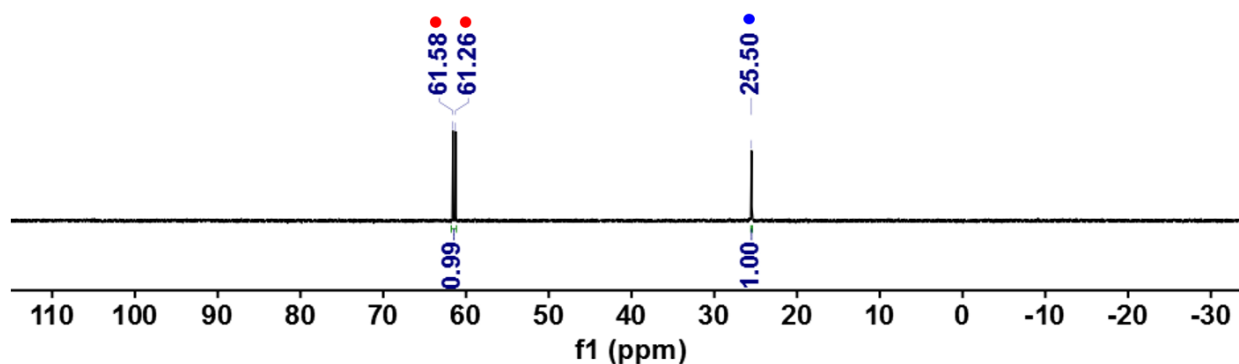


Figure S5. Single-pulse ^{31}P NMR spectra (in C_6D_6 at room temperature) of the reaction mixture of $\{(^{\text{acri}}\text{PNP})\text{Ni}-(\text{N}_2)-\text{Na}(\text{THF})_2\}_2$ (**2**) with benzene for (a) 15 min and (b) 24 hr.

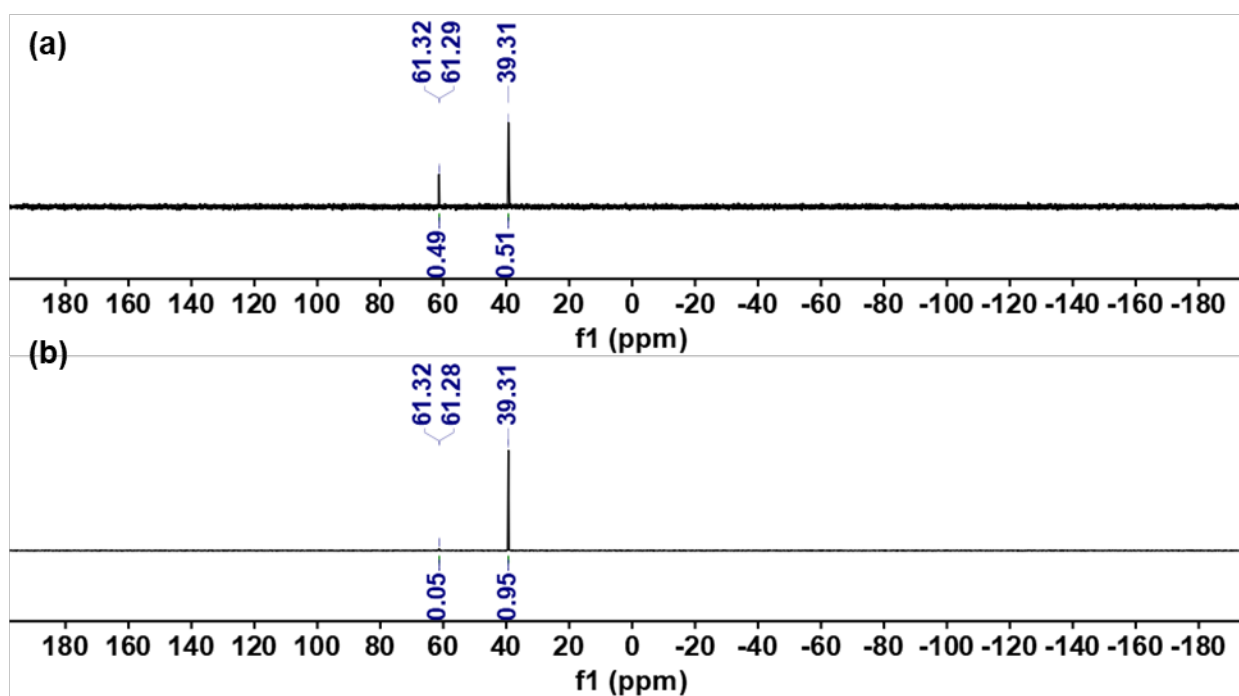


Figure S6. Single-pulse ^{31}P NMR spectra (in C_6D_6 at room temperature) of the reaction of **2** in 5 mL of benzene for (a) 15 min and (b) 24 hrs (●: **3**, ●: **4-Ph**, ●: triphenylphosphine oxide). 4 equivalents of triphenylphosphine oxide was added as an internal standard.

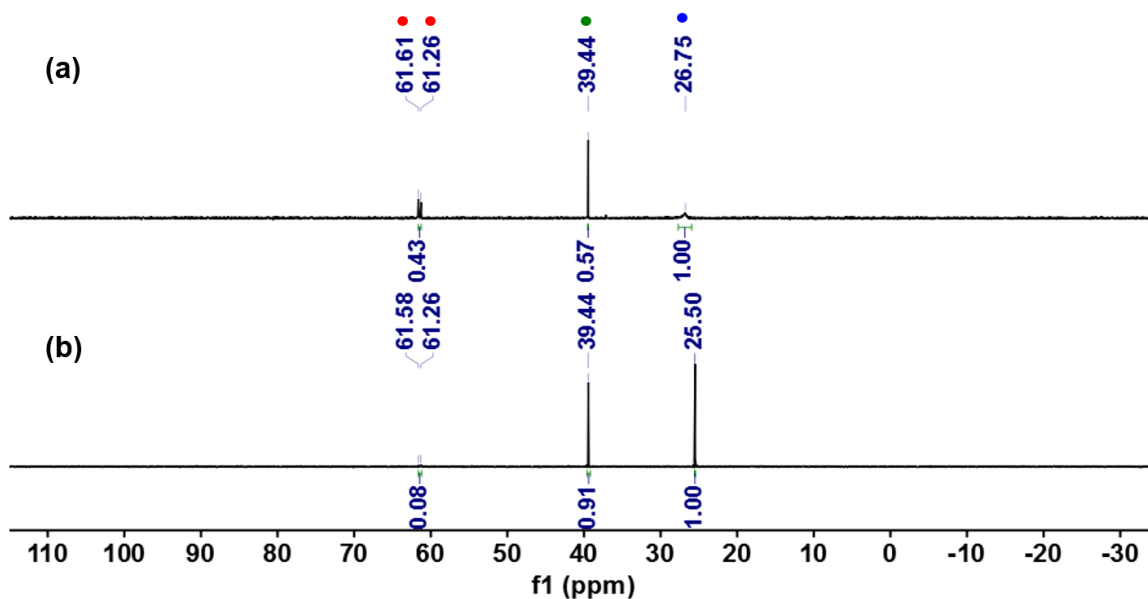


Figure S7. Single-pulse ^{31}P NMR spectrum (in C_6D_6 at room temperature) of the reaction of **2** with 20 equivalents of benzene in 10 mL of pentane for 48 hrs at room temperature (●: **3**, ●: **4-Ph**, ●: triphenylphosphine oxide). 4 equivalents of triphenylphosphine oxide were added as an internal standard.

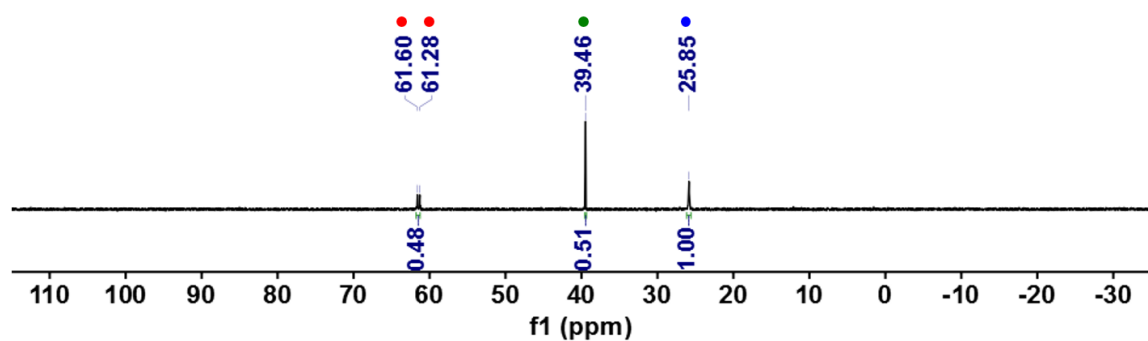


Figure S8. ^1H NMR spectra of a mixture of ($^{\text{acri}}\text{PNP}$)NiH (**3**), ($^{\text{acri}}\text{PNP}$)NiPh (**4-Ph**), OPPh_3 and naphthalene in C_6D_6 at room temperature collected after mixing for (a) 0 hr, (b) 12 hrs and (c) 24 hrs at room temperature (●: **3**, ●: **4-Ph**, ●: triphenylphosphine oxide, ●: C_{10}H_8). Triphenylphosphine oxide was added as an internal standard.

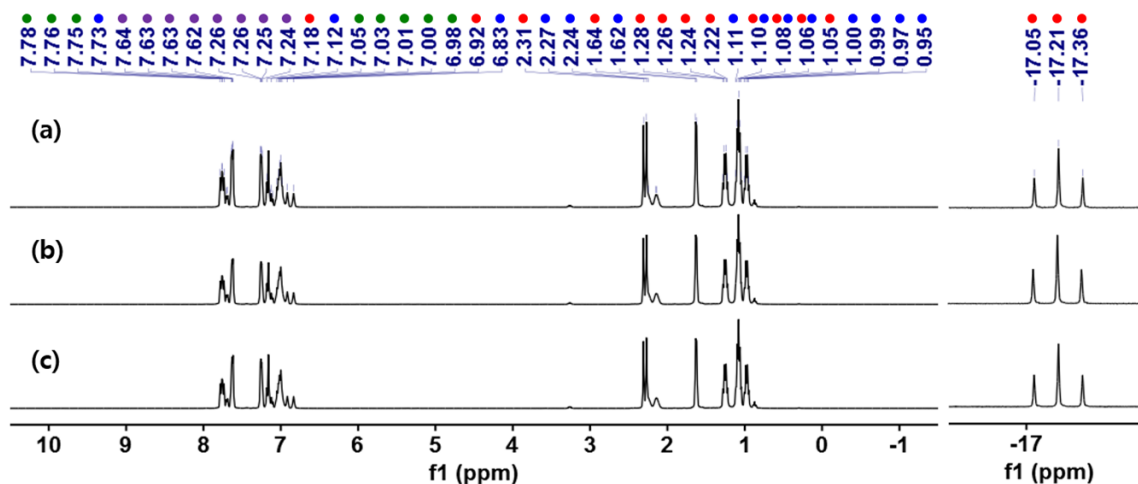


Figure S9. Single-pulse ^{31}P NMR spectra of a mixture of ($^{\text{acri}}\text{PNP}$)NiH (**3**), ($^{\text{acri}}\text{PNP}$)NiPh (**4-Ph**), OPPh_3 and naphthalene in C_6D_6 at room temperature collected after mixing for (a) 0 hr, (b) 12 hrs and (c) 24 hrs at room temperature (●: **3**, ●: **4-Ph**, ●: triphenylphosphine oxide). Triphenylphosphine oxide was added as an internal standard.

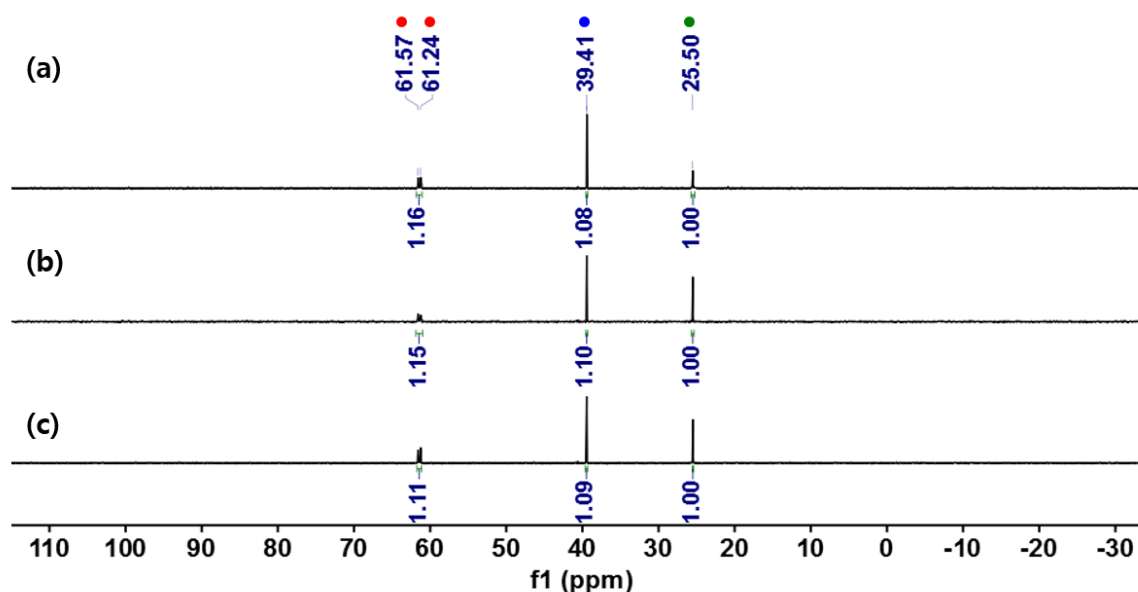


Figure S10. ^1H NMR spectra of a mixture of $(^{\text{acri}}\text{PNP})\text{NiH}$ (**3**), $(^{\text{acri}}\text{PNP})\text{NiPh}$ (**4-Ph**), OPPh_3 and naphthalene in C_6D_6 at room temperature collected after heating for (a) 0 hr, (b) 12 hrs and (c) 24 hrs at $60\text{ }^\circ\text{C}$ (●: **3**, ●: **4-Ph**, ●: triphenylphosphine oxide, ●: C_{10}H_8). Triphenylphosphine oxide was added as an internal standard.

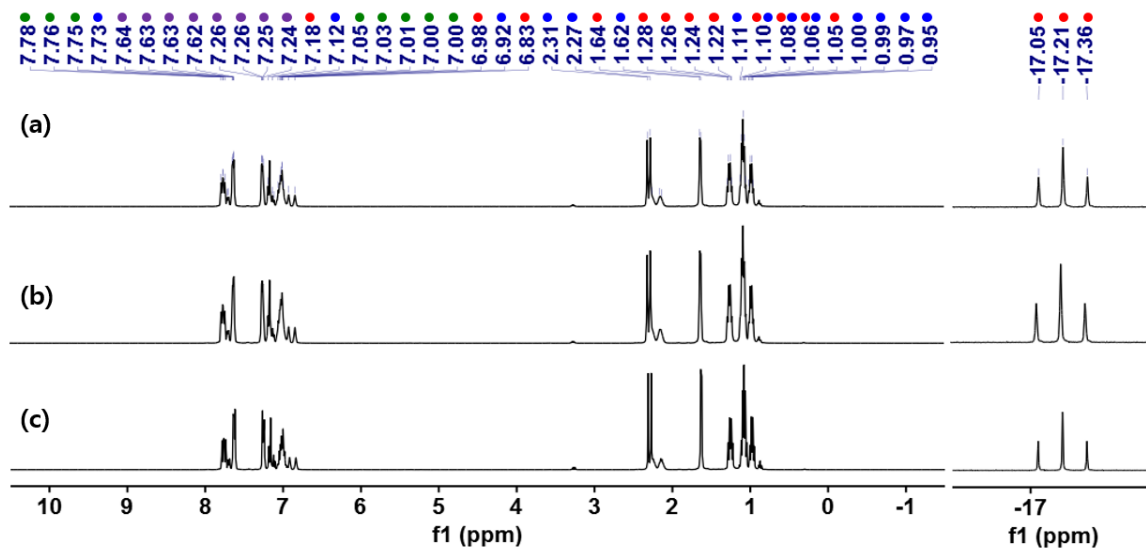


Figure S11. Single-pulse ^{31}P NMR spectra of a mixture of $(^{\text{acri}}\text{PNP})\text{NiH}$ (**3**), $(^{\text{acri}}\text{PNP})\text{NiPh}$ (**4-Ph**), OPPh_3 and naphthalene in C_6D_6 at room temperature collected after heating for (a) 0 hr, (b) 12 hrs and (c) 24 hrs at $60\text{ }^\circ\text{C}$ (●: **3**, ●: **4-Ph**, ●: triphenylphosphine oxide). Triphenylphosphine oxide was added as an internal standard.

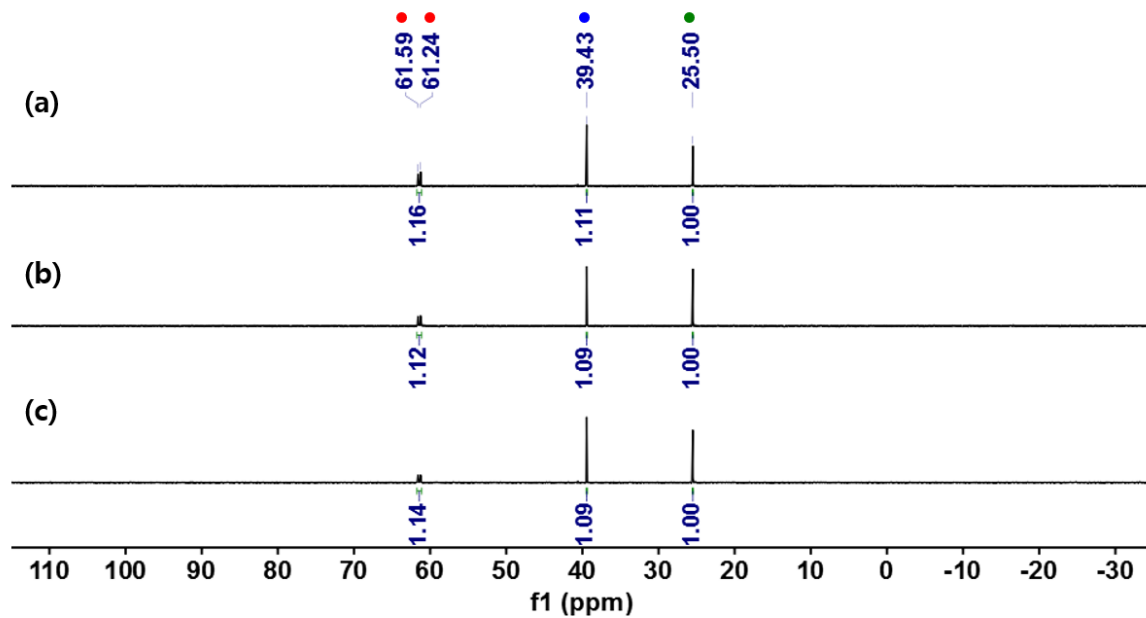


Figure S12. ^1H NMR spectrum of ($^{\text{acri}}\text{PNP}$)NiPh (**4-Ph**) in C_6D_6 at room temperature.

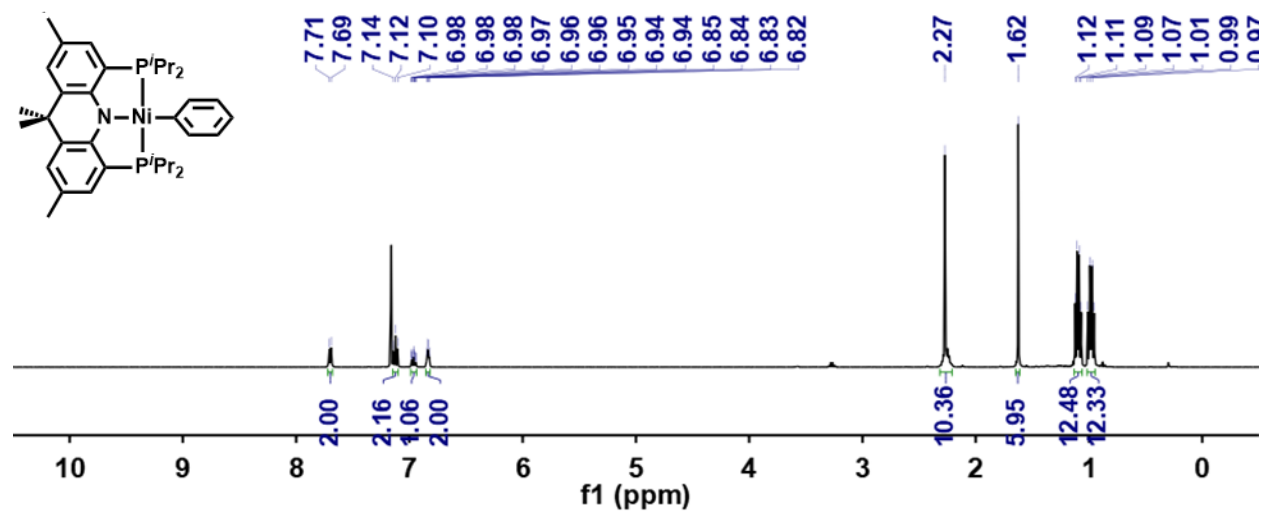


Figure S13. ^{13}C NMR spectrum of ($^{\text{acri}}\text{PNP}$)NiPh (**4-Ph**) in C_6D_6 at room temperature.

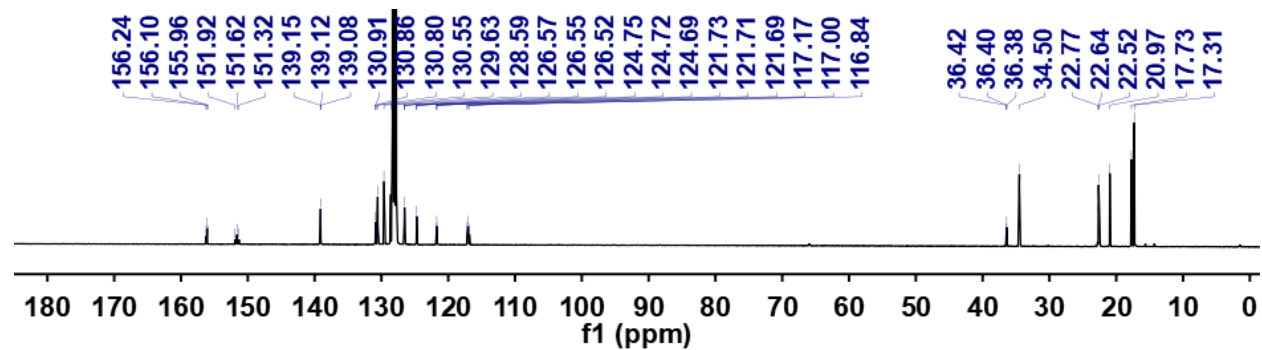


Figure S14. ^{31}P NMR spectrum of ($^{\text{acri}}\text{PNP}$)NiPh (**4-Ph**) in C_6D_6 at room temperature.

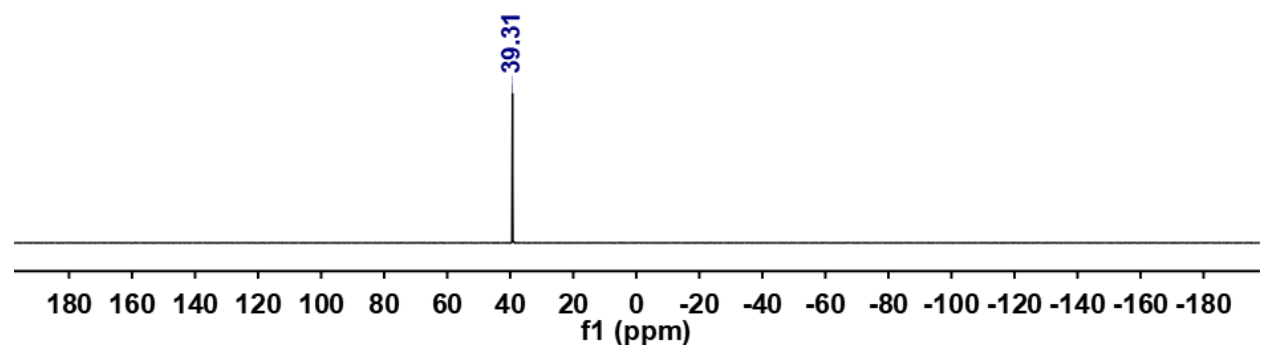


Figure S15. ^1H NMR spectrum of sodium phenoxide in $\text{DMSO-}d_6$ at room temperature.

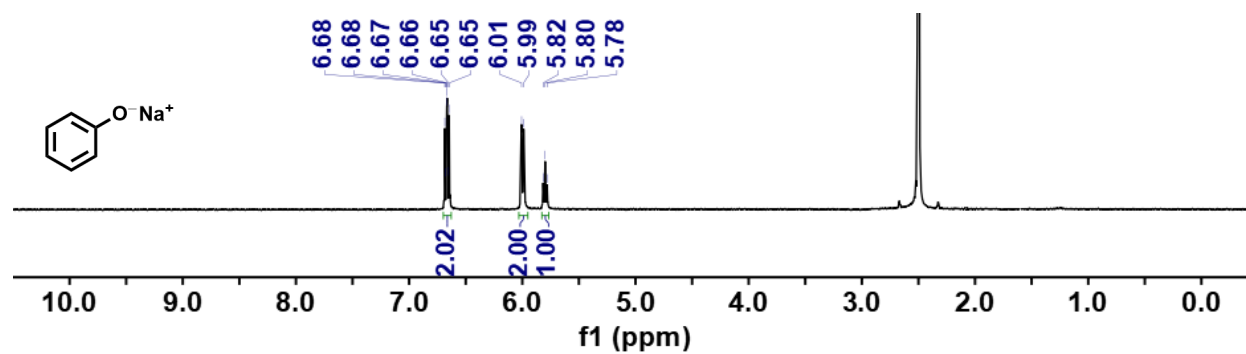


Figure S16. ^1H NMR spectrum of sodium anilide in THF/ C_6D_6 at room temperature (●: THF, ●: diethyl ether).

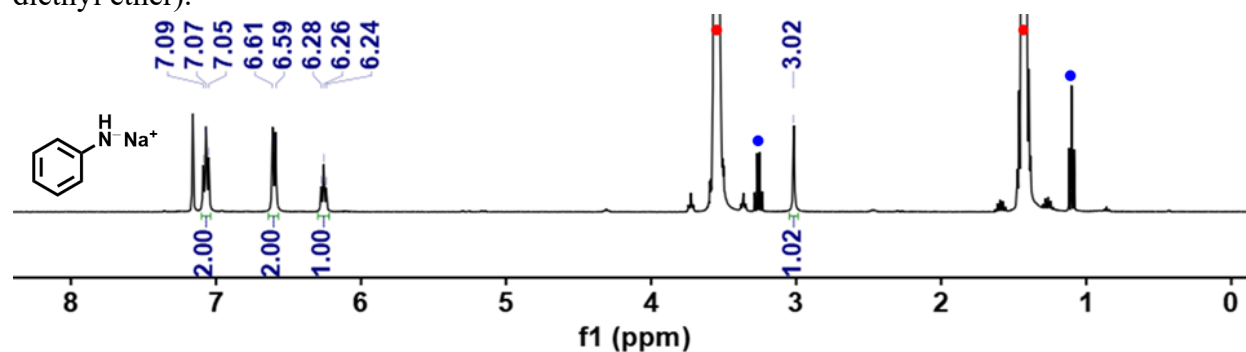


Figure S17. ^1H NMR spectra (in C_6D_6 at room temperature) of the reaction mixture of $\{(\text{acriPNP})\text{Ni}-(\text{N}_2)-\text{Na}(\text{THF})_2\}_2$ (**2**) with (a) 1 equivalent, (b) 2 equivalents and (c) 11 equivalents of triphenylmethane (● : **3**, ● : $(\text{acriPNP})\text{NiC}_6\text{H}_4\text{CHPh}_2$, ● : triphenylmethane).

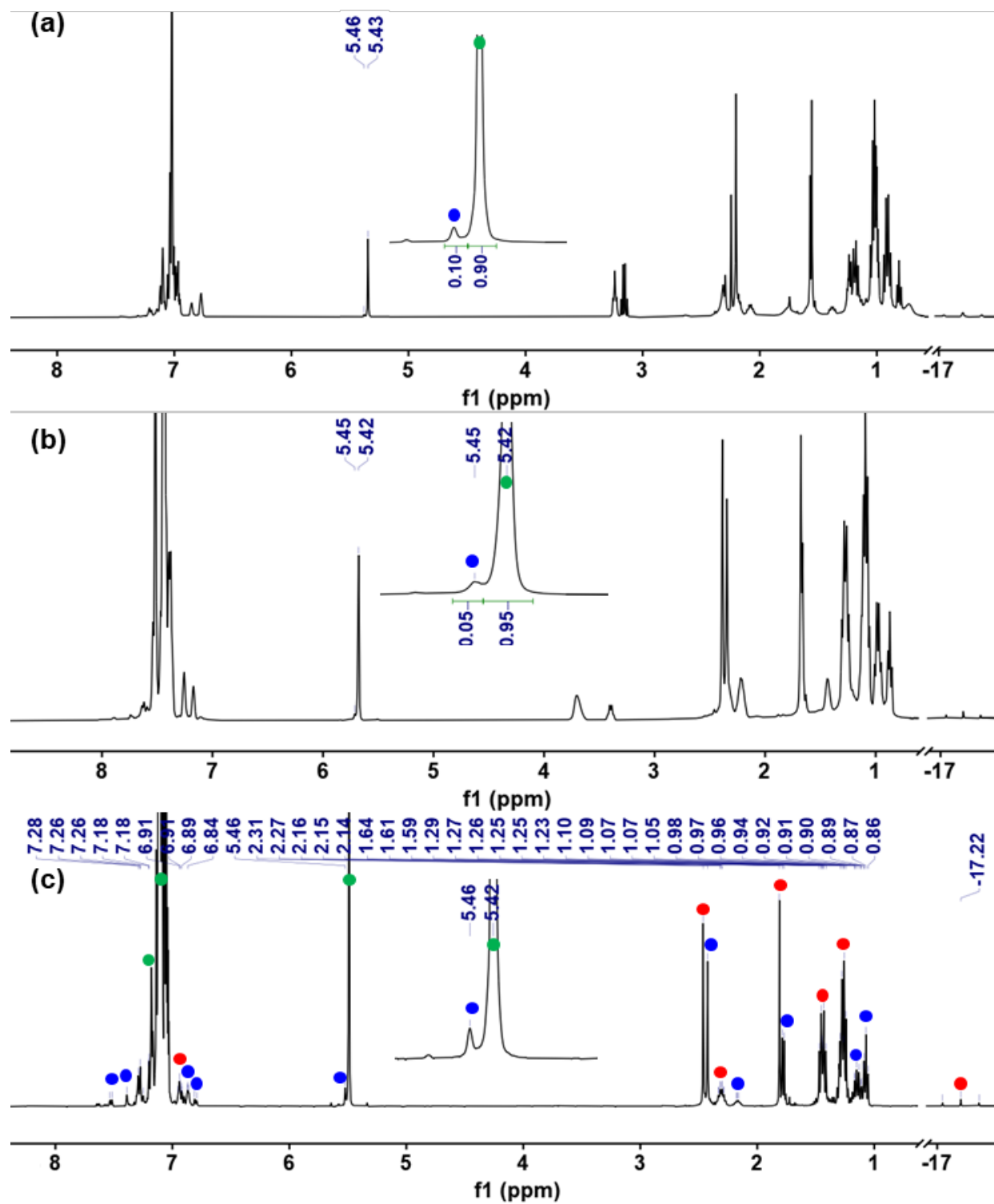


Figure S18. ^{31}P NMR spectra (in C_6D_6 at room temperature) of the reaction mixture of $\{(\text{acriPnP})\text{Ni}-(\text{N}_2)-\text{Na}(\text{THF})_2\}_2$ (**2**) with (a) 1 equivalent, (b) 2 equivalents and (c) 11 equivalents of triphenylmethane (● : **3**, ● : **3-D**, ● : $(\text{acriPnP})\text{NiC}_6\text{H}_4\text{CHPh}_2$, ● : **4-C₆D₅**).

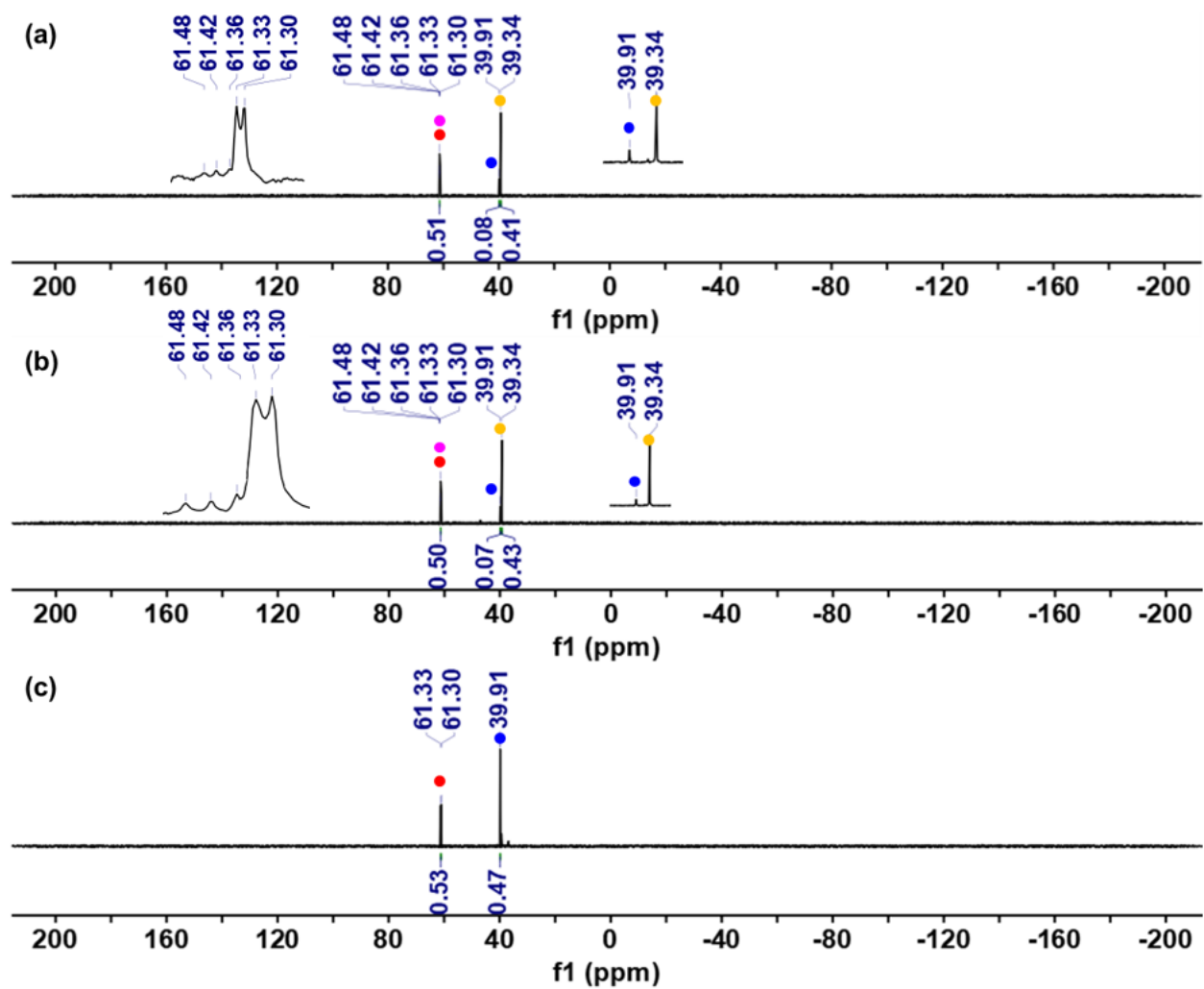


Figure S19. ^1H NMR spectrum of ($^{\text{acri}}\text{PNP}$)NiPh- d_5 (**4-C₆D₅**) in C_6D_6 at room temperature.

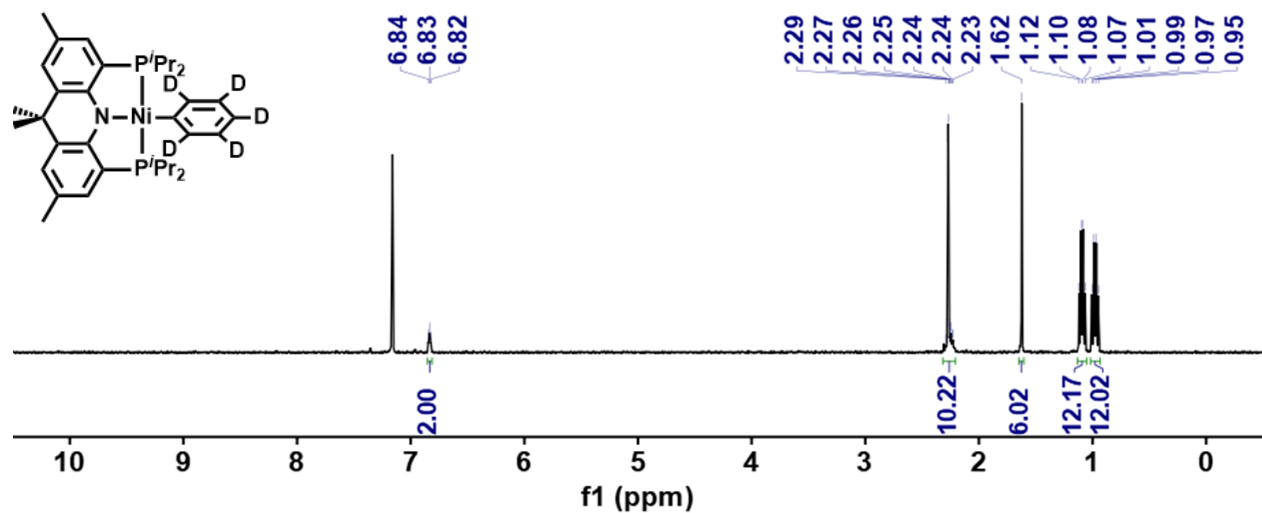


Figure S20. ^{31}P NMR spectrum of ($^{\text{acri}}\text{PNP}$)NiPh- d_5 (**4-C₆D₅**) in C_6D_6 at room temperature.

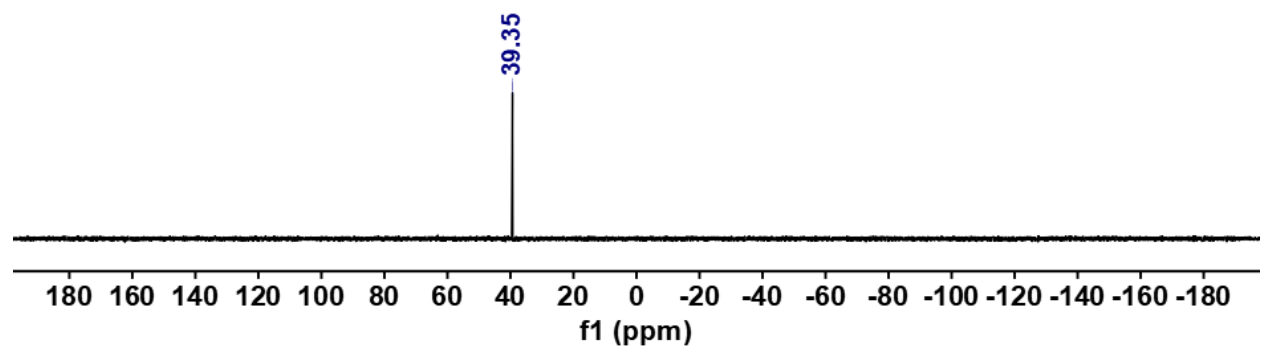


Figure S21. ^1H NMR spectrum of ($^{\text{acri}}\text{PNP}$)NiD (**3-D**) in C_6D_6 at room temperature (●: pentane).

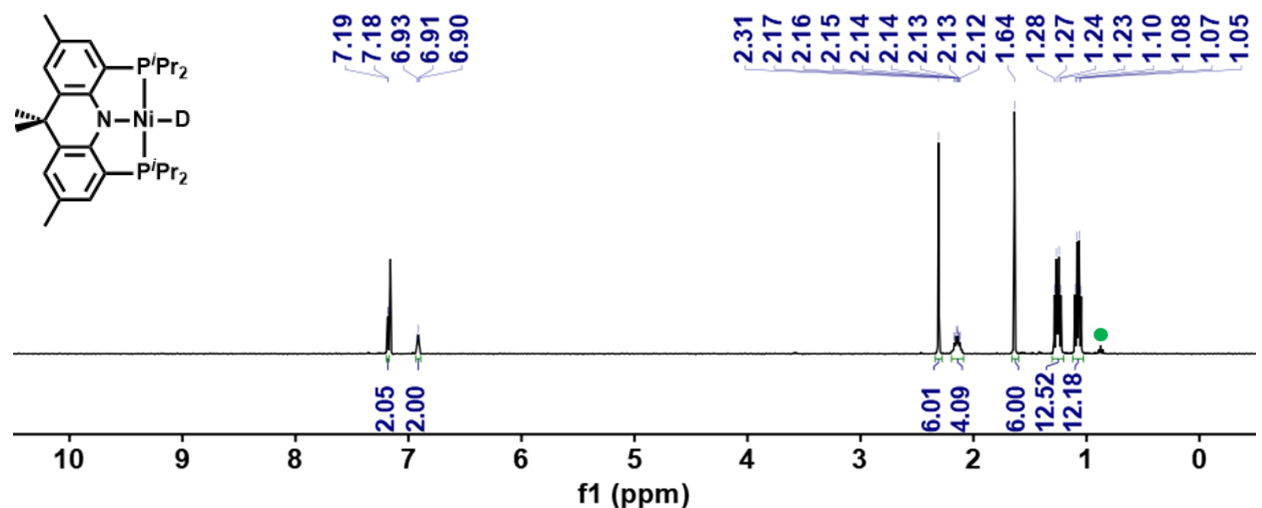


Figure S22. ^{31}P NMR spectrum of ($^{\text{acri}}\text{PNP}$)NiD (**3-D**) in C_6D_6 at room temperature.

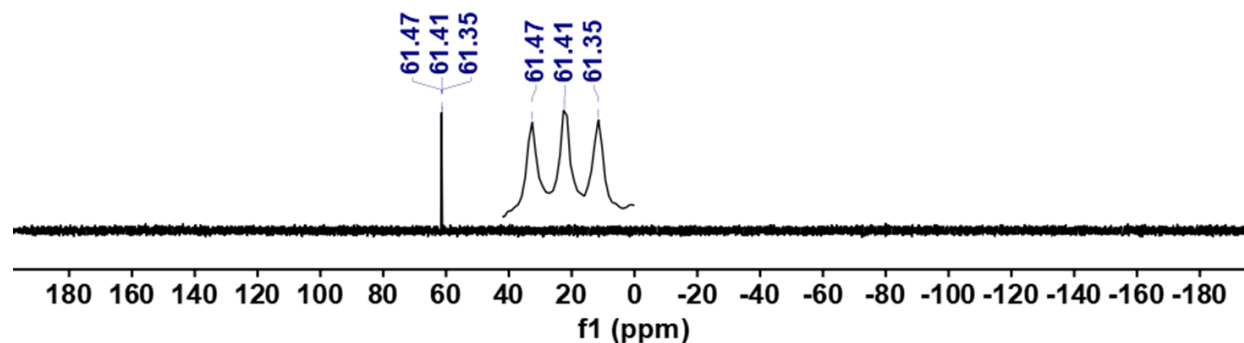


Figure S23. Single-pulse ^{31}P NMR spectrum (in C_6D_6 at room temperature) of the reaction mixture of $\{(\text{acriPNP})\text{Ni}-(\text{N}_2)-\text{Na}(\text{THF})_2\}_2$ (**2**) with naphthalene.

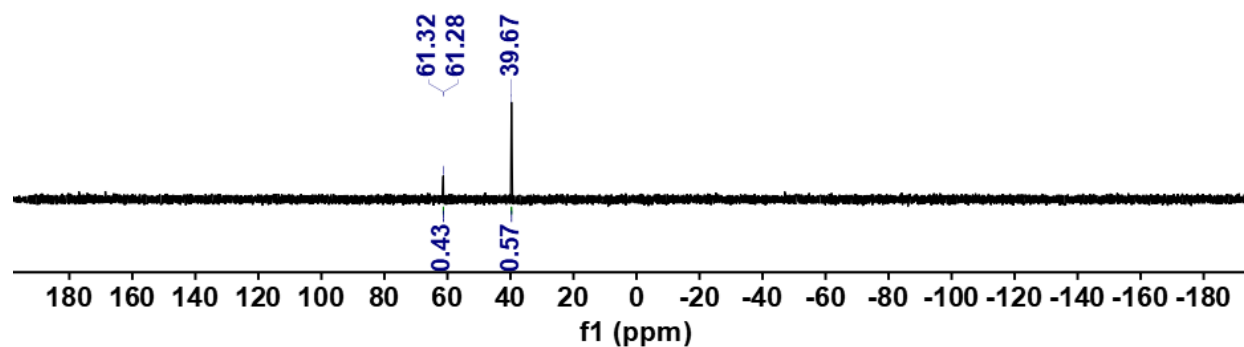


Figure S24. Single-pulse ^{31}P NMR spectrum (in C_6D_6 at room temperature) of the reaction of **2** with 20 equivalents of naphthalene in 10 mL of pentane for 48 hrs (●: **3**, ●: **4-Naph**, ●: **4-Ph**, ●: triphenylphosphine oxide). 4 equivalents of triphenylphosphine oxide were added as an internal standard.

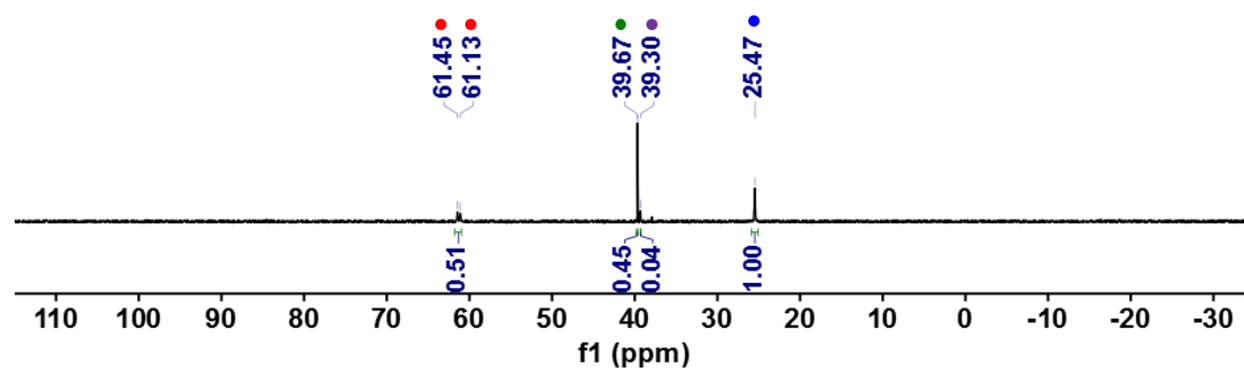


Figure S25. ^1H NMR spectrum of $(^{\text{acri}}\text{PNP})\text{Ni}(2\text{-naphthyl})$ (**4-Naph**) in C_6D_6 at room temperature.

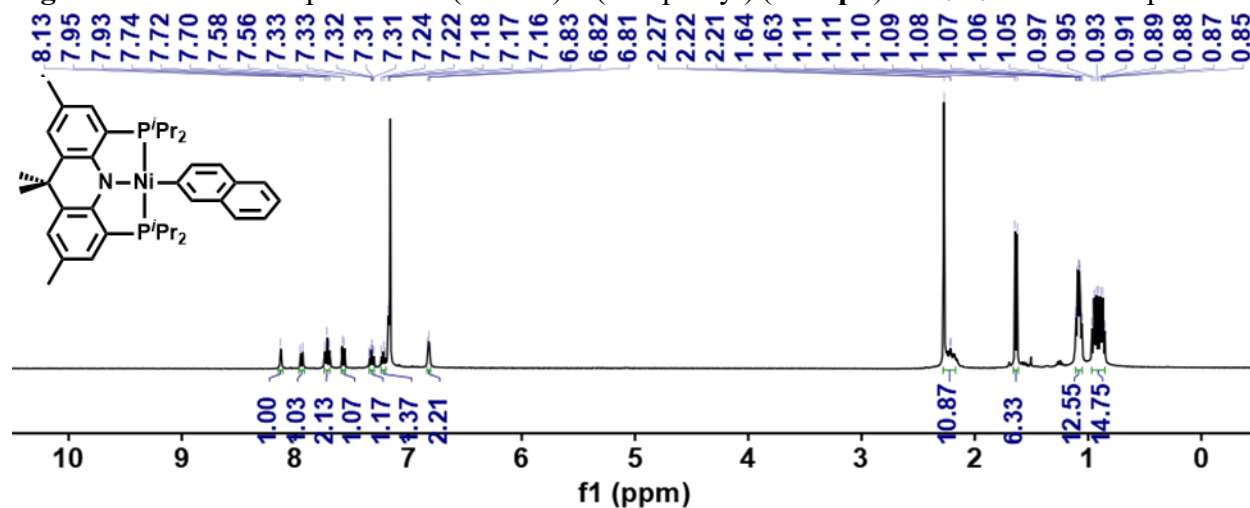


Figure S26. ^{13}C NMR spectrum of $(^{\text{acri}}\text{PNP})\text{Ni}(2\text{-naphthyl})$ (**4-Naph**) in C_6D_6 at room temperature.

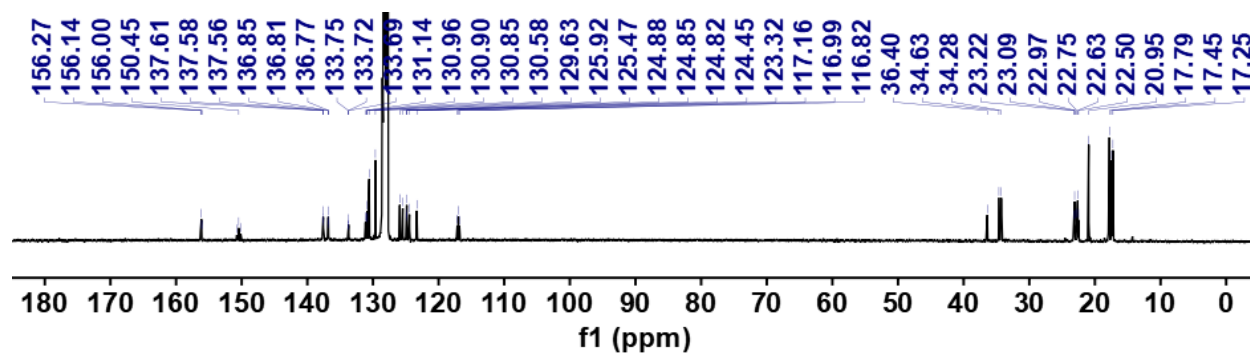


Figure S27. ^{31}P NMR spectrum of $(^{\text{acri}}\text{PNP})\text{Ni}(2\text{-naphthyl})$ (**4-Naph**) in C_6D_6 at room temperature.

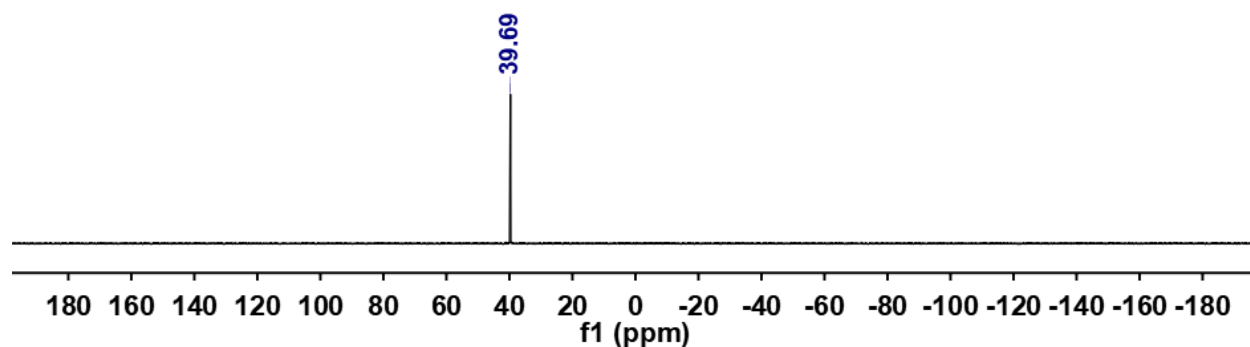


Figure S28. Single-pulse ^{31}P NMR spectrum (in C_6D_6 at room temperature) of the reaction mixture of $\{(\text{acriPNP})\text{Ni}-(\text{N}_2)-\text{Na}(\text{THF})_2\}_2$ (**2**) with anthracene.

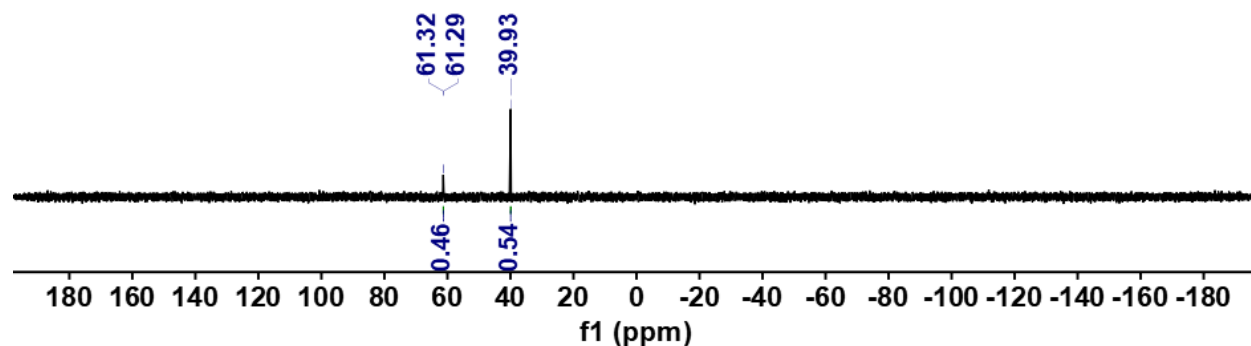


Figure S29. Single-pulse ^{31}P NMR spectrum (in $\text{C}_6\text{D}_6/\text{THF}$ at room temperature) of the reaction of **2** with 20 equivalents of anthracene in 10 mL of pentane for 48 hrs (●: **3**, ●: **4-Anth**, ●: triphenylphosphine oxide). 4 equivalents of triphenylphosphine oxide was added as an internal standard.

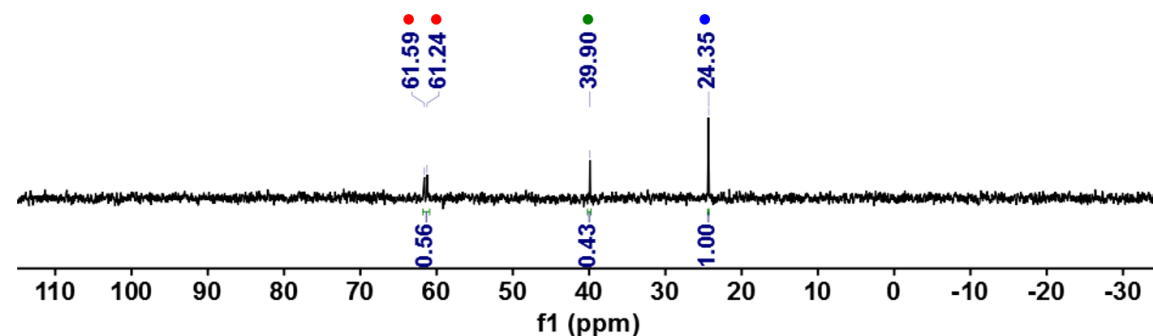


Figure S30. ^1H NMR spectrum of $(\text{acriPNP})\text{Ni}(2\text{-anthracenyl})$ (**4-Anth**) in C_6D_6 at room temperature.

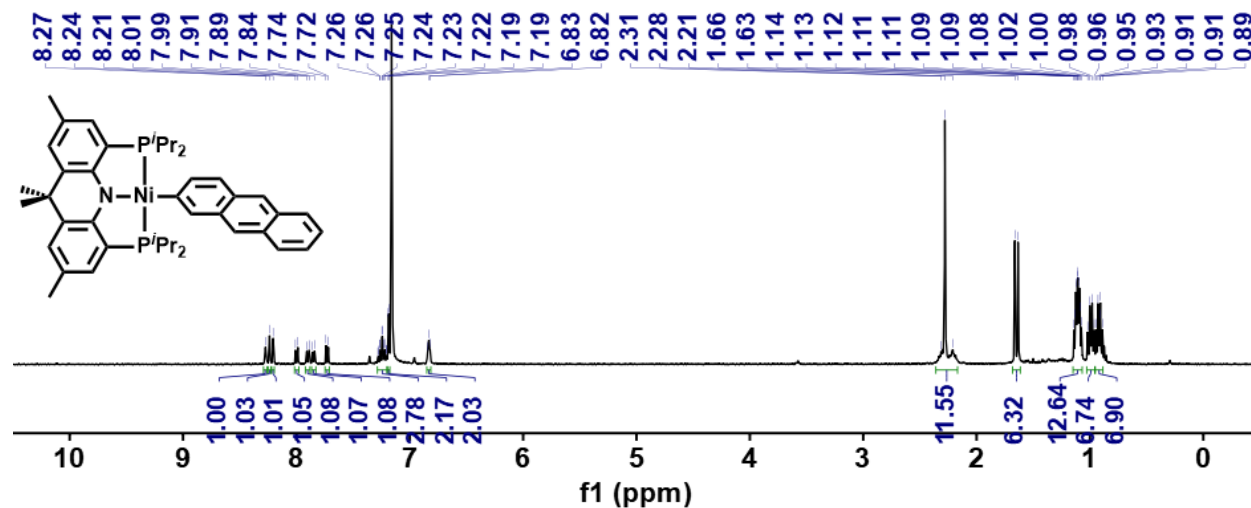


Figure S31. ^{13}C NMR spectrum of ($^{\text{acri}}\text{PNP}$)Ni(2-anthracenyl) (**4-Anth**) in C_6D_6 at room temperature.

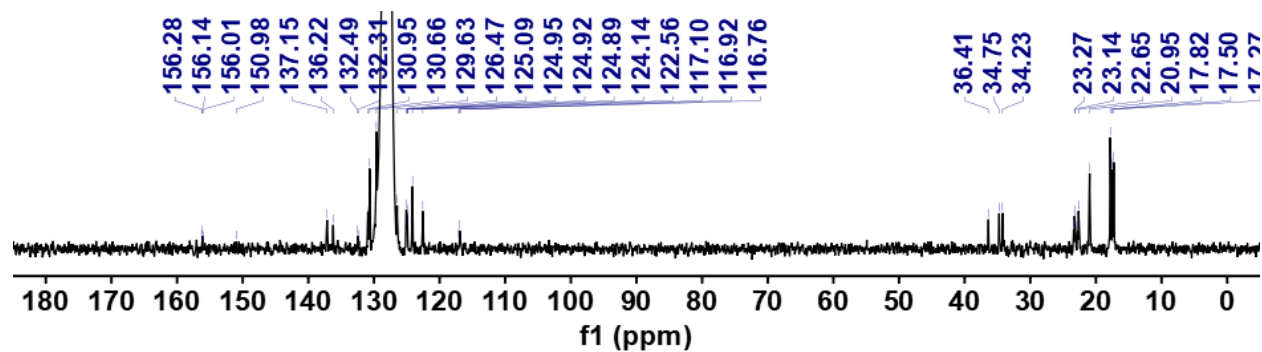


Figure S32. ^{31}P NMR spectrum of ($^{\text{acri}}\text{PNP}$)Ni(2-anthracenyl) (**4-Anth**) in C_6D_6 at room temperature.

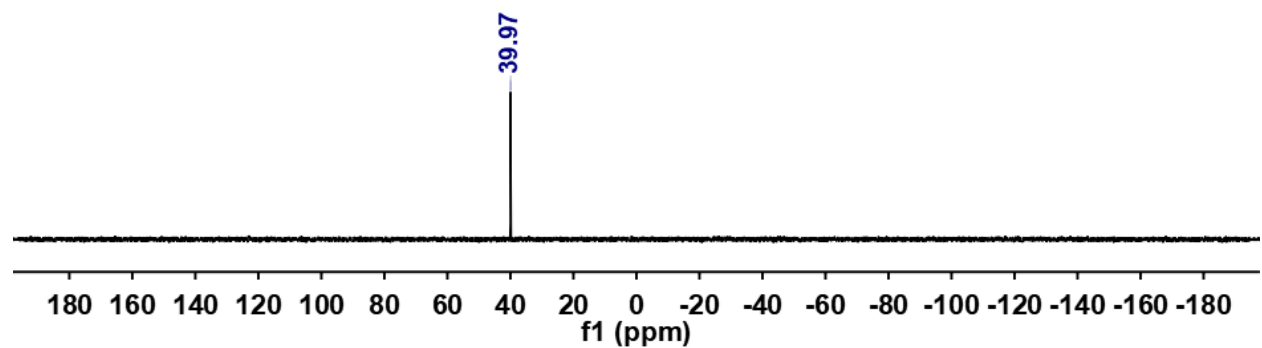


Figure S33. Single-pulse ^{31}P NMR spectra (in toluene/ C_6D_6 at room temperature) of the reaction mixture of $\{(\text{acriPNP})\text{Ni}-(\text{N}_2)-\text{Na}(\text{THF})_2\}_2$ (**2**) with toluene for (a) 15 min and (b) 24 hr.

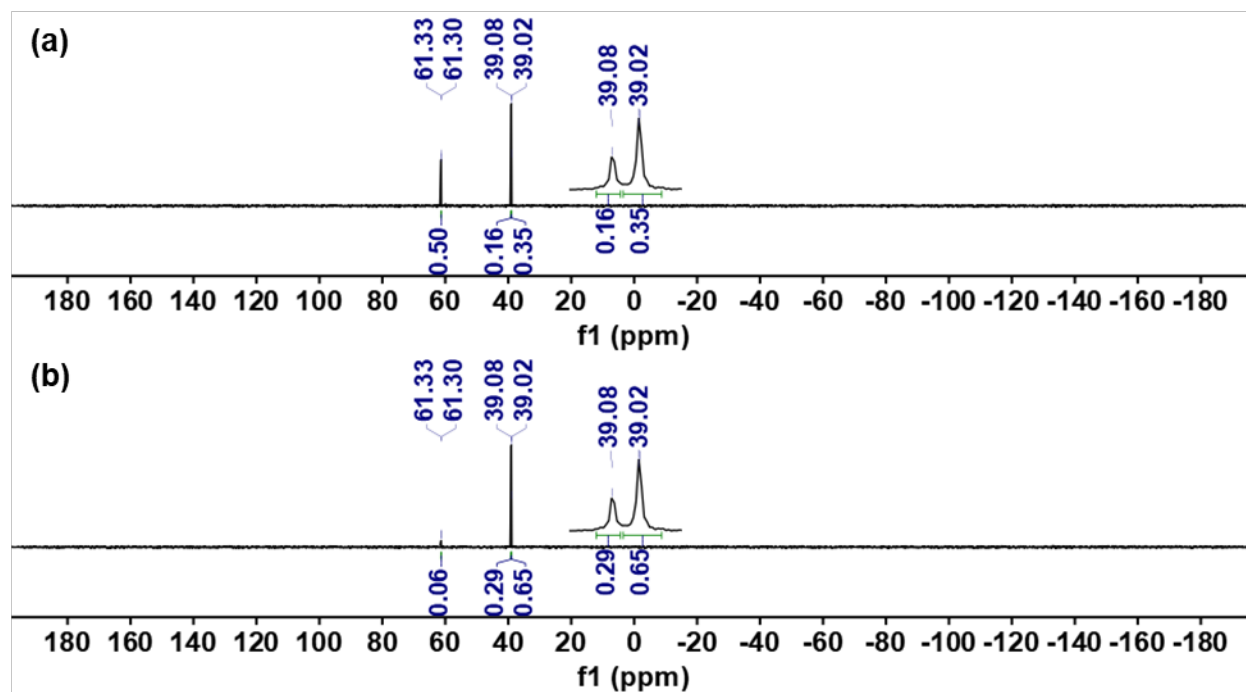


Figure S34. Single-pulse ^{31}P NMR spectra (in C_6D_6 at room temperature) of the reaction of **2** in 5 mL of toluene for (a) 15 min and (b) 24 hrs (●: **3**, ●: **4-pTol**, ●: **4-mTol**, ●: triphenylphosphine oxide). 4 equivalents of triphenylphosphine oxide was added as an internal standard.

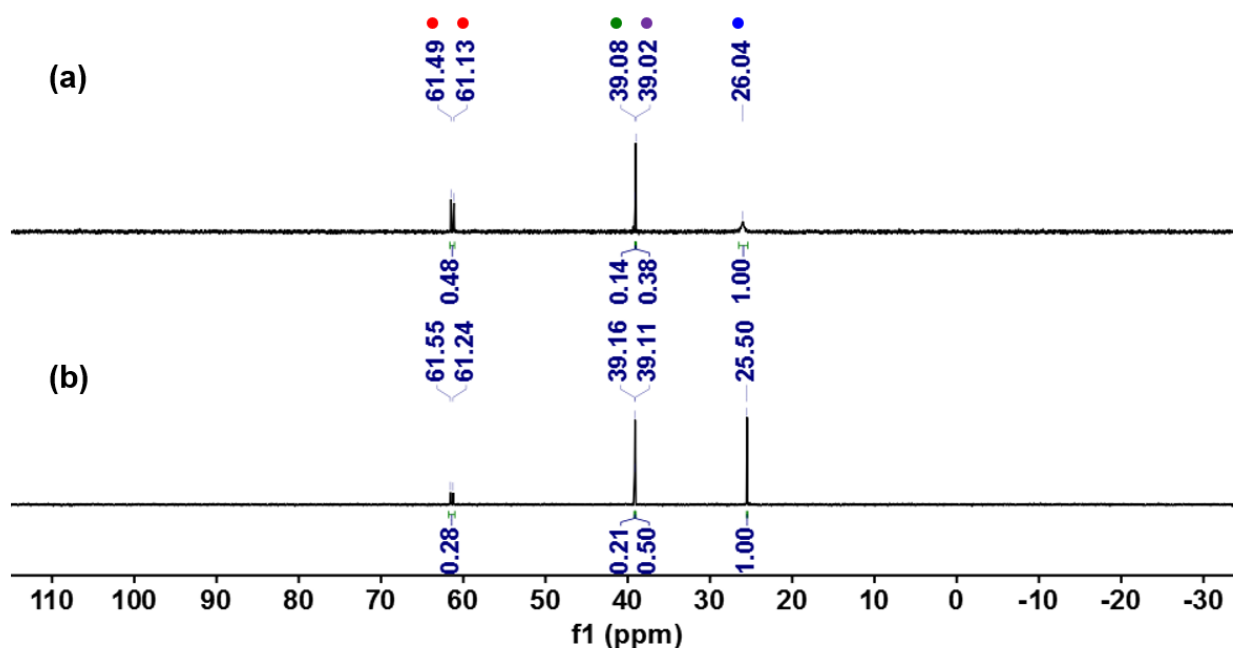


Figure S35. Single-pulse ^{31}P NMR spectrum of the reaction of **2** with 20 equivalents of toluene for 48 hrs (●: **3**, ●: **4-*p*Tol**, ●: **4-*m*Tol**, ●: triphenylphosphine oxide). 4 equivalents of triphenylphosphine oxide were added as an internal standard.

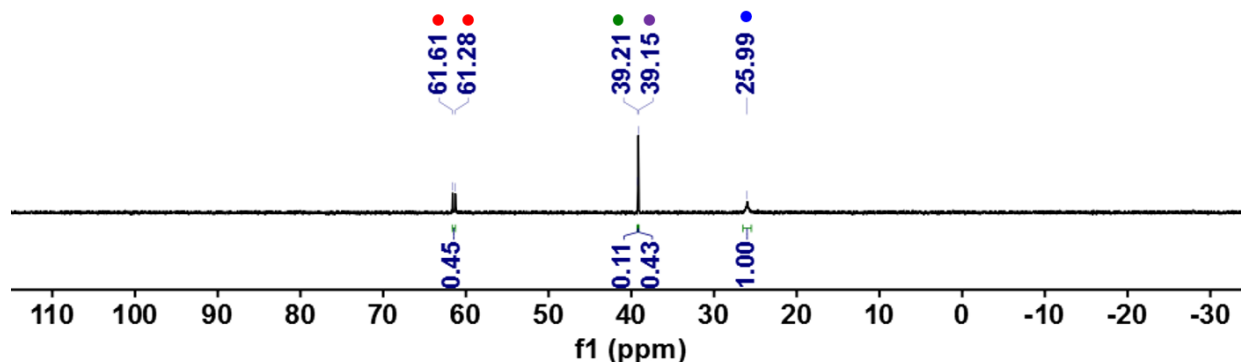


Figure S36. ^1H NMR spectrum of (^{acri}PNP)Ni(*o*-tolyl) (**4-*o*Tol**) in C_6D_6 at room temperature.

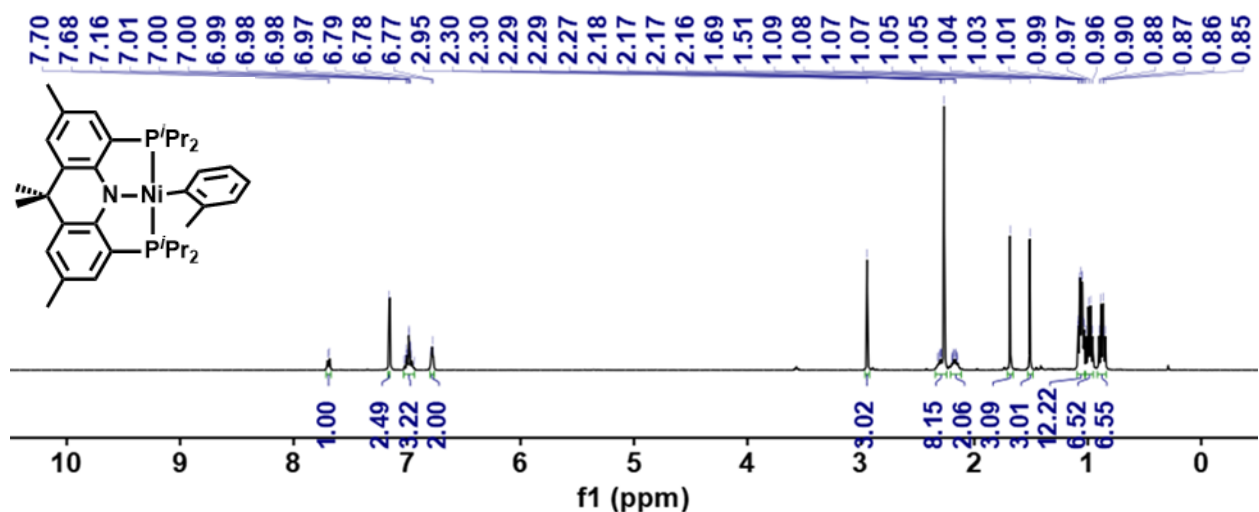


Figure S37. ^{13}C NMR spectrum of (^{acri}PNP)Ni(*o*-tolyl) (**4-*o*Tol**) in C_6D_6 at room temperature.

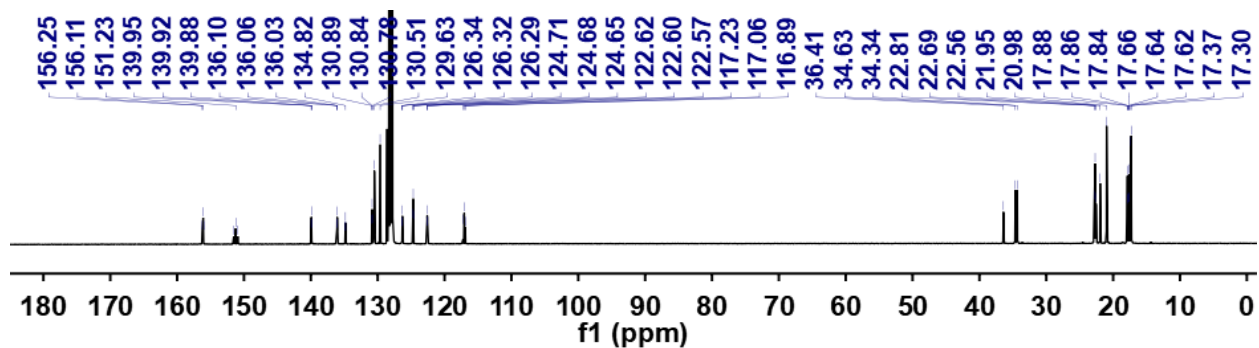


Figure S38. ^{31}P NMR spectrum of ($^{\text{acri}}\text{PNP}$)Ni(*o*-tolyl) (**4-*o*Tol**) in C_6D_6 at room temperature.

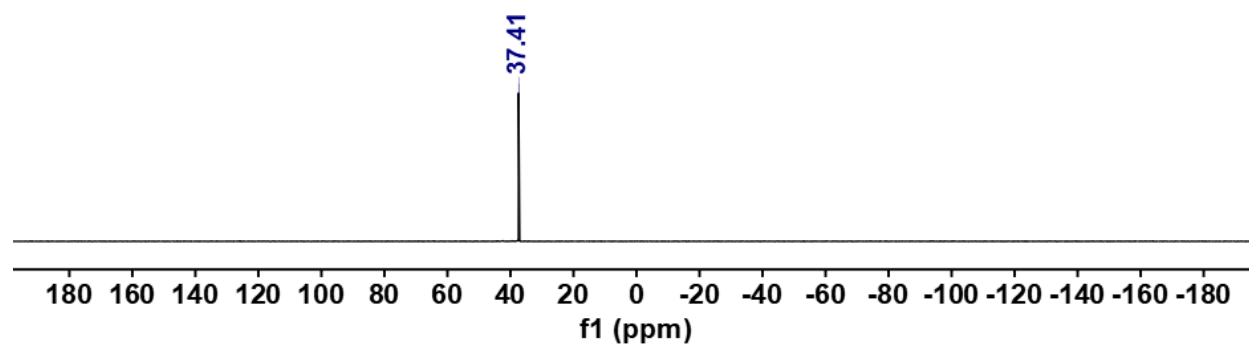


Figure S39. ^1H NMR spectrum of ($^{\text{acri}}\text{PNP}$)Ni(*m*-tolyl) (**4-*m*Tol**) in C_6D_6 at room temperature.

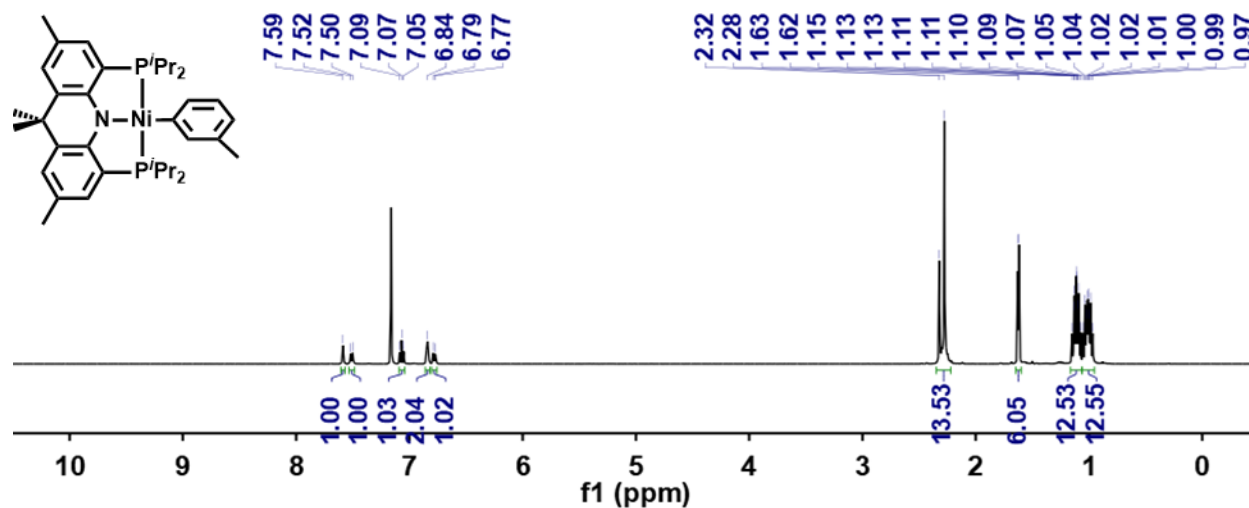


Figure S40. ^{13}C NMR spectrum of ($^{\text{acri}}\text{PNP}$)Ni(*m*-tolyl) (**4-*m*Tol**) in C_6D_6 at room temperature.

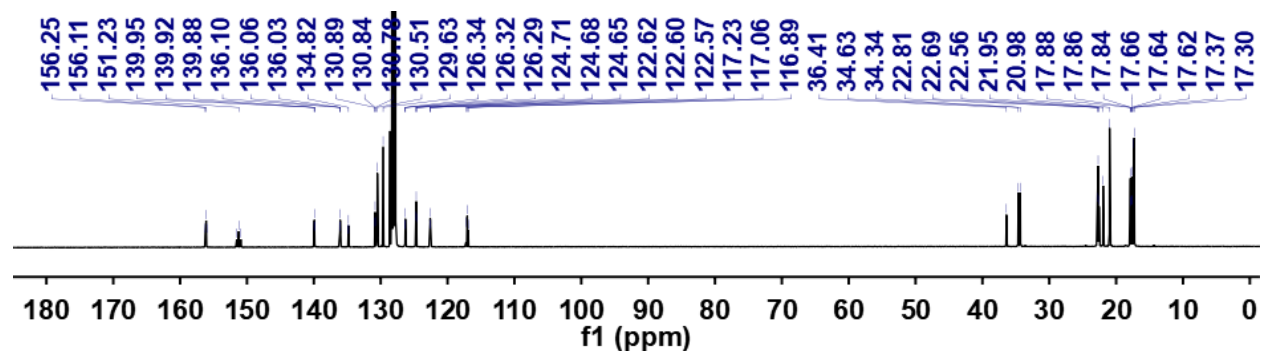


Figure S41. ^{31}P NMR spectrum of ($^{\text{acri}}\text{PNP}$)Ni(*m*-tolyl) (**4-*m*Tol**) in C_6D_6 at room temperature.

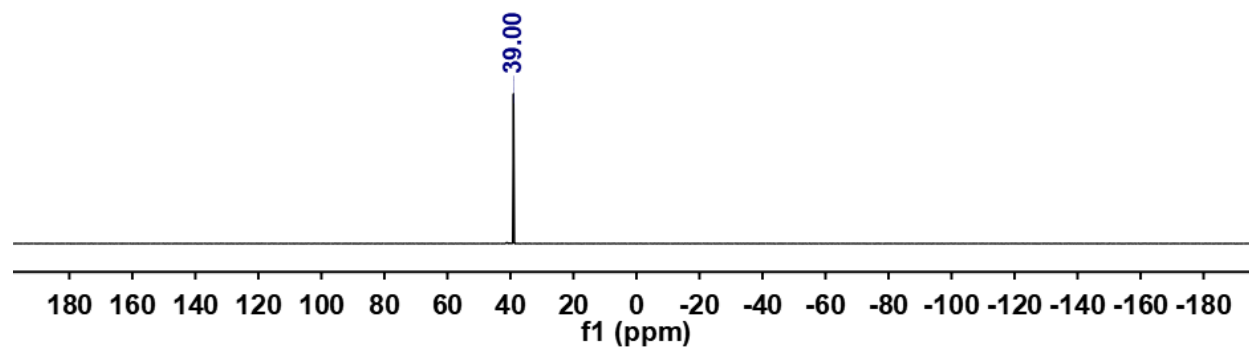


Figure S42. ^1H NMR spectrum of ($^{\text{acri}}\text{PNP}$)Ni(*p*-tolyl) (**4-*p*Tol**) in C_6D_6 at room temperature.

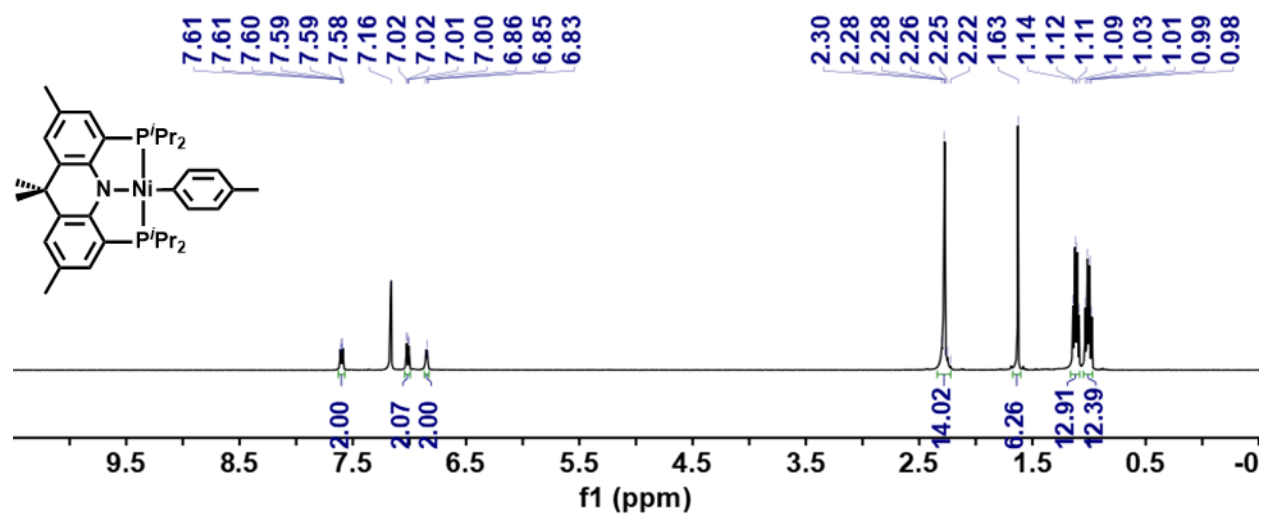


Figure S43. ^{13}C NMR spectrum of ($^{\text{acri}}\text{PNP}$)Ni(*p*-tolyl) (**4-*p*Tol**) in C_6D_6 at room temperature.

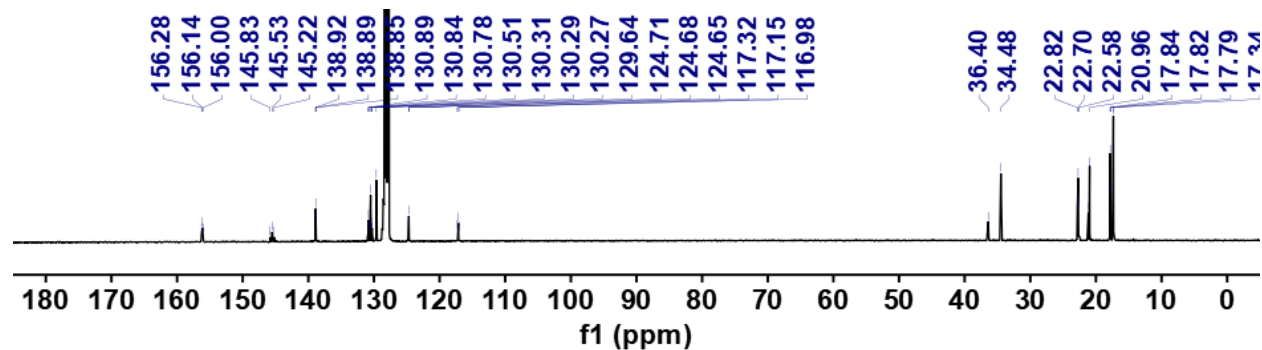


Figure S44. ^{31}P NMR spectrum of ($^{\text{acri}}\text{PNP}$)Ni(*p*-tolyl) (**4-*p*Tol**) in C_6D_6 at room temperature.

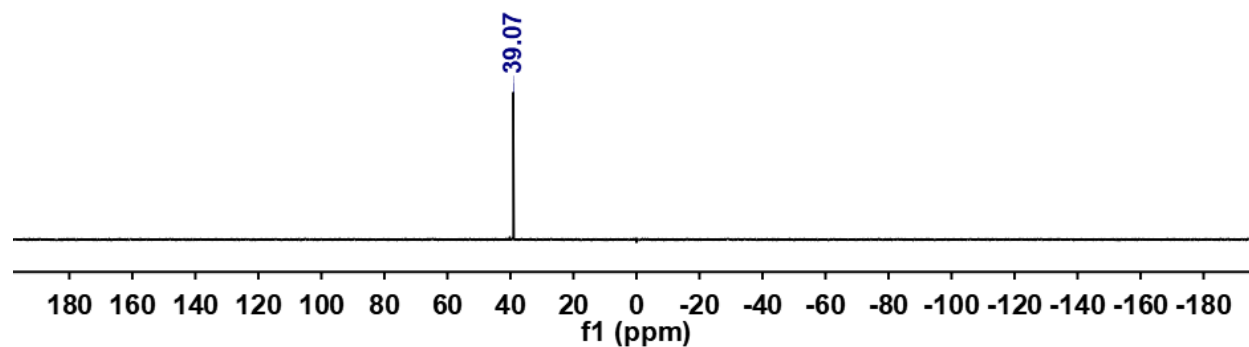


Figure S45. ^1H NMR spectrum of ($^{\text{acri}}\text{PNP}$)Ni(benzyl) in C_6D_6 at room temperature (●: pentane).

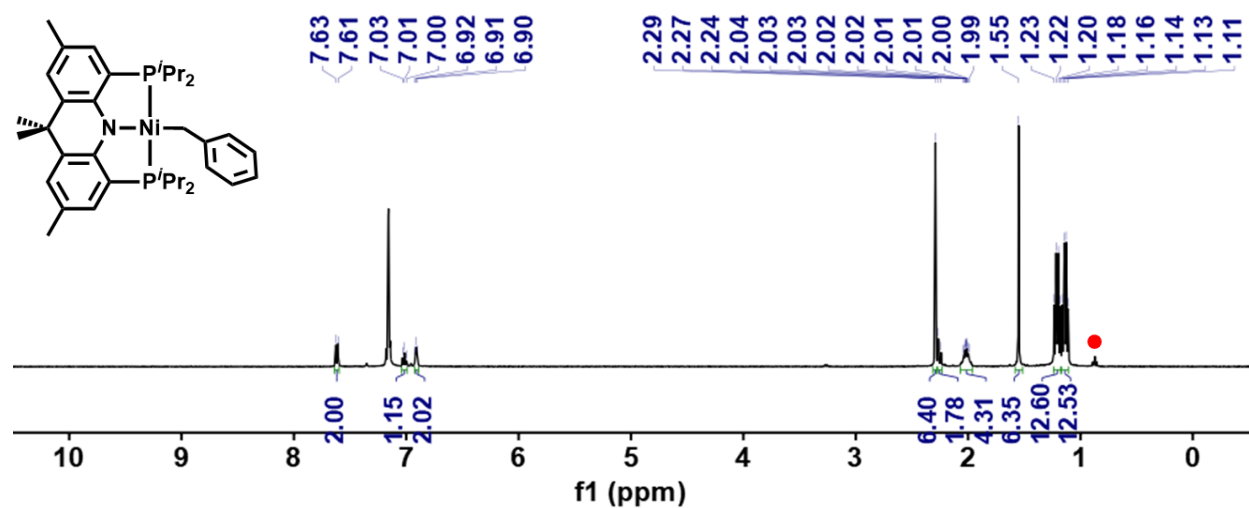


Figure S46. ^{13}C NMR spectrum of ($^{\text{acri}}\text{PNP}$)Ni(benzyl) in C_6D_6 at room temperature.

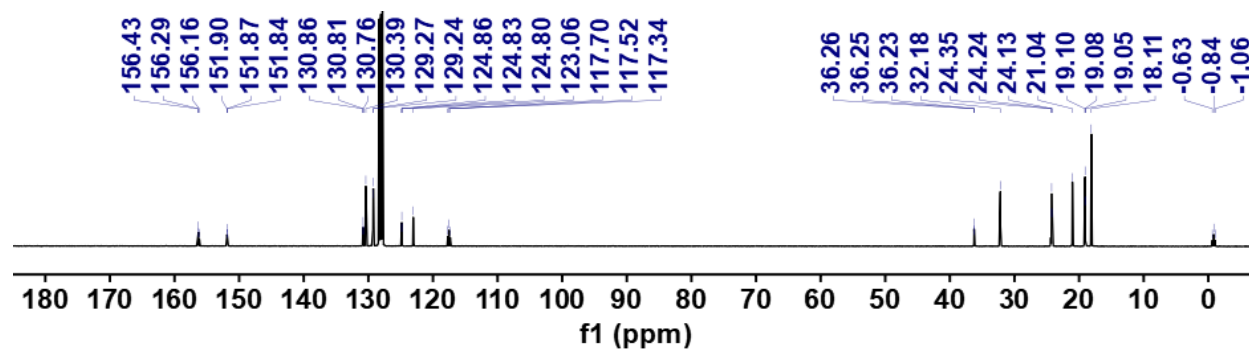


Figure S47. ^{31}P NMR spectrum of $(^{\text{acri}}\text{PNP})\text{Ni}(\text{benzyl})$ in C_6D_6 at room temperature.

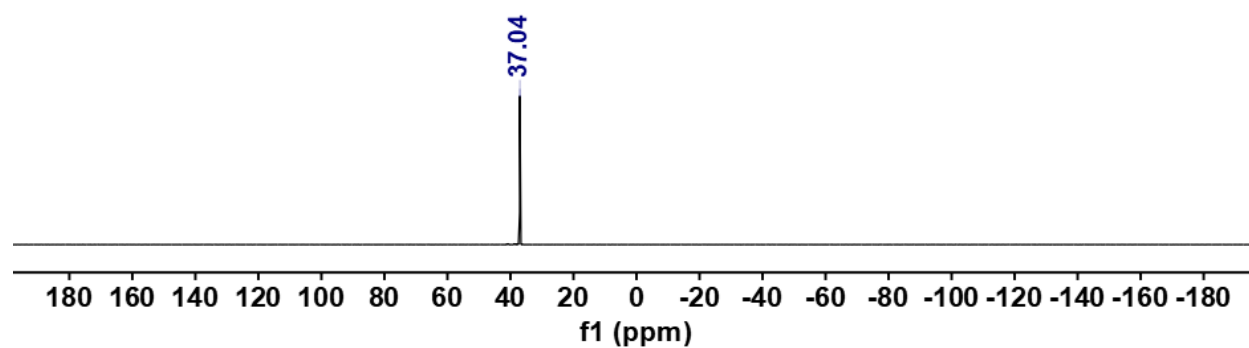


Figure S48. ^1H NMR spectrum (in $\text{THF}/\text{C}_6\text{D}_6$ at room temperature) of the reaction mixture of triethyl phosphonoacetate with NaH (●: THF, ●: methylene proton of remaining ethyl diethylphosphonoacetate, ●: methine proton of ethyl sodiodiethylphosphonoacetate).

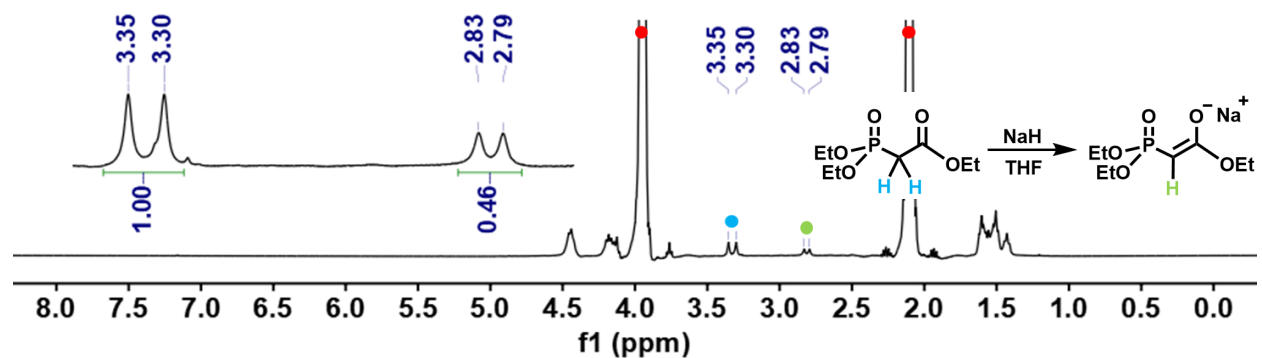


Figure S49. ^1H NMR spectrum of $\{(^{\text{acri}}\text{PNP})\text{Ni}-(\text{N}_2)-\text{K}(\text{THF})_2\}_2$ (**2-K**) in $\text{THF}-d_8$ at room temperature (●: THF, ●: pentane).

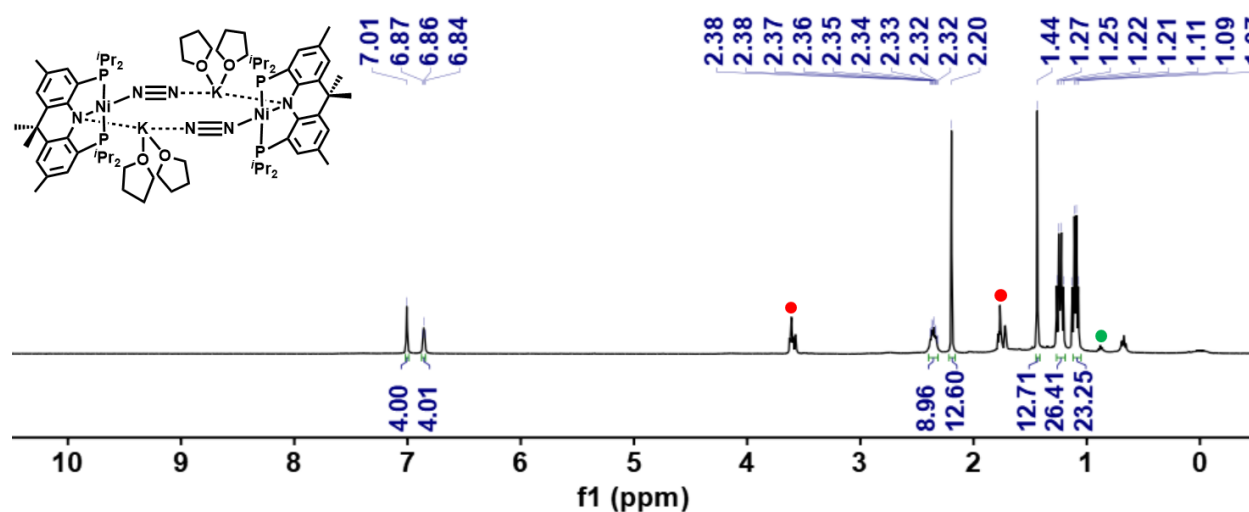


Figure S50. ^{13}C NMR spectrum of $\{(\text{acriPnP})\text{Ni}-(\text{N}_2)-\text{K}(\text{THF})_2\}_2$ (**2-K**) in $\text{THF-}d_8$ at room temperature (●: pentane).

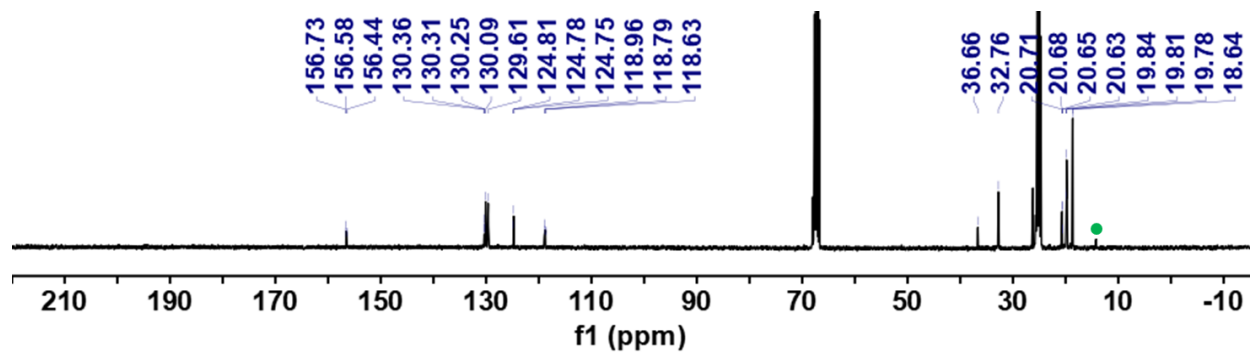


Figure S51. ^{31}P NMR spectrum of $\{(\text{acriPnP})\text{Ni}-(\text{N}_2)-\text{K}(\text{THF})_2\}_2$ (**2-K**) in $\text{THF-}d_8$ at room temperature.

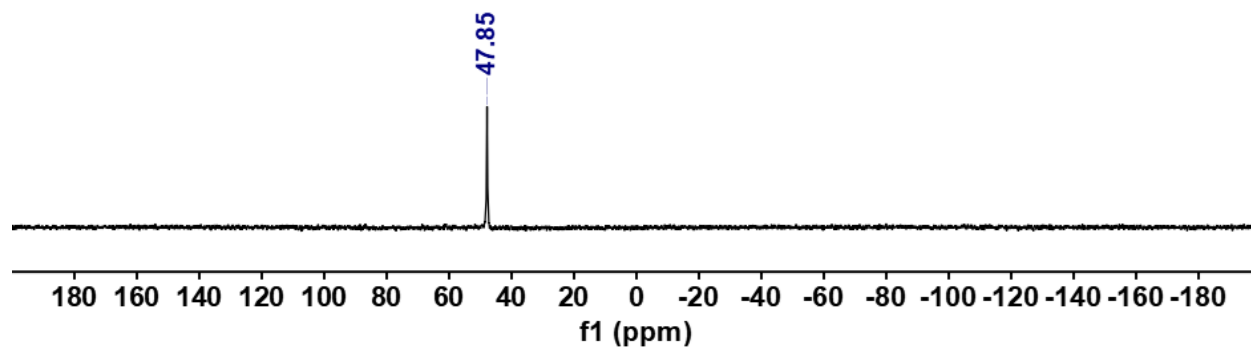


Figure S52. ^{31}P NMR spectra in C_6D_6 (a) of $\{(\text{acriPnP})\text{Ni}-(\text{N}_2)-\text{K}(\text{THF})_2\}_2$ (**2-K**), (b) stirring for 12 hrs at room temperature and (c) heating at 40°C for 12 hrs (● : **3-D**, ● : **4-C₆D₅**, ● : unknown species).

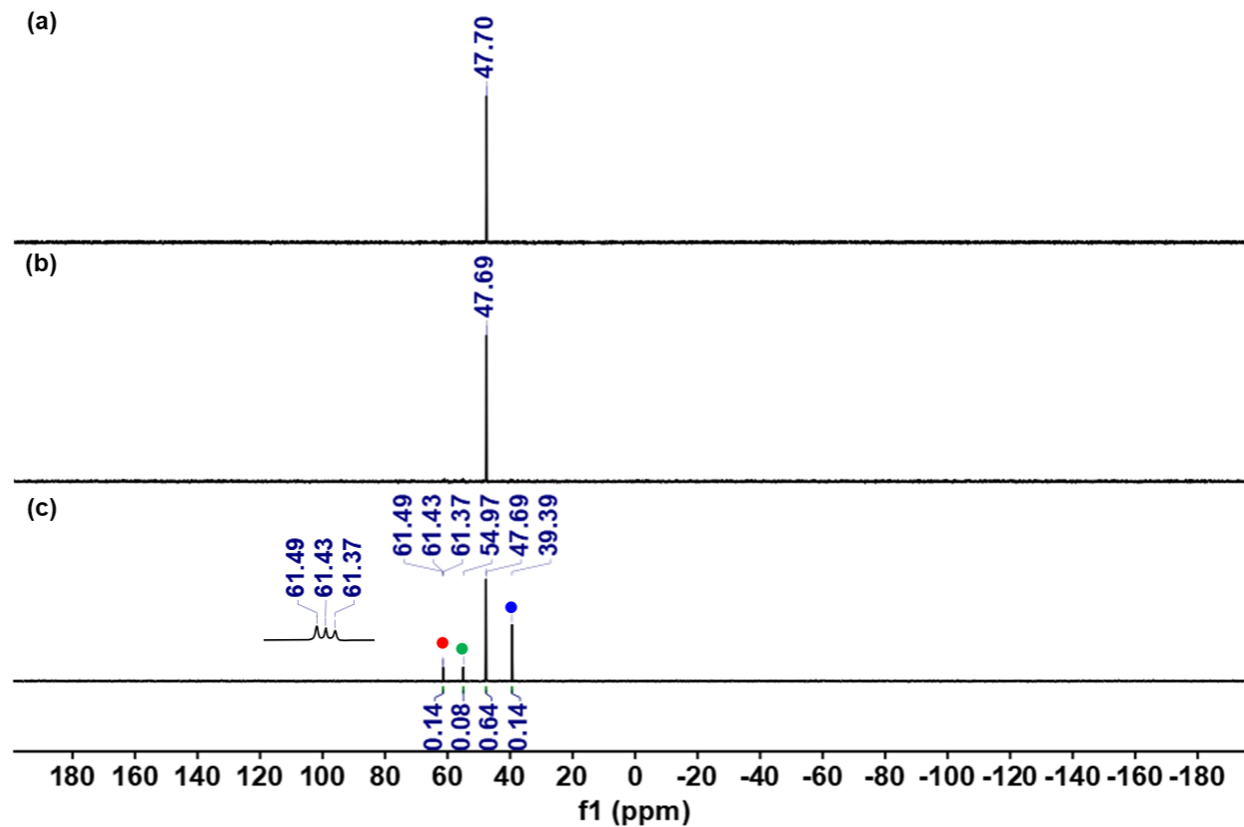


Figure S53. ^1H NMR spectrum of $\{(\text{acriPNP})\text{Ni}-(\text{N}_2)\text{-Li}(\text{THF})_2\}_2$ (**2-Li**) in $\text{THF-}d_8$ at room temperature. (●: THF, ●: pentane).

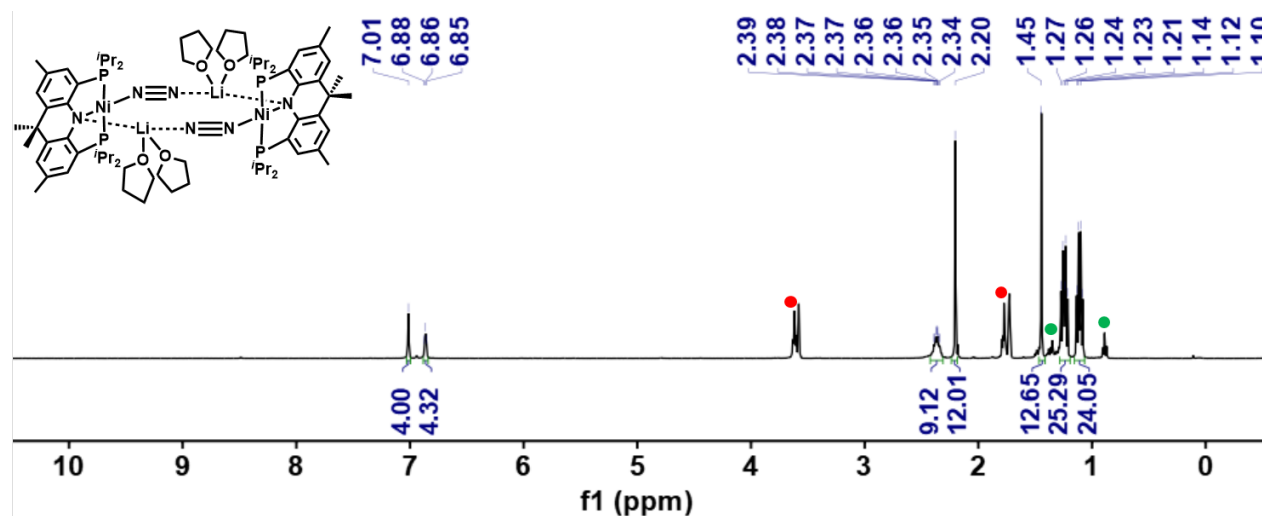


Figure S54. ^{13}C NMR spectrum of $\{(\text{acriPNP})\text{Ni}-(\text{N}_2)\text{-Li}(\text{THF})_2\}_2$ (**2-Li**) in $\text{THF-}d_8$ at room temperature (●: pentane).

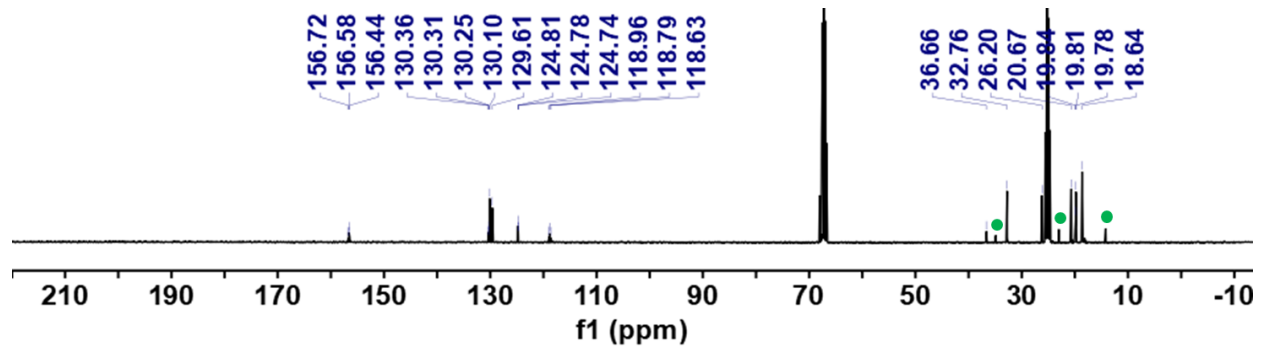


Figure S55. ^{31}P NMR spectrum of $\{(\text{acriPNP})\text{Ni}-(\text{N}_2)\text{-Li}(\text{THF})_2\}_2$ (**2-Li**) in $\text{THF-}d_8$ at room temperature.

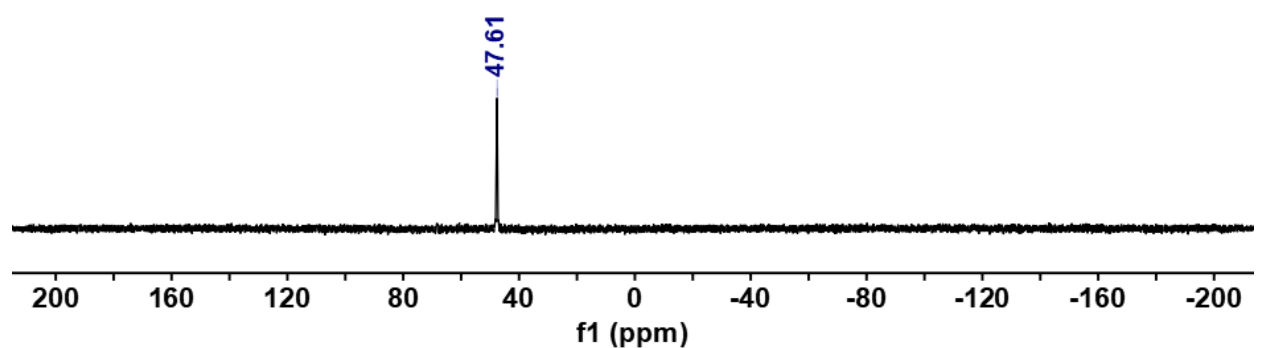


Figure S56. ^{31}P NMR spectra in C_6D_6 (a) of $\{(\text{acriPNP})\text{Ni}-(\text{N}_2)-\text{Li}(\text{THF})_2\}_2$ (**2-Li**), (b) stirring for 12 hrs at room temperature and (c) heating at 40°C for 12 hrs (● : **3-D**, ● : **4-C₆D₅**, ● : $(\text{acriPNP})\text{Li}(\text{THF})$).

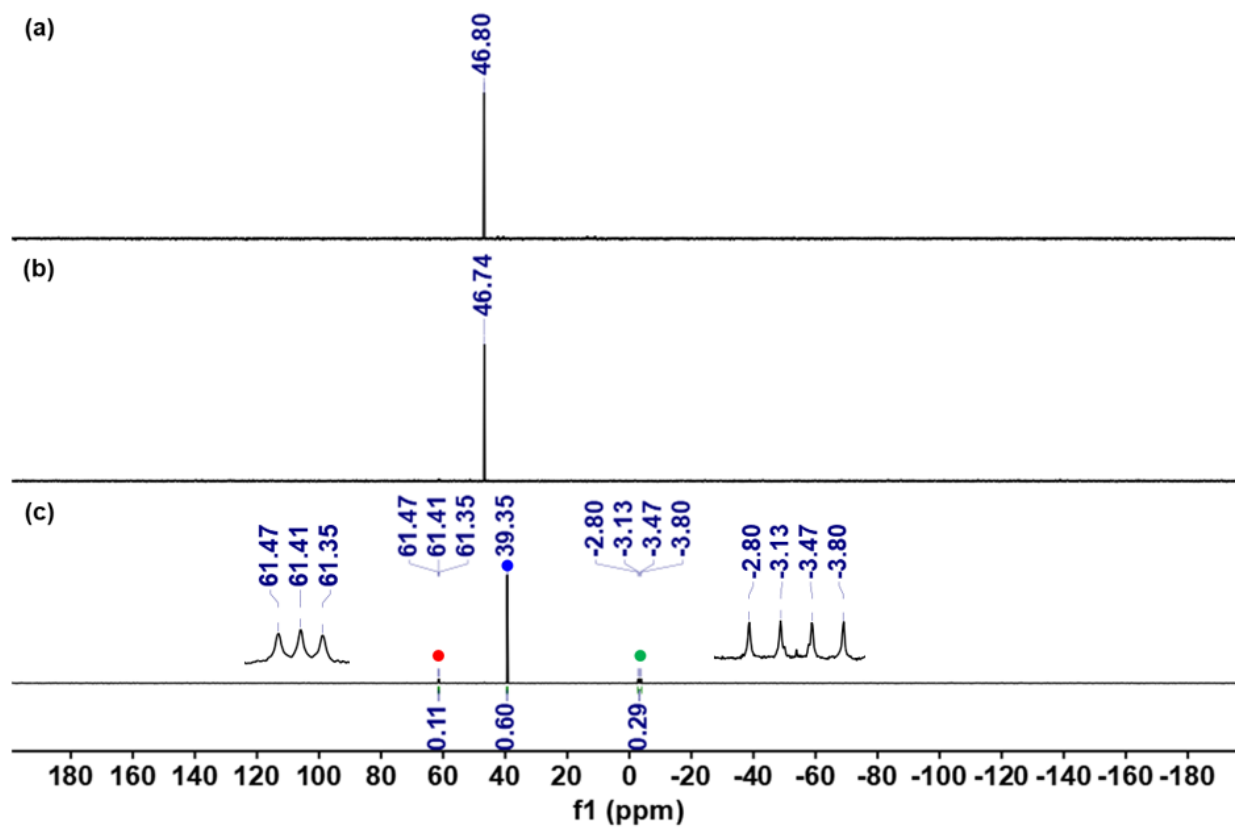


Figure S57. ^{31}P NMR spectra of the reaction of (a) $(^{\text{acri}}\text{PNP})\text{NiCl}$ and (b) $(^{\text{acri}}\text{PNP})\text{NiH}$ (**3**) with excess benzene and sodium at room temperature.

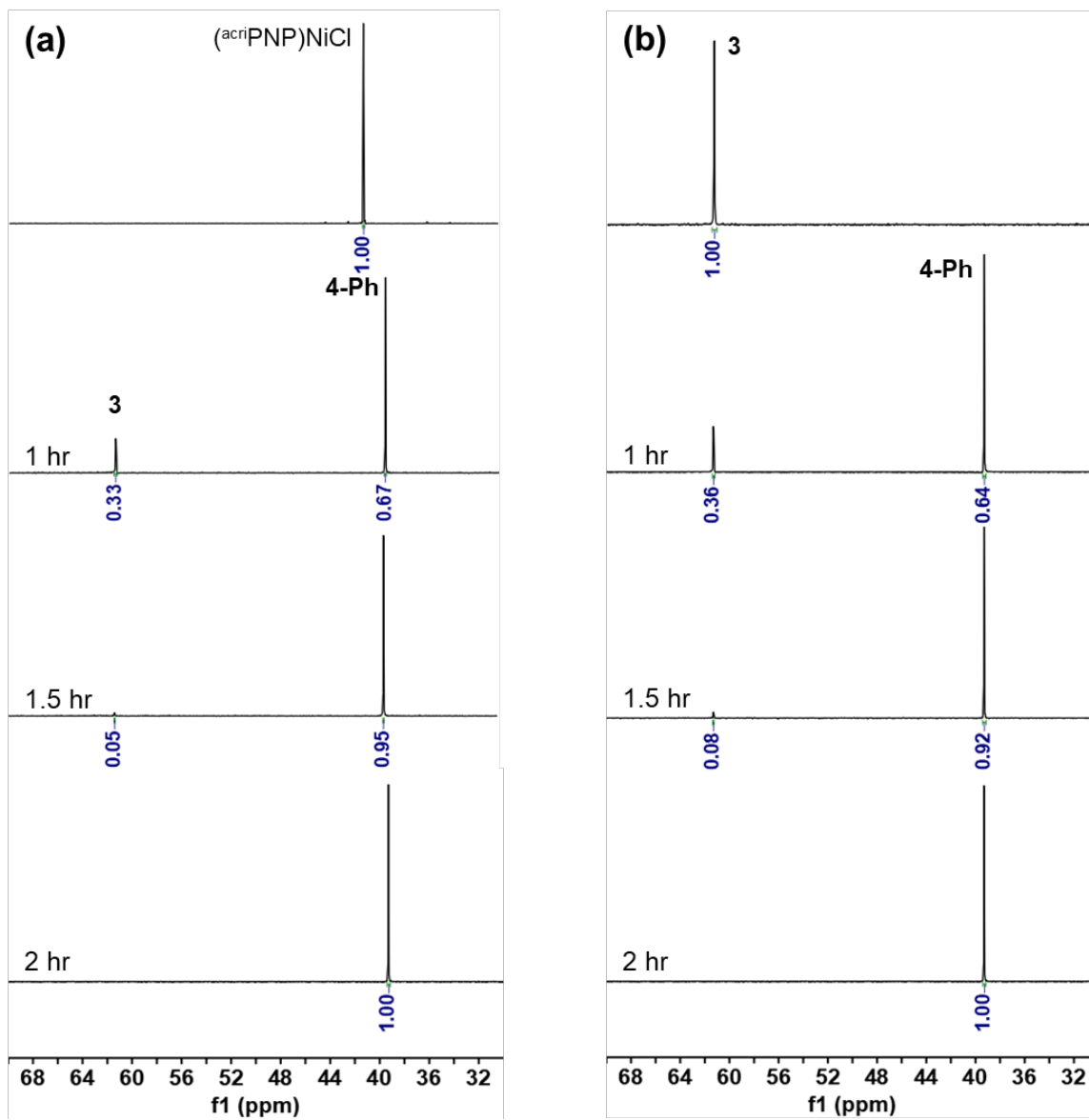


Figure S58. ^{31}P NMR spectra of the reaction of **2** with (a) benzene and (b) benzene- d_6 . (c) Plot of $\ln[2]$ vs. time with a linear least-square fit (red, **2** + benzene; blue, **2** + benzene- d_6).

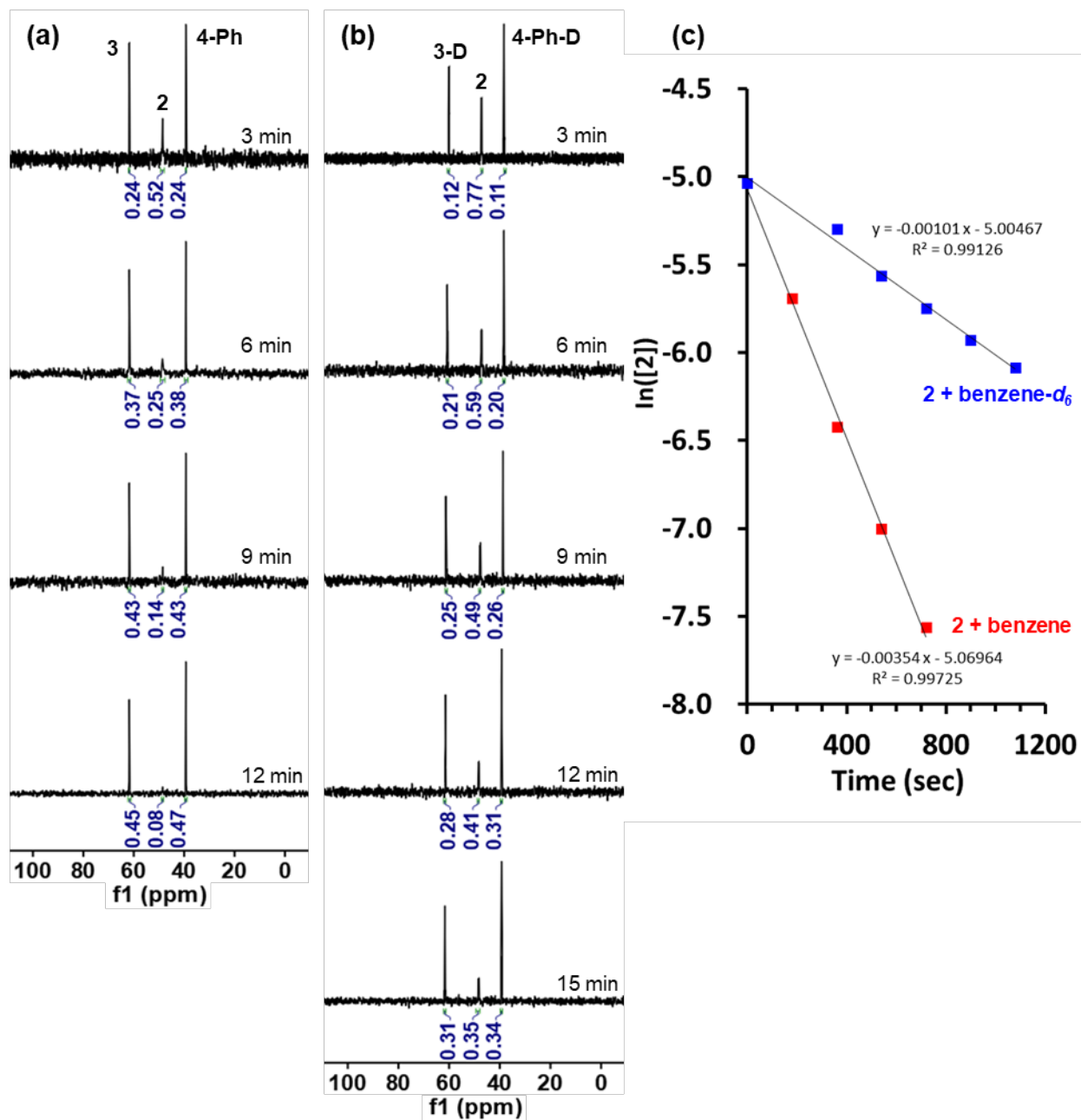


Figure S59. ^1H NMR spectrum (in benzene/benzene- d_6 at room temperature) of the reaction mixture of $\{(\text{acriPNP})\text{Ni}-(\text{N}_2)-\text{Na}(\text{THF})_2\}_2$ (**2**) with benzene/benzene- d_6 (1:1) (● : **3**, ● : **3-D**, ● : **4-Ph**, ● : **4-C₆D₅**).

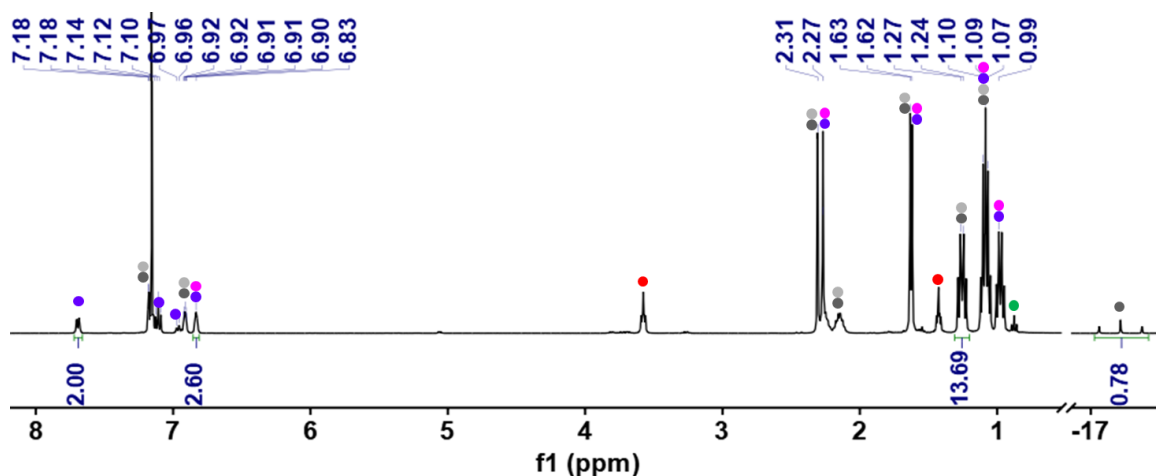


Figure S60. ^{31}P NMR spectrum (in benzene/benzene- d_6 at room temperature) of the reaction mixture of $\{(\text{acriPNP})\text{Ni}-(\text{N}_2)-\text{Na}(\text{THF})_2\}_2$ (**2**) with benzene/benzene- d_6 (1:1) (● : **3**, ● : **3-D**, ● : **4-Ph**, ● : **4-C₆D₅**, ● : THF, ● : pentane).

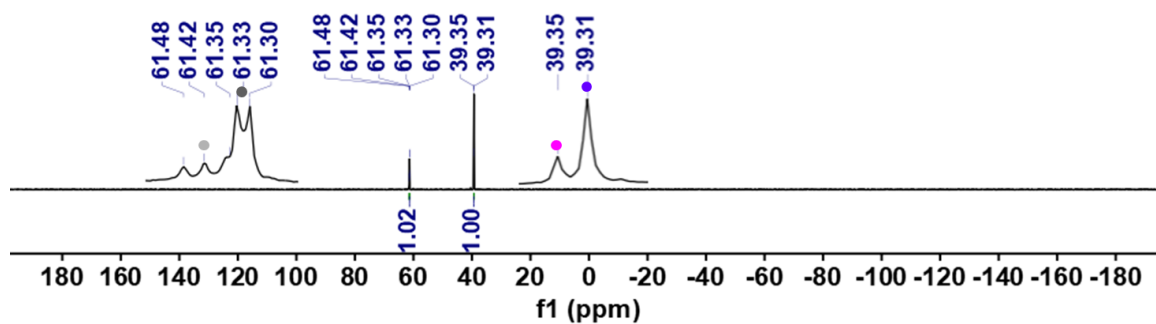


Figure S61. ^1H NMR spectrum of $(\text{acriPNP})\text{Ni}(\text{CH}=\text{CH}_2)$ (**5**) in C_6D_6 at room temperature.

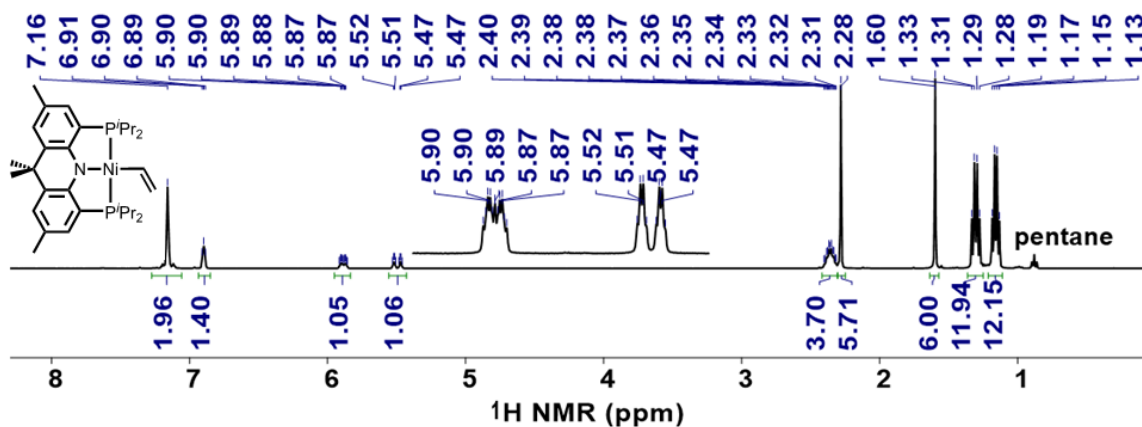


Figure S62. ^1H NMR spectrum of $(^{\text{acri}}\text{PNP})\text{Ni}(\text{CH}=\text{CH}_2)$ (**5**) in acetonitrile- d_3 at room temperature.

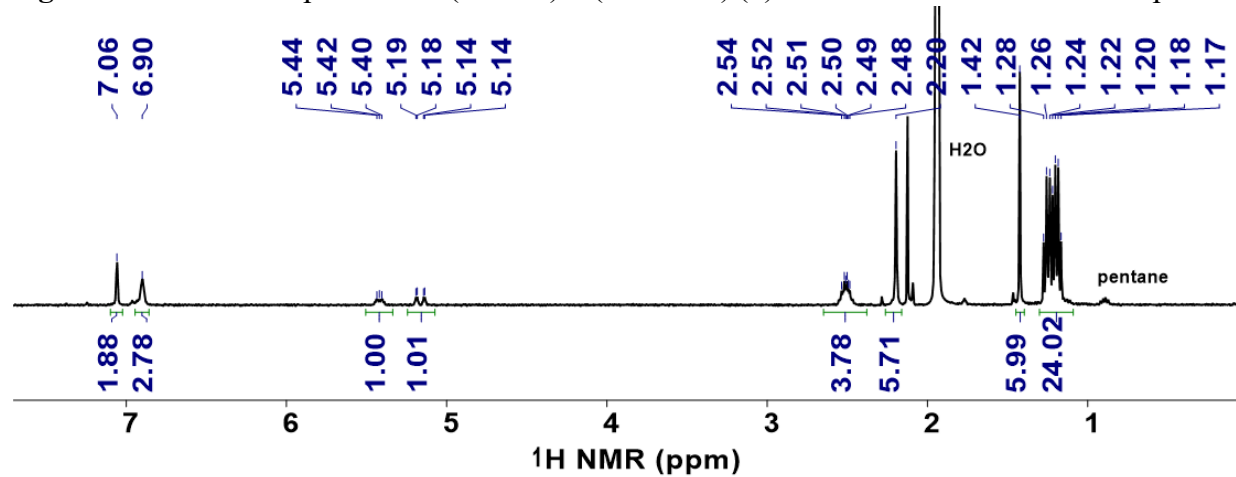


Figure S63. ^{13}C NMR spectrum of $(^{\text{acri}}\text{PNP})\text{Ni}(\text{CH}=\text{CH}_2)$ (**5**) in C_6D_6 at room temperature.

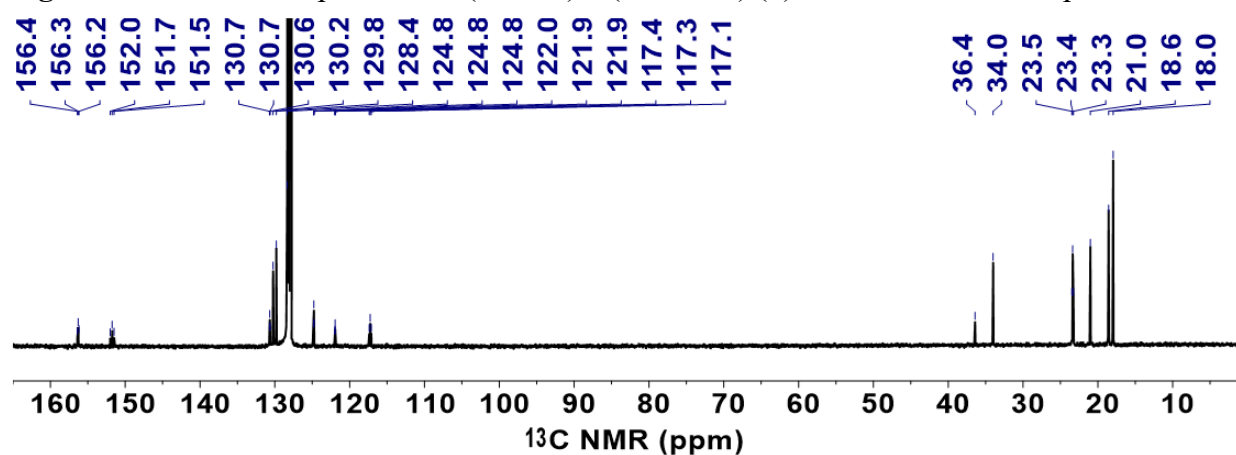


Figure S64. ^{31}P NMR spectrum of $(^{\text{acri}}\text{PNP})\text{Ni}(\text{CH}=\text{CH}_2)$ (**5**) in C_6D_6 at room temperature.

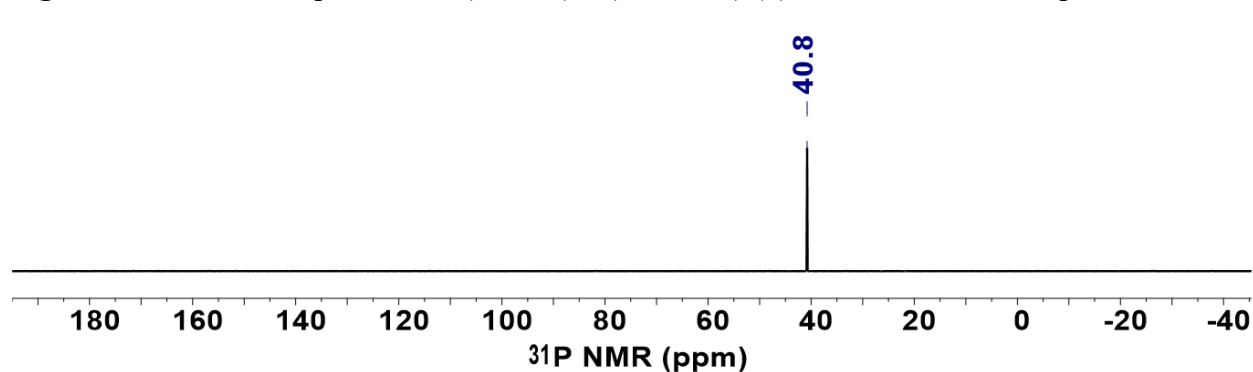


Figure S65. COSY NMR spectrum of $(^{acri}PNP)Ni(CH=CH_2)$ (**5**) in C_6D_6 .

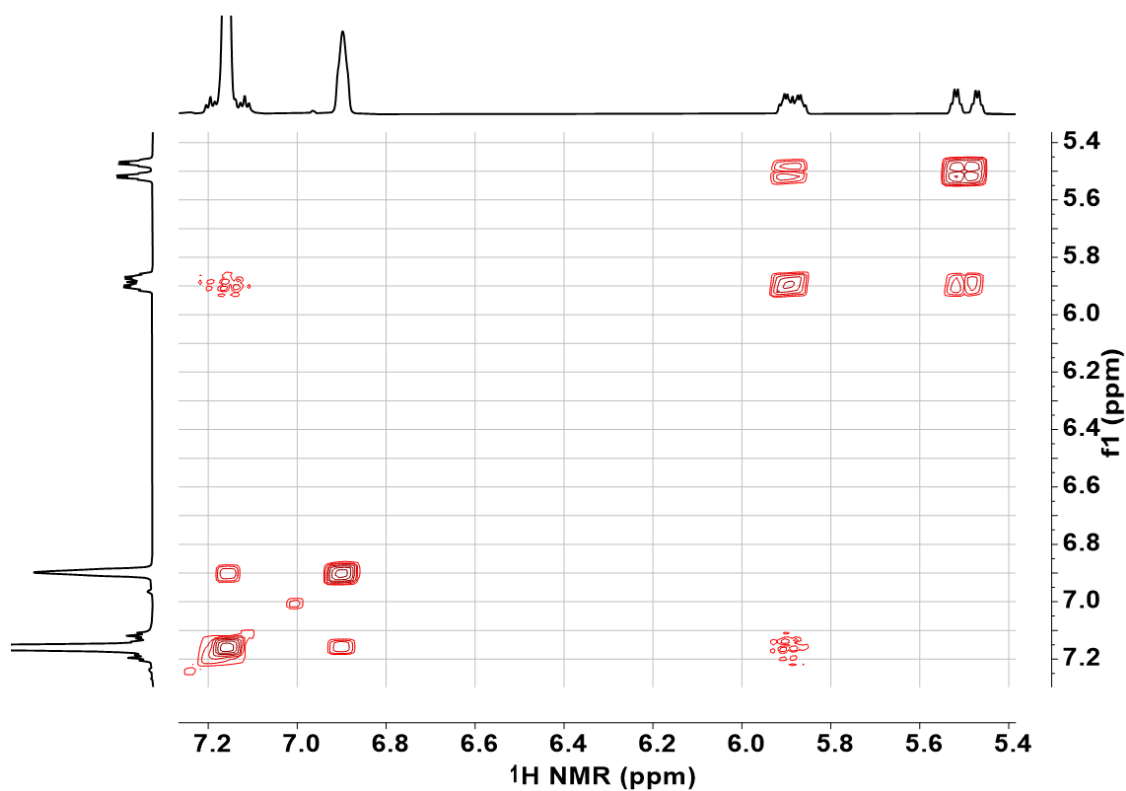


Figure S66. HSQC NMR spectrum of $(^{acri}PNP)Ni(CH=CH_2)$ (**5**) in C_6D_6 (blue: CH_2 , red: CH).

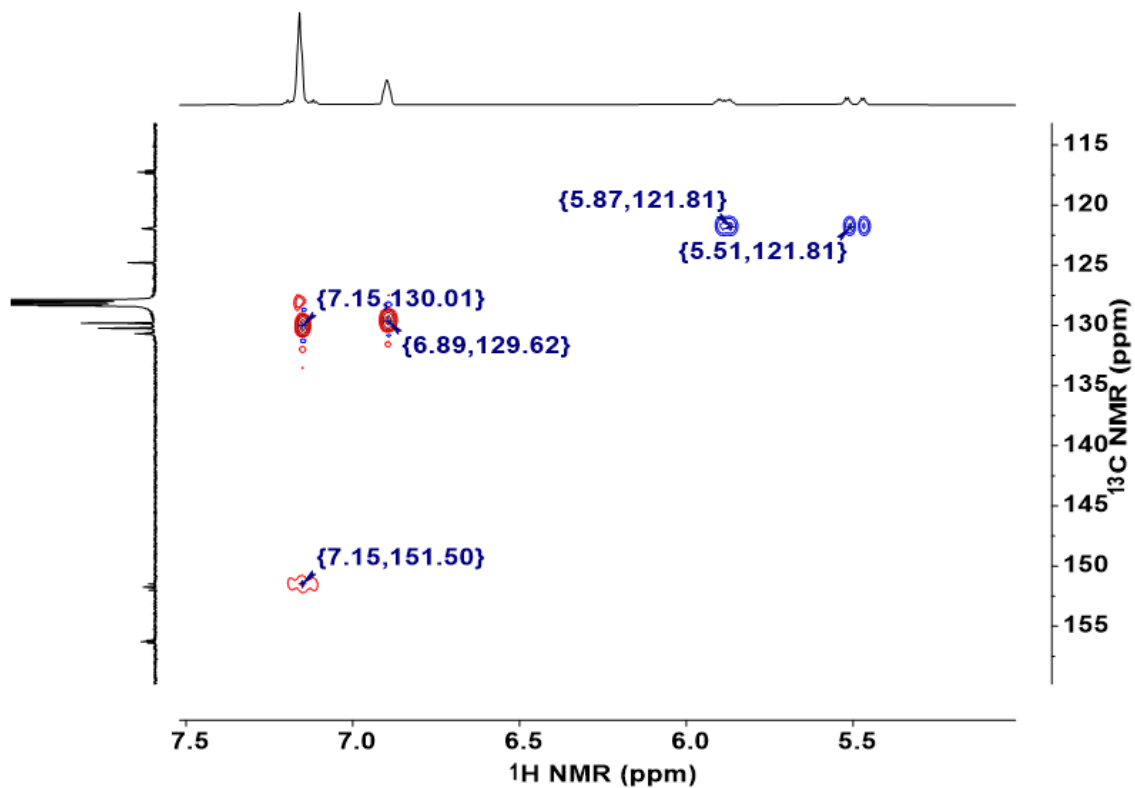


Figure S67. Crude ^{31}P NMR spectra of an aliquot from the reduction of **5** in the presence of 15-C-5 after 1.5 h and 20.5 h (~0.1 mL of THF- d_8 was added to facilitate NMR lock).

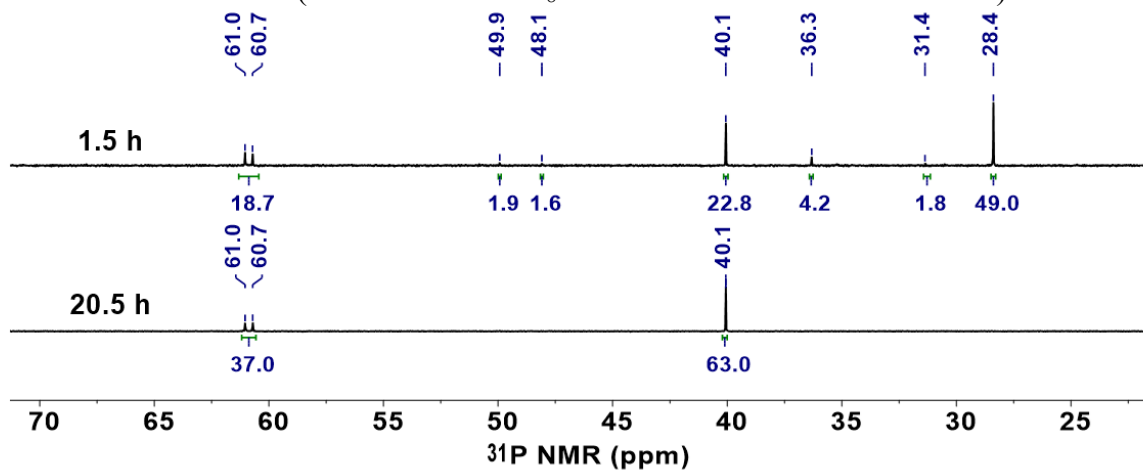


Figure S68. Crude ^{31}P NMR spectra of an aliquot from the reduction of (^{acri}PNP)NiPh (**4-Ph**) in the presence of glyme (~0.1 mL of THF- d_8 was added to facilitate NMR lock).

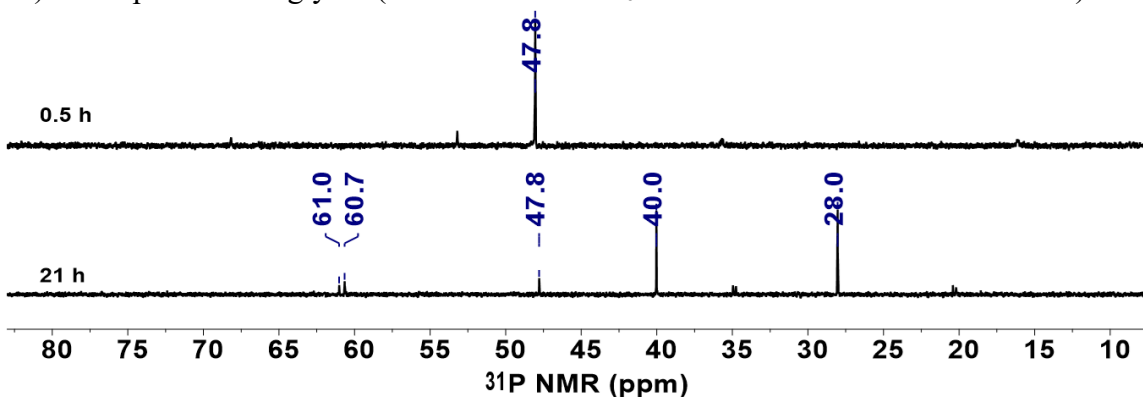


Figure S69. Crude ^1H NMR spectrum in 1.0 mL glyme (●) and 0.1 mL C_6D_6 and PhLi (1.8 mg) to give *in situ* methyl vinyl ether (●) and lithium methoxide (●).

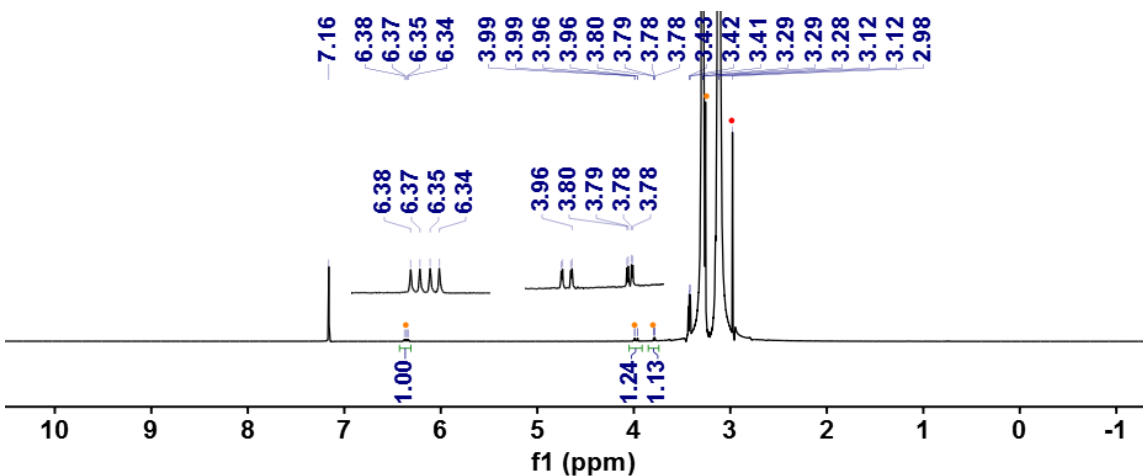


Figure S70. Crude ^1H NMR spectrum in C_6D_6 of PhLi in excess 15-C-5 to give *in situ* lithium tetraethylene glycoxide vinyl ether.

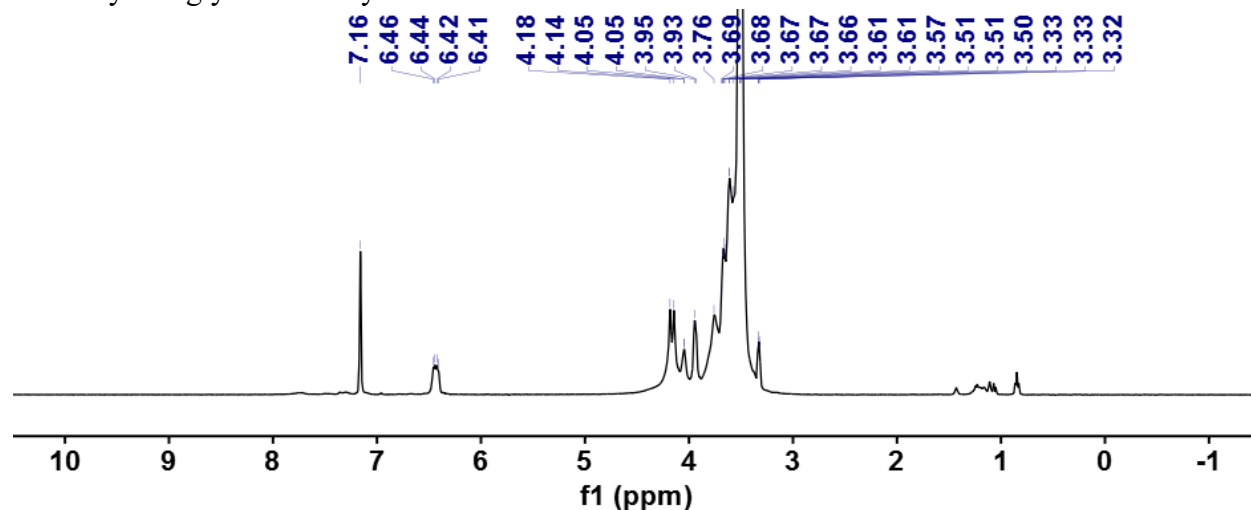


Figure S71. ^1H NMR spectra in C_6D_6 of (1) $\text{Na}\{\text{O}(\text{C}_2\text{H}_4\text{O})_4\}\text{Na}$ isolated from reduction of **5** in the presence of 15-C-5 and (2) $\text{Na}\{\text{O}(\text{C}_2\text{H}_4\text{O})_4\}\text{Na}$ isolated from reaction of Na and tetraethylene glycol (Aldrich, 99%). (●): tetraethylene glycoxide vinyl ether.

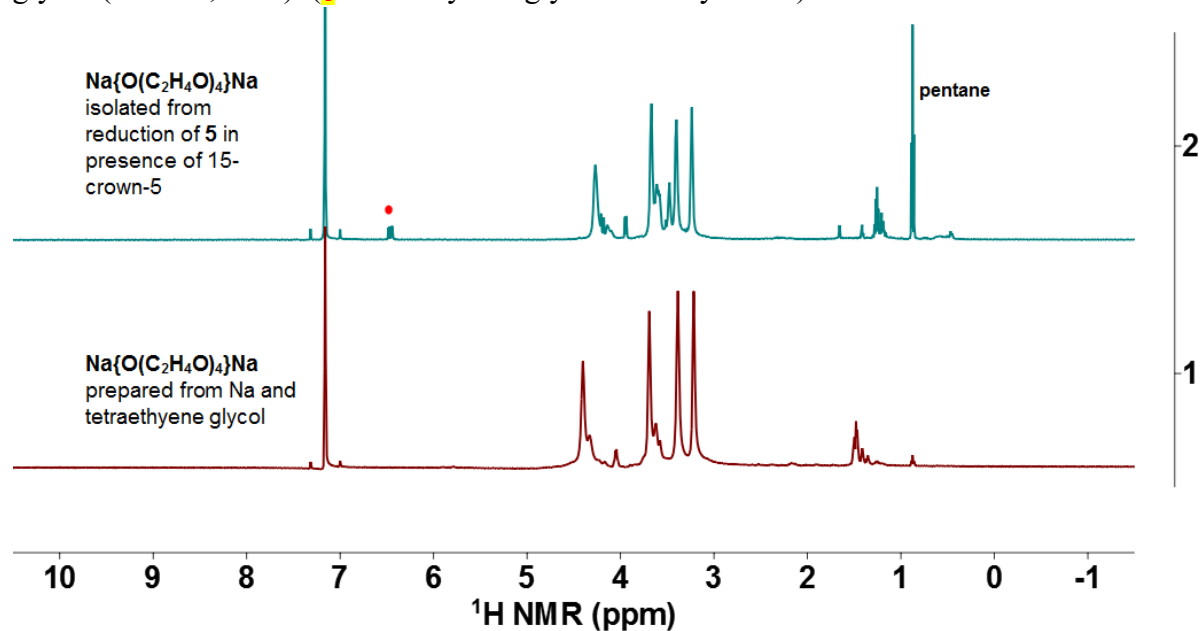


Figure S72. Crude ^{31}P NMR spectrum of an aliquot from the reaction of **2** with 15-C-5 and PhLi after 5h (~ 0.1 mL of THF- d_8 was added to facilitate NMR lock).

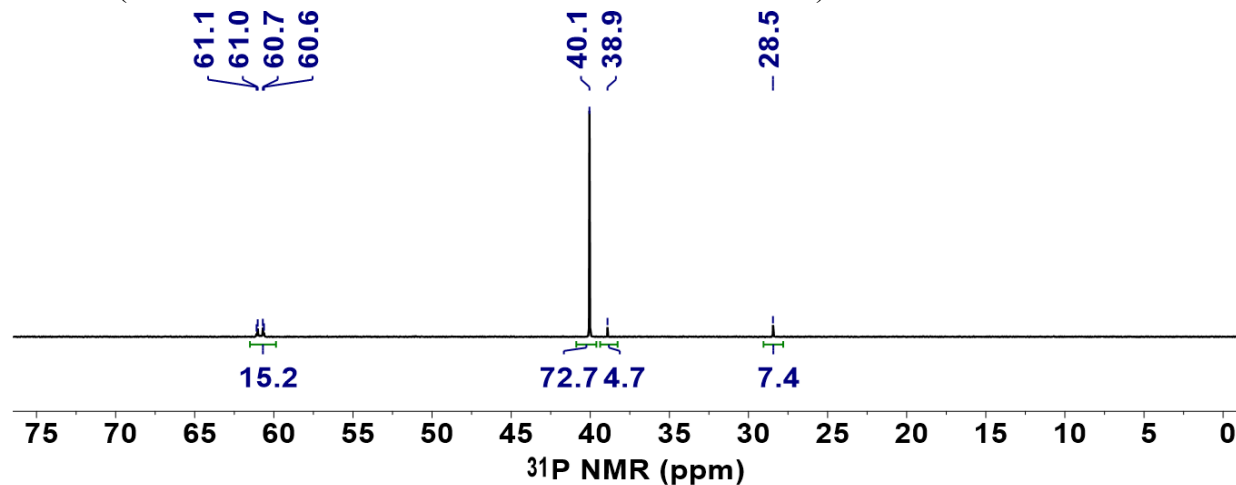


Figure S73. ^1H NMR spectra (in C_6D_6 at room temperature) of $(\text{acriPNP})\text{Ni}\cdot\text{C}_{10}\text{H}_8$ (**1** $\cdot\text{C}_{10}\text{H}_8$) collected after mixing for (a) 0 hr, (b) 12 hrs and (c) 24 hrs at room temperature (●: **1**, ●: C_6D_6 , ●: C_{10}H_8).

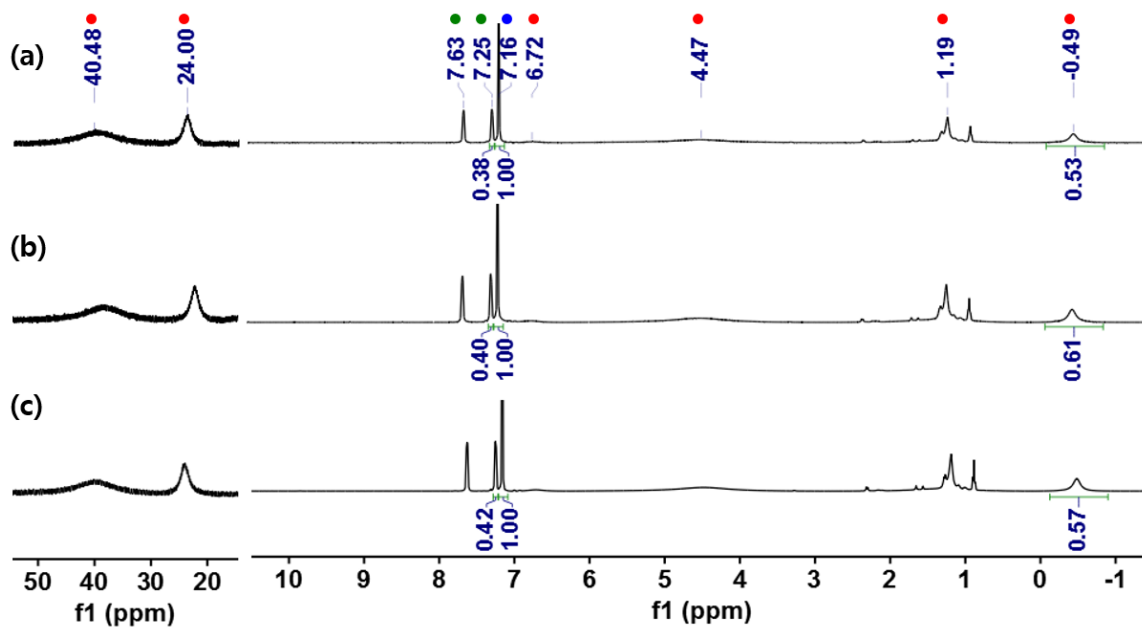


Figure S74. ^1H NMR spectra (in C_6D_6 at room temperature) of $(^{\text{acri}}\text{PNP})\text{Ni}\cdot\text{C}_{10}\text{H}_8$ ($\mathbf{1}\cdot\text{C}_{10}\text{H}_8$) collected after heating at $60\text{ }^\circ\text{C}$ for (a) 0 hr, (b) 12 hrs and (c) 24 hrs at room temperature (●: $\mathbf{1}$, ●: C_6D_6 , ●: C_{10}H_8).

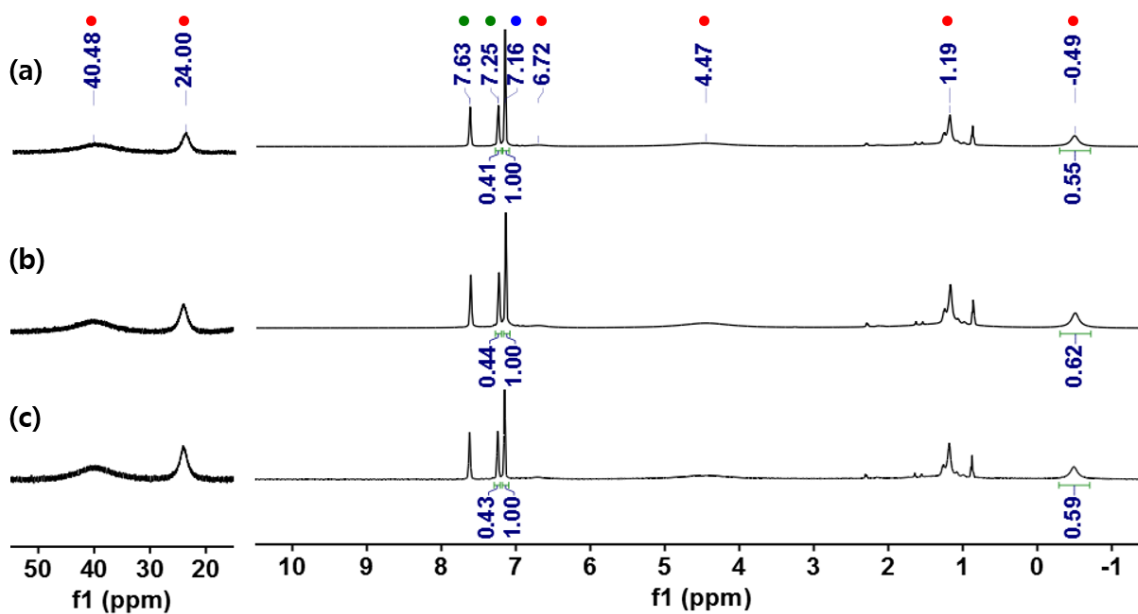


Figure S75. ^1H NMR spectra (in $\text{C}_6\text{D}_6/\text{THF-}d_8$ at room temperature) of $(^{\text{acri}}\text{PNP})\text{Ni}\cdot\text{C}_{10}\text{H}_8$ ($\mathbf{1}\cdot\text{C}_{10}\text{H}_8$) and $\text{NaBAR}^{\text{F}}_4$ collected after mixing at room temperature for (a) 0 hr, (b) 12 hrs and (c) 24 hrs (●: $\mathbf{1}$, ●: C_6D_6 , ●: C_{10}H_8).

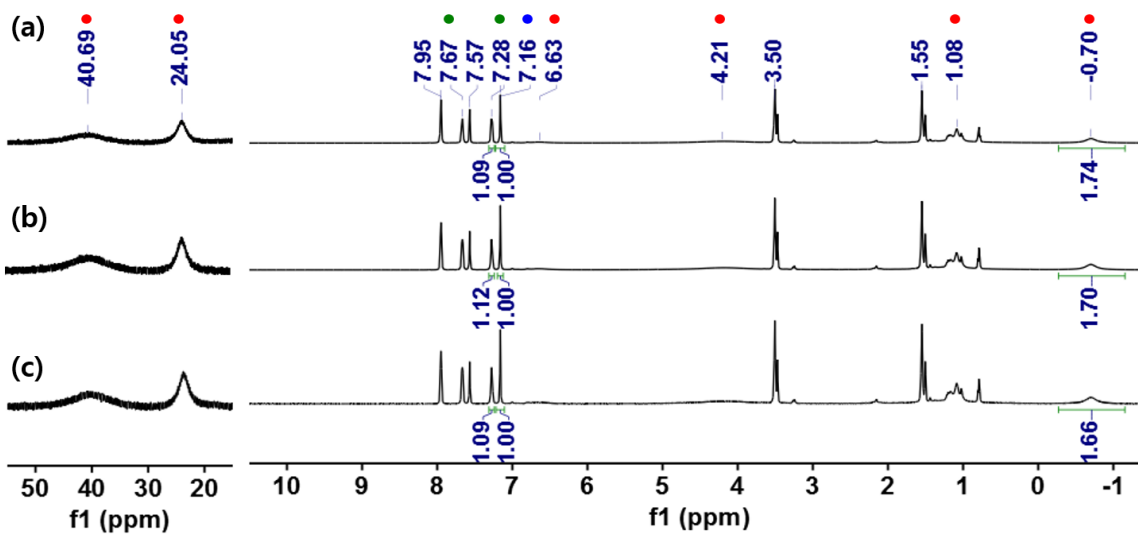


Figure S76. ^1H NMR spectra (in $\text{C}_6\text{D}_6/\text{THF-}d_8$ at room temperature) of $(\text{acriPNP})\text{Ni}\cdot\text{C}_{10}\text{H}_8$ ($\mathbf{1}\cdot\text{C}_{10}\text{H}_8$) and $\text{NaBAR}^{\text{F}}_4$ collected after heating at $60\text{ }^\circ\text{C}$ for (a) 0 hr, (b) 12 hrs and (c) 24 hrs (●: $\mathbf{1}$, ●: C_6D_6 , ●: C_{10}H_8).

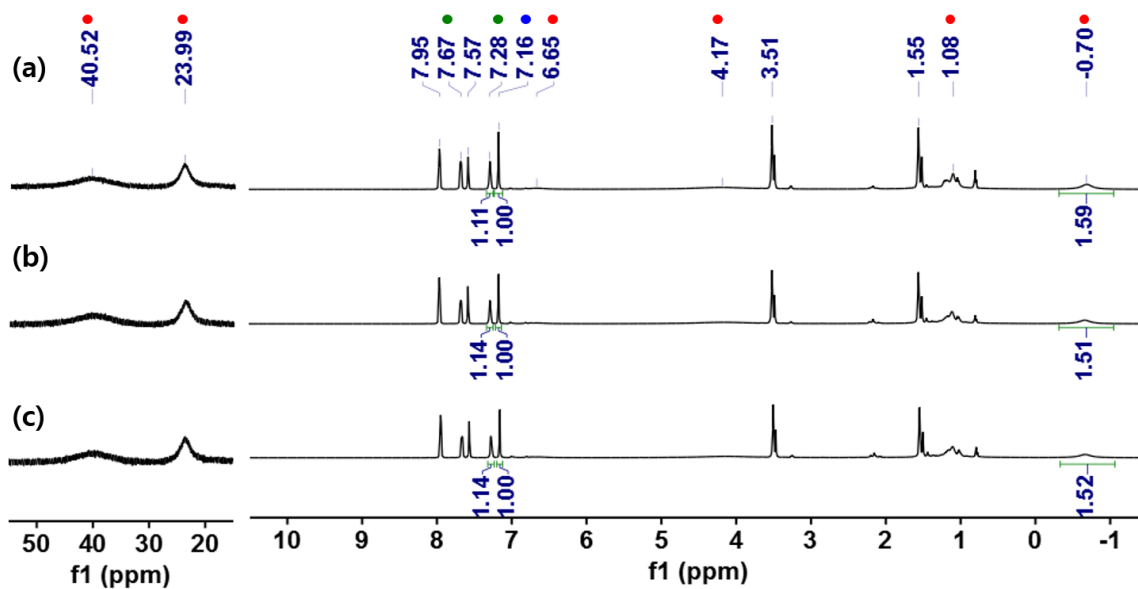


Figure S77. MAS ^{23}Na NMR spectra of (a) NaH isolated from the reaction of $\mathbf{2}$ and benzene, (b) authentic NaH , (c) NaOH solution in H_2O and (d) NaCl at room temperature.

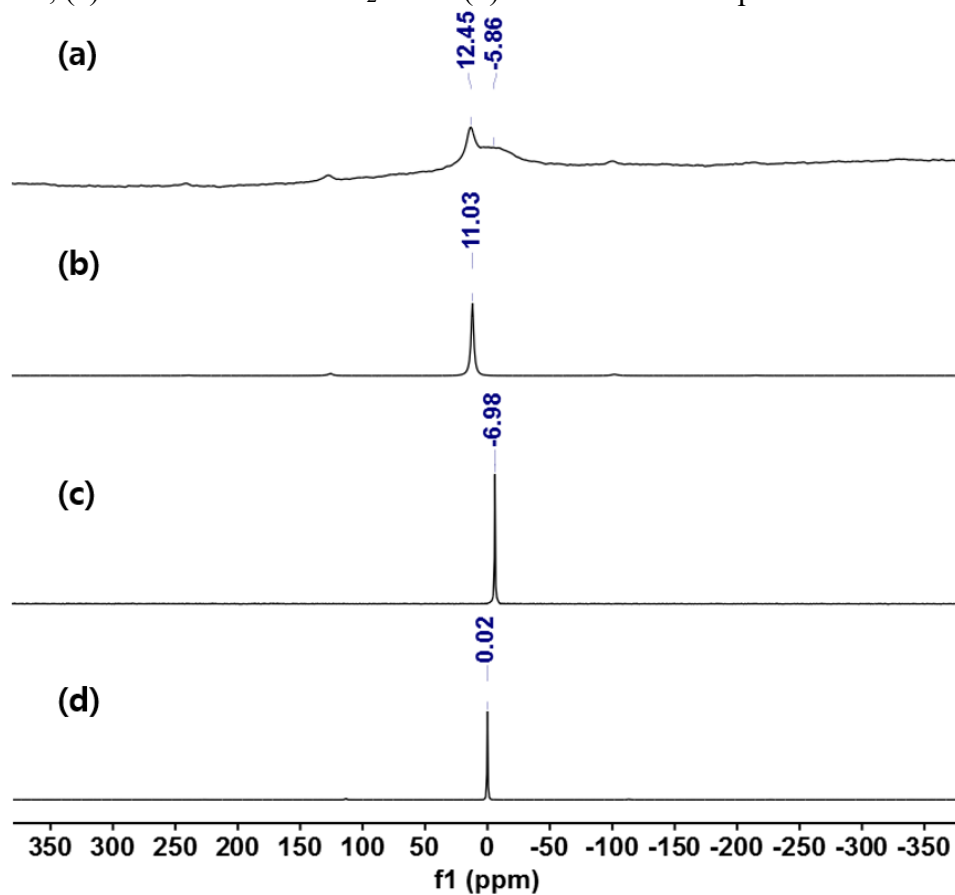


Figure S78. Reaction of $\{(\text{acriPNP})\text{Ni}-(\text{N}_2)-\text{Na}(\text{THF})_2\}_2$ (**2**) with toluene followed by (a) ^{31}P NMR spectroscopy (in toluene/ $\text{THF-}d_8$ at room temperature) and (b) X-band EPR spectroscopy (in toluene/ $\text{THF-}d_8$ at room temperature, collected at 10 K) for 5 min, 25 min and 2 hrs.

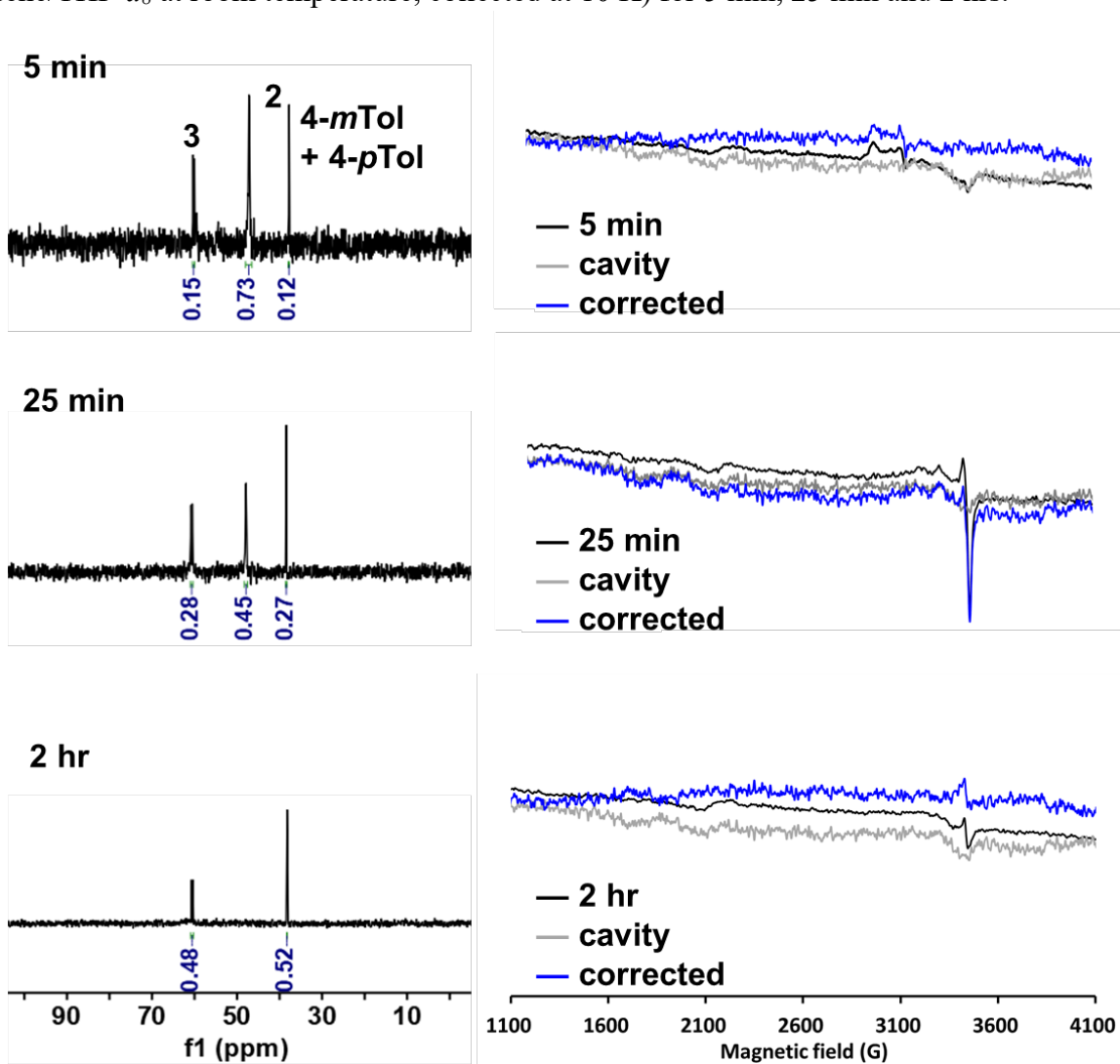


Figure S80. Solid-state structure of (^{acri}PNP)NiPh (**4-Ph**). Hydrogen atoms are omitted for clarity.

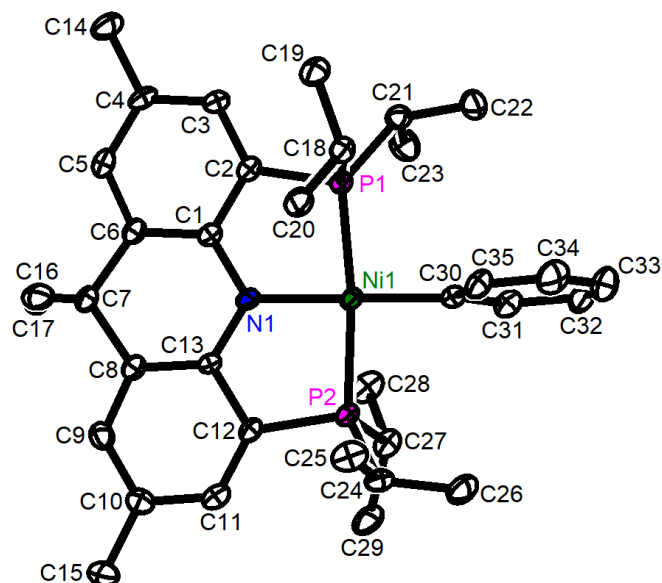


Table S2. Selected bond distances and angles for (^{acri}PNP)NiPh (**4-Ph**) (Å and °).

Bond distance		Bond angle	
$d_{\text{Ni1-N1}}$	1.934(3)	$\angle\text{N1-Ni1-C30}$	178.4(2)
$d_{\text{Ni1-P1}}$	2.162(1)	$\angle\text{P1-Ni1-P2}$	172.13(4)
$d_{\text{Ni1-P2}}$	2.163(1)	$\angle\text{N1-Ni1-P1}$	86.2(1)
$d_{\text{Ni1-C30}}$	1.902(4)	$\angle\text{N1-Ni1-P2}$	86.3(1)

Figure S81. Solid-state structure of (^{acri}PNP)Ni(2-naphthyl) (**4-Naph**). Hydrogen atoms are omitted for clarity.

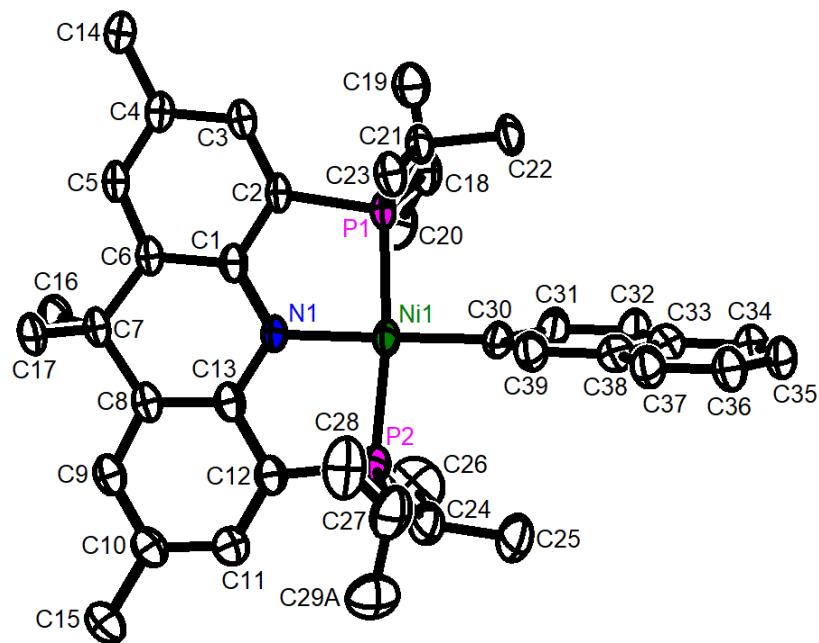


Table S3. Selected bond distances and angles for (^{acri}PNP)Ni(2-naphthyl) (**4-Naph**) (Å and °).

Bond distance		Bond angle	
$d_{\text{Ni1-N1}}$	1.927(2)	$\angle\text{N1-Ni1-C30}$	179.0(1)
$d_{\text{Ni1-P1}}$	2.1582(8)	$\angle\text{P1-Ni1-P2}$	172.09(3)
$d_{\text{Ni1-P2}}$	2.1625(9)	$\angle\text{N1-Ni1-P1}$	86.30(7)
$d_{\text{Ni1-C30}}$	1.900(2)	$\angle\text{N1-Ni1-P2}$	86.46(7)

Figure S82. Solid-state structure of (^{acri}PNP)Ni(2-anthracenyl) (**4-Anth**). Hydrogen atoms are omitted for clarity.

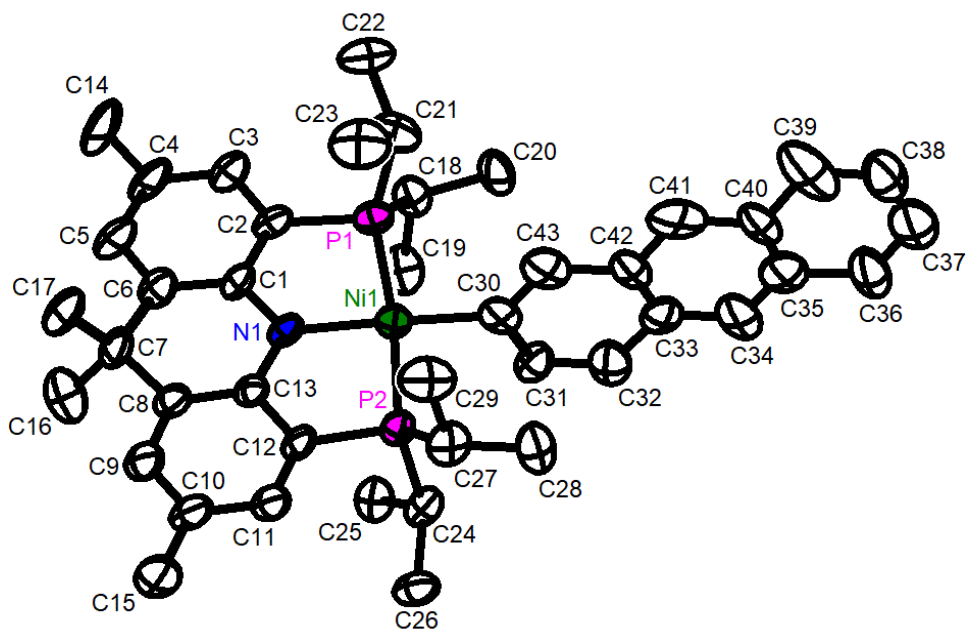


Table S4. Selected bond distances and angles for (^{acri}PNP)Ni(2-anthracenyl) (**4-Anth**) (Å and °).

Bond distance		Bond angle	
$d_{\text{Ni1-N1}}$	1.9241(1)	$\angle\text{N1-Ni1-C30}$	178.073(2)
$d_{\text{Ni1-P1}}$	2.1624(1)	$\angle\text{P1-Ni1-P2}$	171.896(2)
$d_{\text{Ni1-P2}}$	2.1626(1)	$\angle\text{N1-Ni1-P1}$	86.755(2)
$d_{\text{Ni1-C30}}$	1.9084(1)	$\angle\text{N1-Ni1-P2}$	86.227(2)

Figure S83. Solid-state structure of (^{acri}PNP)Ni(*o*-tolyl) (**4-*o*Tol**). Hydrogen atoms are omitted for clarity.

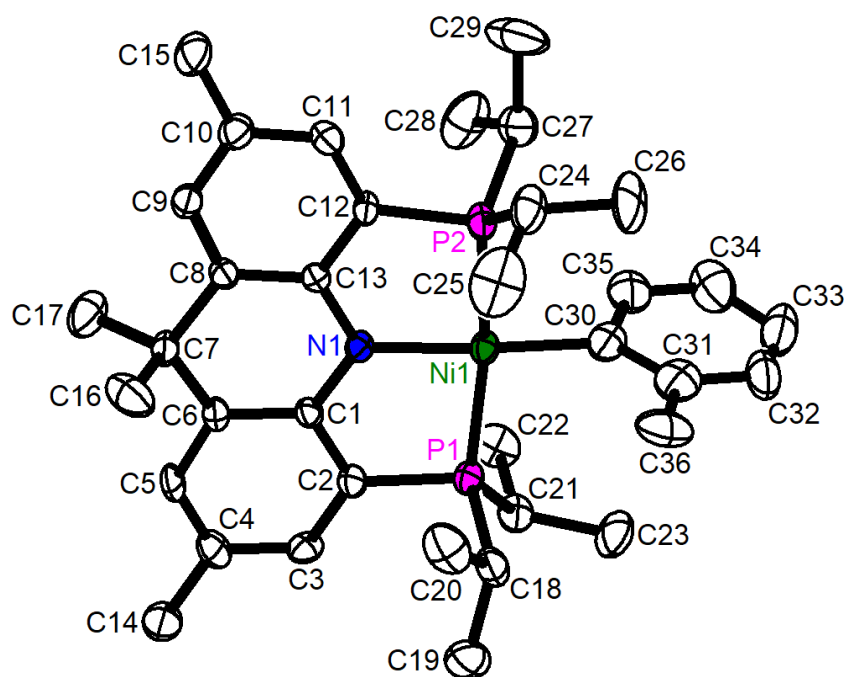


Table S5. Selected bond distances and angles for (^{acri}PNP)Ni(*o*-tolyl) (**4-*o*Tol**) (Å and °).

Bond distance		Bond angle	
$d_{\text{Ni1-N1}}$	1.934(5)	$\angle\text{N1-Ni1-C30}$	173.2(3)
$d_{\text{Ni1-P1}}$	2.184(2)	$\angle\text{P1-Ni1-P2}$	171.21(8)
$d_{\text{Ni1-P2}}$	2.184(1)	$\angle\text{N1-Ni1-P1}$	86.2(2)
$d_{\text{Ni1-C30}}$	1.950(9)	$\angle\text{N1-Ni1-P2}$	86.1(2)

Figure S84. Solid-state structure of (^{acri}PNP)Ni(*m*-tolyl) (**4-*m*Tol**). Hydrogen atoms are omitted for clarity.

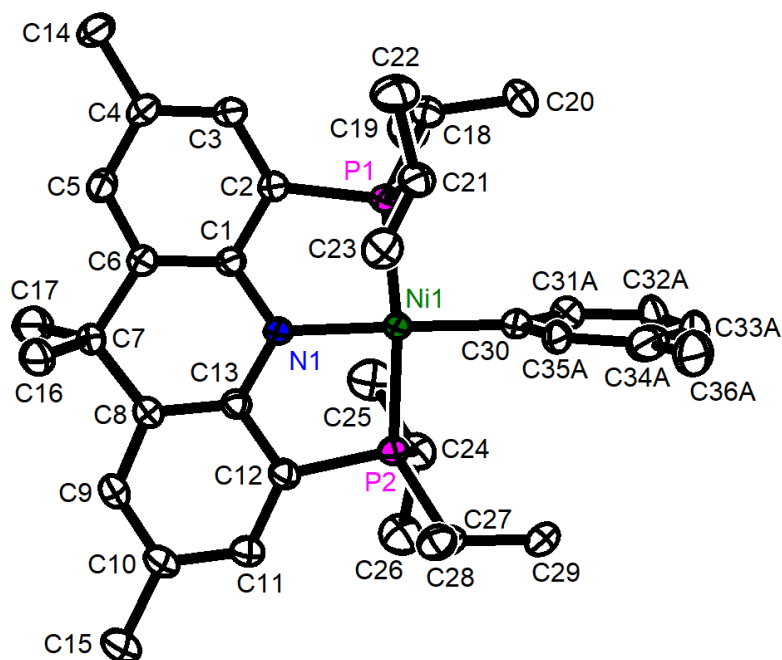


Table S6. Selected bond distances and angles for (^{acri}PNP)Ni(*m*-tolyl) (**4-*m*Tol**) (Å and °).

Bond distance		Bond angle	
$d_{\text{Ni1-N1}}$	1.9241(1)	$\angle\text{N1-Ni1-C30}$	178.073(2)
$d_{\text{Ni1-P1}}$	2.1624(1)	$\angle\text{P1-Ni1-P2}$	171.896(2)
$d_{\text{Ni1-P2}}$	2.1626(1)	$\angle\text{N1-Ni1-P1}$	86.755(2)
$d_{\text{Ni1-C30}}$	1.9084(1)	$\angle\text{N1-Ni1-P2}$	86.227(2)

Figure S85. Solid-state structure of (^{acri}PNP)Ni(*p*-tolyl) (**4-*p*Tol**). Hydrogen atoms are omitted for clarity.

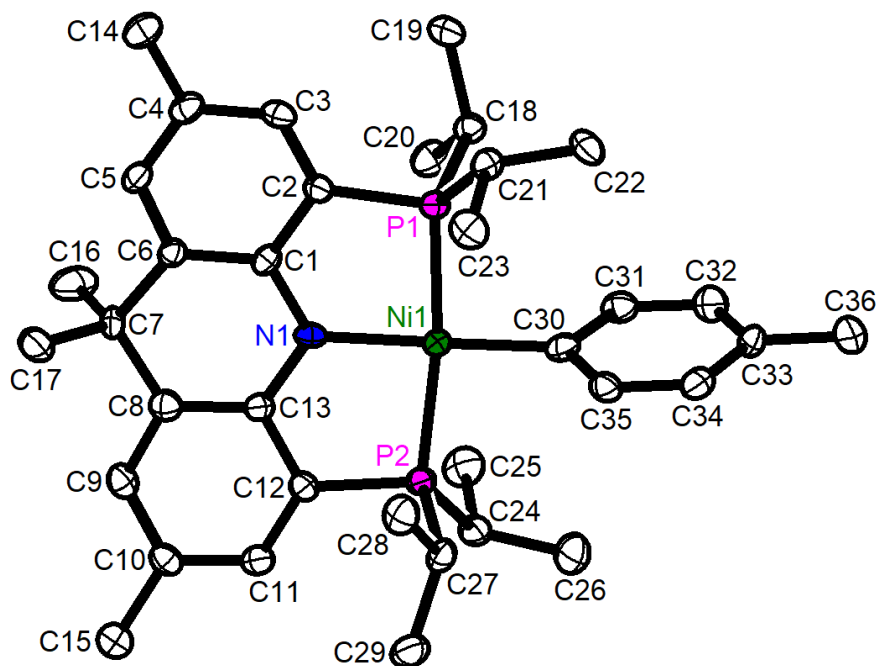


Table S7. Selected bond distances and angles for (^{acri}PNP)Ni(*p*-tolyl) (**4-*p*Tol**) (Å and °).

Bond distance		Bond angle	
$d_{\text{Ni1-N1}}$	1.933(5)	$\angle\text{N1-Ni1-C30}$	178.5(2)
$d_{\text{Ni1-P1}}$	2.169(2)	$\angle\text{P1-Ni1-P2}$	172.26(7)
$d_{\text{Ni1-P2}}$	2.167(2)	$\angle\text{N1-Ni1-P1}$	86.6(2)
$d_{\text{Ni1-C30}}$	1.908(6)	$\angle\text{N1-Ni1-P2}$	86.2(2)

Figure S86. Solid-state structure of (^{acri}PNP)Ni(benzyl). Hydrogen atoms are omitted for clarity.

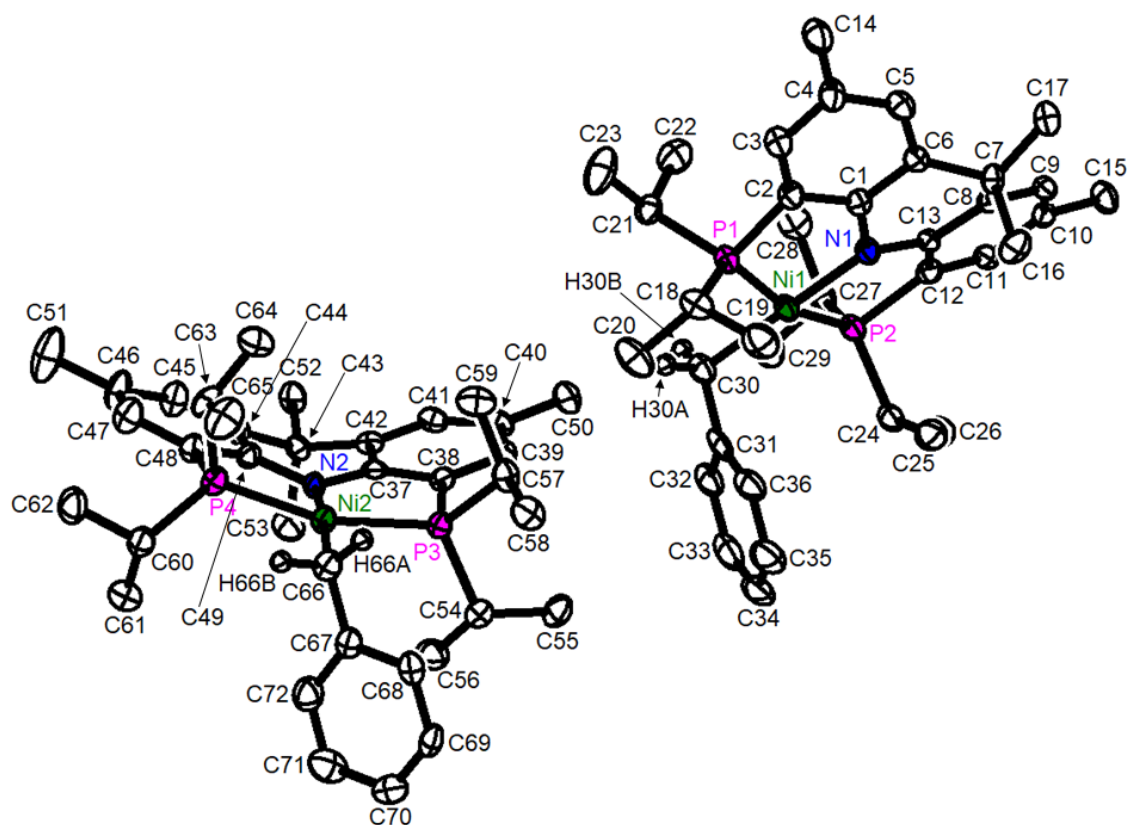


Table S8. Selected bond distances and angles for (^{acri}PNP)Ni(benzyl) (Å and °).

Bond distance		Bond angle	
$d_{\text{Ni1-N1}}$	1.924(4)	$\angle\text{N1-Ni1-C30}$	176.9(2)
$d_{\text{Ni1-P1}}$	2.178(2)	$\angle\text{P1-Ni1-P2}$	165.11(6)
$d_{\text{Ni1-P2}}$	2.213(2)	$\angle\text{N1-Ni1-P1}$	86.1(1)
$d_{\text{Ni1-C30}}$	2.008(5)	$\angle\text{N1-Ni1-P2}$	85.3(1)
$d_{\text{Ni2-N2}}$	1.938(4)	$\angle\text{N2-Ni2-C66}$	173.3(2)
$d_{\text{Ni2-P3}}$	2.174(2)	$\angle\text{P3-Ni2-P4}$	163.01(6)
$d_{\text{Ni2-P4}}$	2.199(2)	$\angle\text{N2-Ni2-P3}$	85.6(1)
$d_{\text{Ni2-C66}}$	1.990(5)	$\angle\text{N2-Ni2-P4}$	85.9(1)

Figure S87. Solid-state structure of (^{acri}PNP)Ni(CH=CH₂) (**5**). Hydrogen atoms are omitted for clarity. Asymmetric unit contains two molecules of (^{acri}PNP)Ni(CH=CH₂). The one on the left shows crystallographic positional disorder at the vinyl ligand.

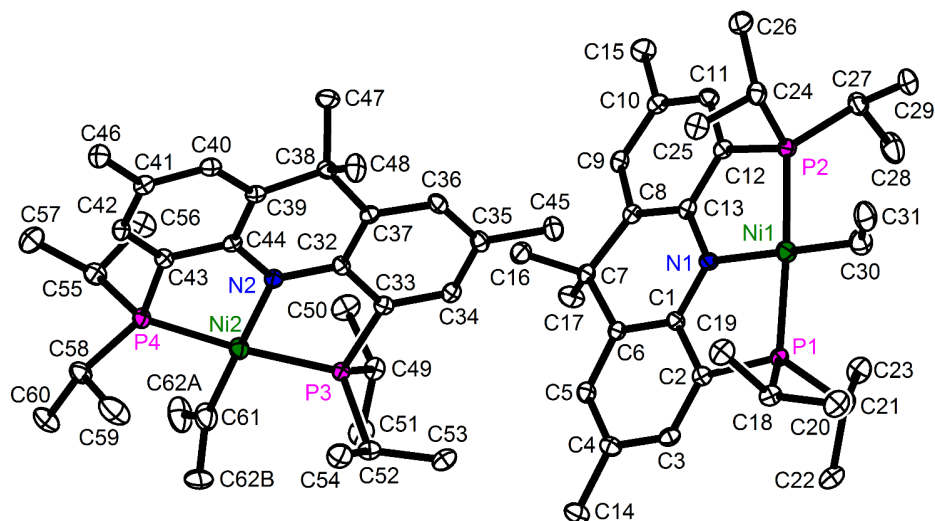


Table S9. Selected bond distances and angles for (^{acri}PNP)Ni(CH=CH₂) (**5**) (Å and °).

Bond distance		Bond angle	
d _{Ni1-N1}	1.932(2)	∠N1-Ni1-C30	178.52(12)
d _{Ni1-P1}	2.1611(8)	∠P1-Ni1-P2	172.43(3)
d _{Ni1-P2}	2.1677(8)	∠N1-Ni1-P1	86.42(7)
d _{Ni1-C30}	1.890(3)	∠N1-Ni1-P2	86.81(7)
d _{C30-C31}	1.337(4)	∠Ni1-C30-C31	129.9(3)
d _{Ni2-N2}	1.933(2)	∠N2-Ni2-C61	179.14(12)
d _{Ni2-P3}	2.1644(8)	∠P3-Ni2-P4	172.96(3)
d _{Ni2-P4}	2.1679(8)	∠N2-Ni2-P3	86.63(7)
d _{Ni2-C60}	1.894(3)	∠N2-Ni2-P4	86.55(7)
d _{C61-C62a}	1.313(5)	∠Ni2-C61-C62a	131.1(3)
d _{C61-C62b}	1.268(13)	∠Ni2-C61-C62b	137.2(8)

Figure S88. Core structures of (a) **2**, (b) $\{\text{Na}\}\{(\text{acriPnP})\text{Ni}(\text{CO})\}$, (c) $\{\text{Na}(\text{12-crown-4})_2\}\{(\text{acriPnP})\text{Ni}(\text{CO})\}^6$ and (d) $(\text{acriPnP})\text{NiCl}$.¹ The distances of a nitrogen atom from the red plane defined by two carbon and one nickel are shown.

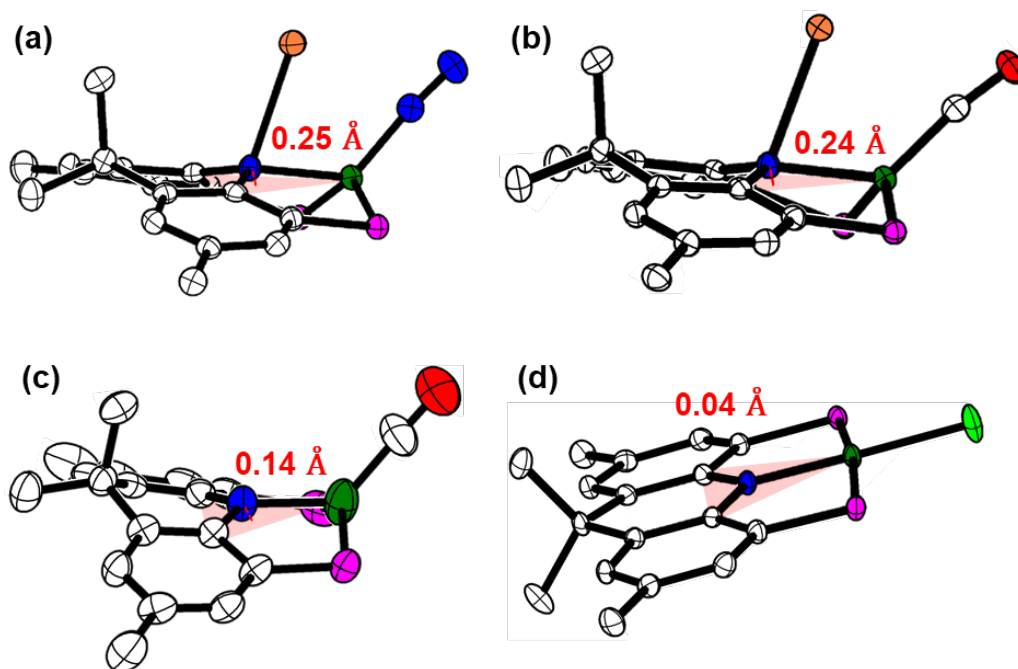


Figure S89. Structural comparisons of $\{(\text{acriPnP})\text{Ni}(\text{N}_2)\text{Na}(\text{THF})_2\}_2$ (**2**, black) with two different nickel species; $(\text{acriPnP})\text{Ni}\cdot\text{C}_{10}\text{H}_8$ (**1**· C_{10}H_8 , blue),¹ and $(\text{acriPnP})\text{NiPh}$ (**4-Ph**, red) based on the XRD data; bond lengths in Å.

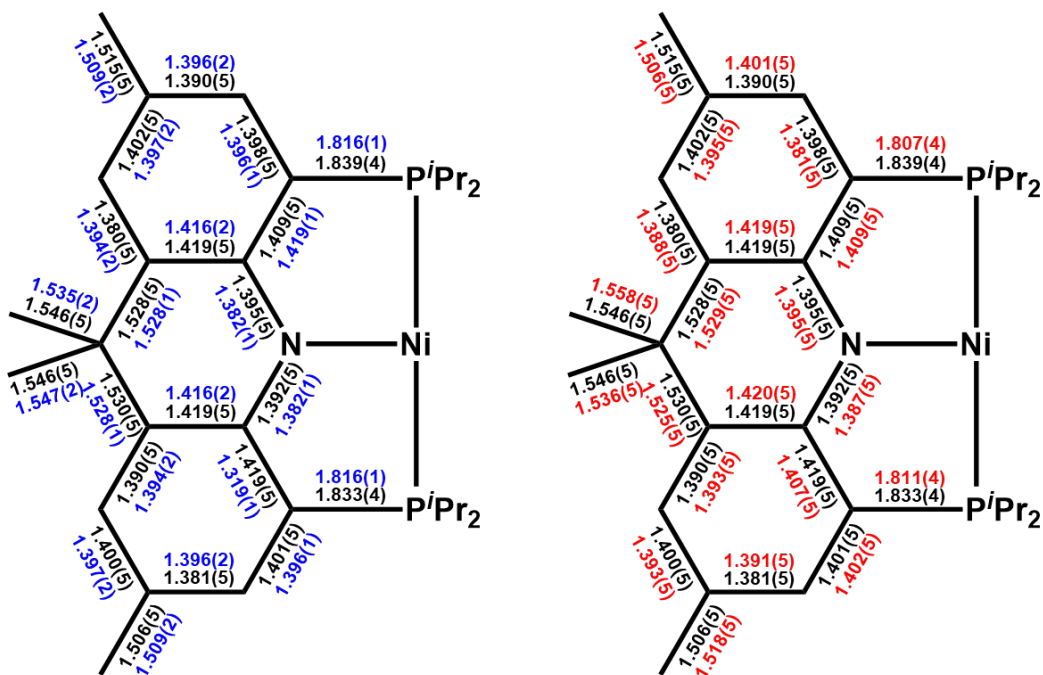


Figure S90. UV-Vis spectra of $\{(\text{acriPNP})\text{Ni}-(\text{N}_2)-\text{Na}(\text{THF})_2\}_2$ (**2**, red line), $(\text{acriPNP})\text{NiPh}$ (**4-Ph**, blue line), $(\text{acriPNP})\text{Ni}(2\text{-naphthyl})$ (**4-Naph**, green line) and $(\text{acriPNP})\text{Ni}(2\text{-anthracenyl})$ (**4-Anth**, dotted black line) in THF at room temperature.

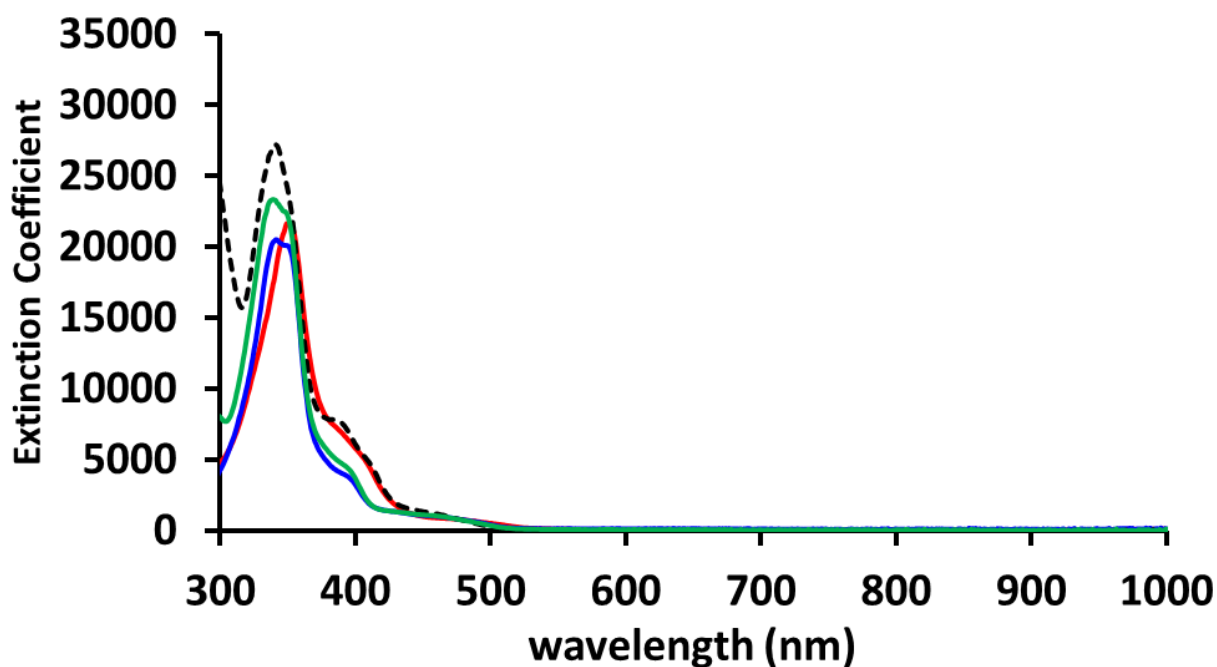


Figure S91. UV-Vis spectra of $(\text{acriPNP})\text{Ni}(o\text{-tolyl})$ (**4-*o*Tol**, red line), and $(\text{acriPNP})\text{Ni}(m\text{-tolyl})$ (**4-*m*Tol**, blue line), $(\text{acriPNP})\text{Ni}(p\text{-tolyl})$ (**4-*p*Tol**, green line) and $(\text{acriPNP})\text{Ni}(\text{benzyl})$ (dotted black line) in THF at room temperature.

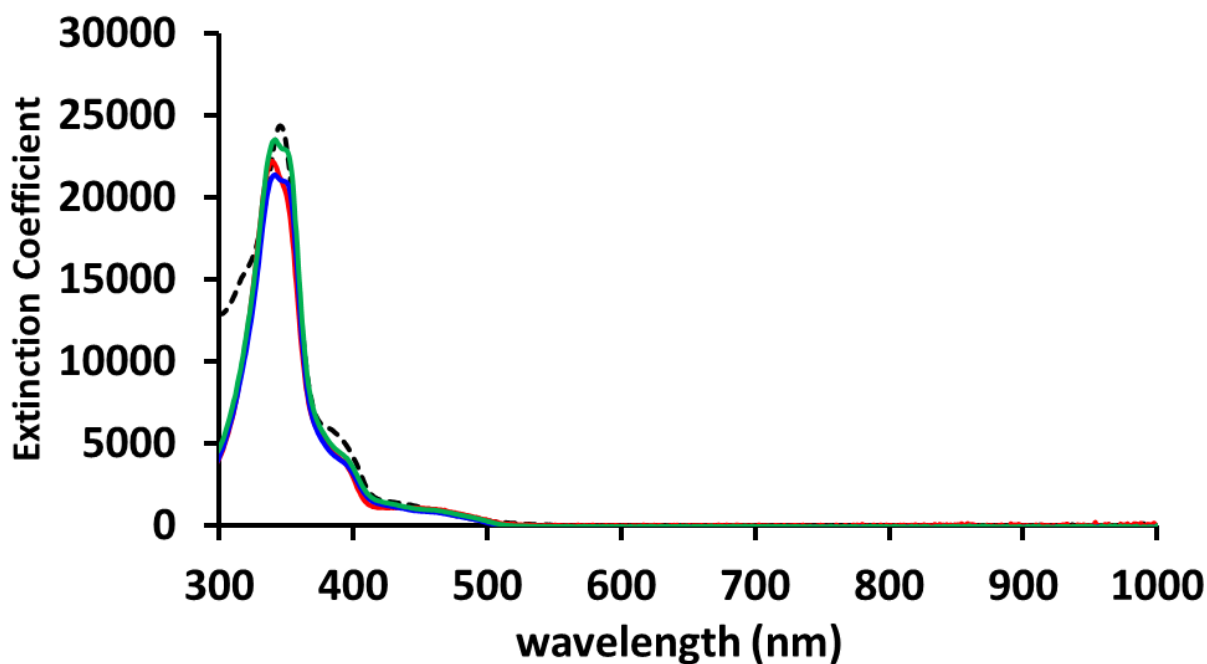


Figure S92. Calibration curve of the benzophenone radical in THF at room temperature.

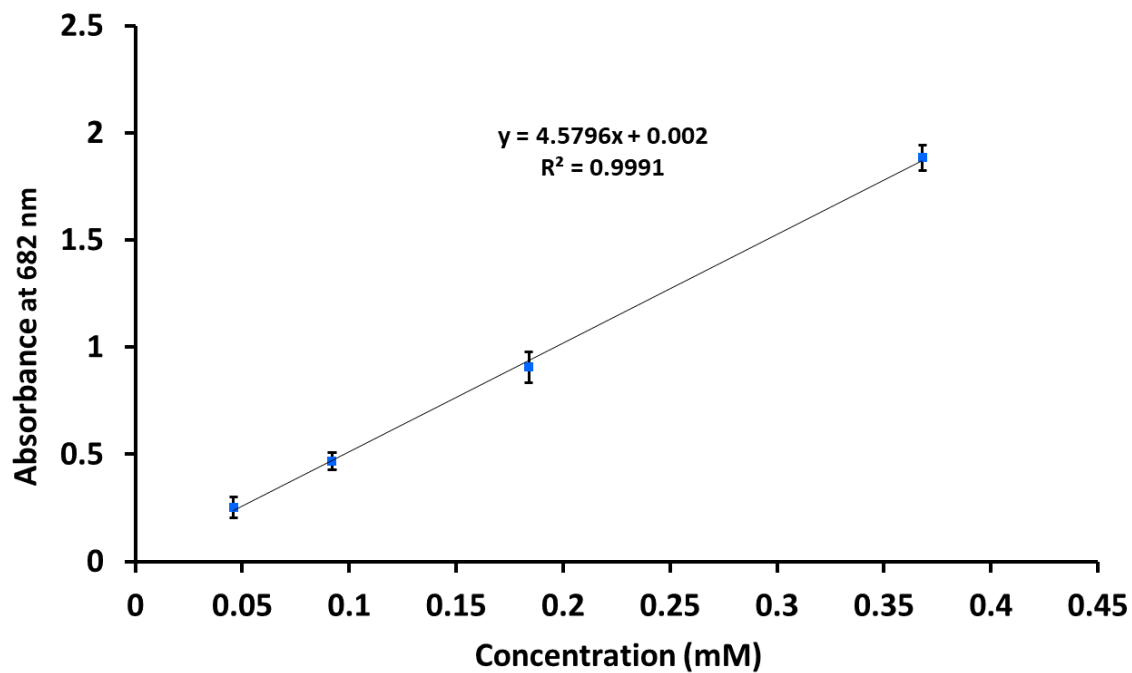


Figure S93. UV-Vis spectra of benzophenone radical in THF at room temperature with various concentrations.

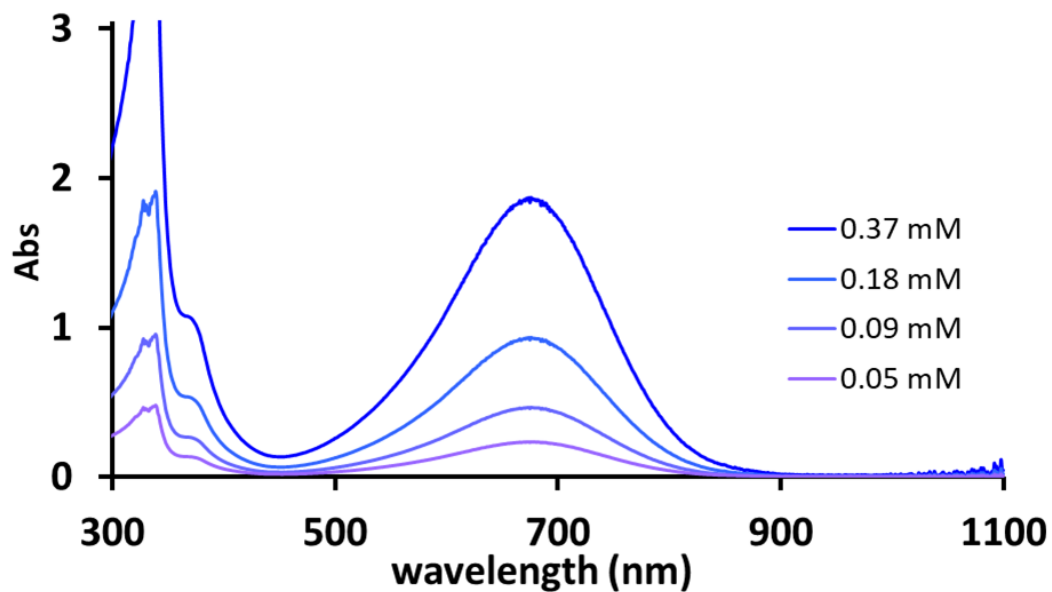


Figure S94. UV-Vis spectrum of [Na(18-crown-6)DME][C₁₀H₈] in THF at room temperature.¹¹

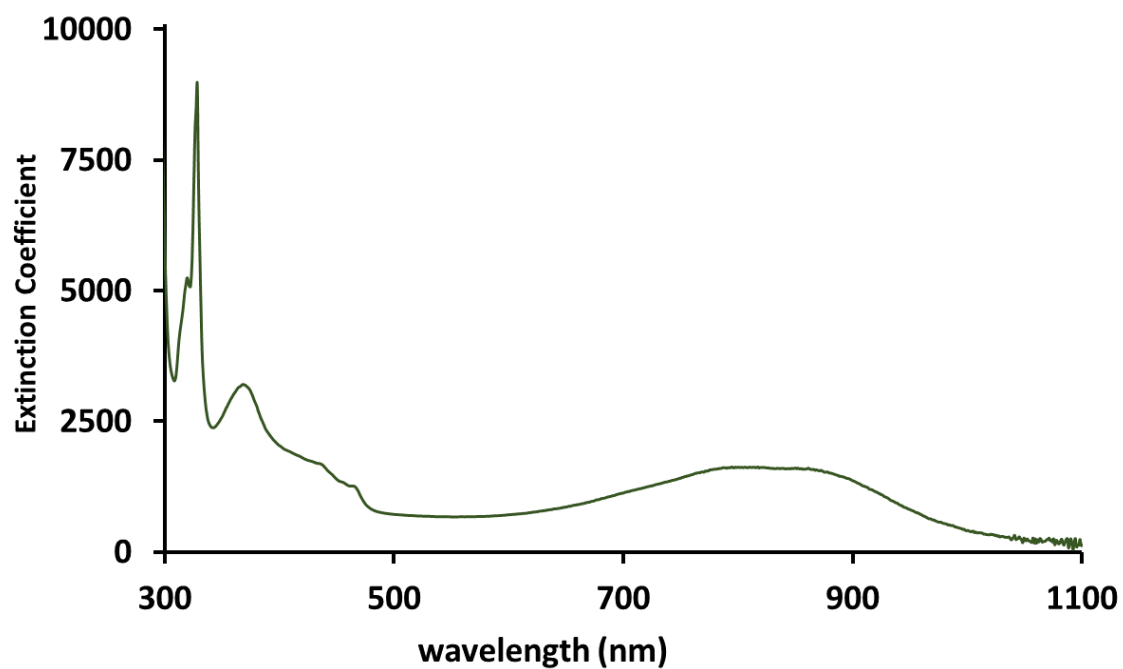


Figure S95. Photo images of (a) NH₃(l) and the solution of (b) a black powder isolated from the reaction of **2** in benzene and (c) an authentic sample of Na(0) in NH₃(l).

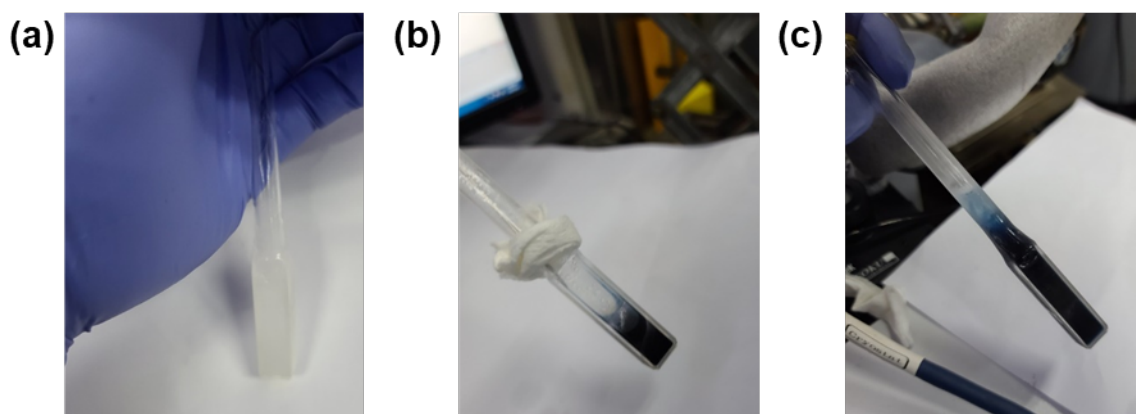


Figure S96. Plots of the normalized signal intensities (I/I_0) versus gradient strength (G) (a) and plots of $\ln(I/I_0)$ versus G^2 (b). The corresponding data obtained from pulsed gradient spin echo experiments for $\{(\text{acriPNP})\text{Ni}-(\text{N}_2)-\text{Na}(\text{THF})_2\}_2$ (**2**, blue), $(\text{acriPNP})\text{NiPh}$ (**4-Ph**, black), $(\text{acriPNP})\text{Ni}(2\text{-naphthyl})$ (**4-Naph**, red) and $\{(\text{acriPNP})\text{Ni}\}_2\text{-}\mu\text{-CO}_2\text{-}\kappa^2\text{C},\text{O}$ (green) in $\text{THF-}d_8$ at room temperature.

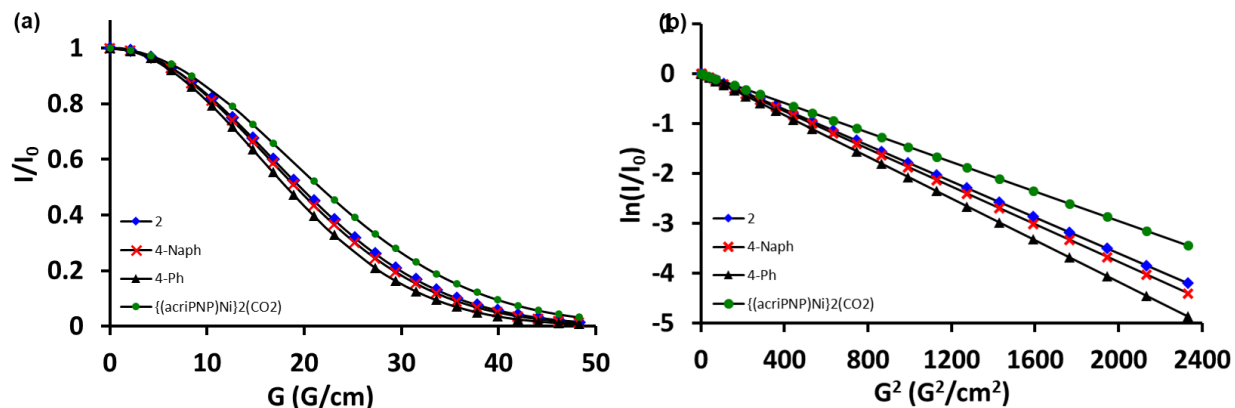


Table S10. Diffusion constants and hydrodynamic radii (R_{solution}) for **2**, **4-Ph**, **4-Naph** and $\{(\text{acriPNP})\text{Ni}\}_2\text{-}\mu\text{-CO}_2\text{-}\kappa^2\text{C},\text{O}$.⁶

Compound	Diffusion constant ($\times 10^{-10} \text{ m}^2 \text{ s}^{-1}$)	R_{solution} (\AA)
4-Ph	12.34	2.92
4-Naph	11.61	3.10
2	11.12	3.24
$\{(\text{acriPNP})\text{Ni}\}_2\text{-}\mu\text{-CO}_2\text{-}\kappa^2\text{C},\text{O}$	9.27	3.87

Figure S97. IR spectra of $\{(\text{acriPNP})\text{Ni}-(\text{N}_2)-\text{Na}(\text{THF})_2\}_2$ (**2**, red line), $\{(\text{acriPNP})\text{Ni}-(\text{N}_2)-\text{K}(\text{THF})_2\}_2$ (**2-K**, blue line) and $\{(\text{acriPNP})\text{Ni}-(\text{N}_2)-\text{Li}(\text{THF})_2\}_2$ (**2-Li**, green line) (KBr pellet).

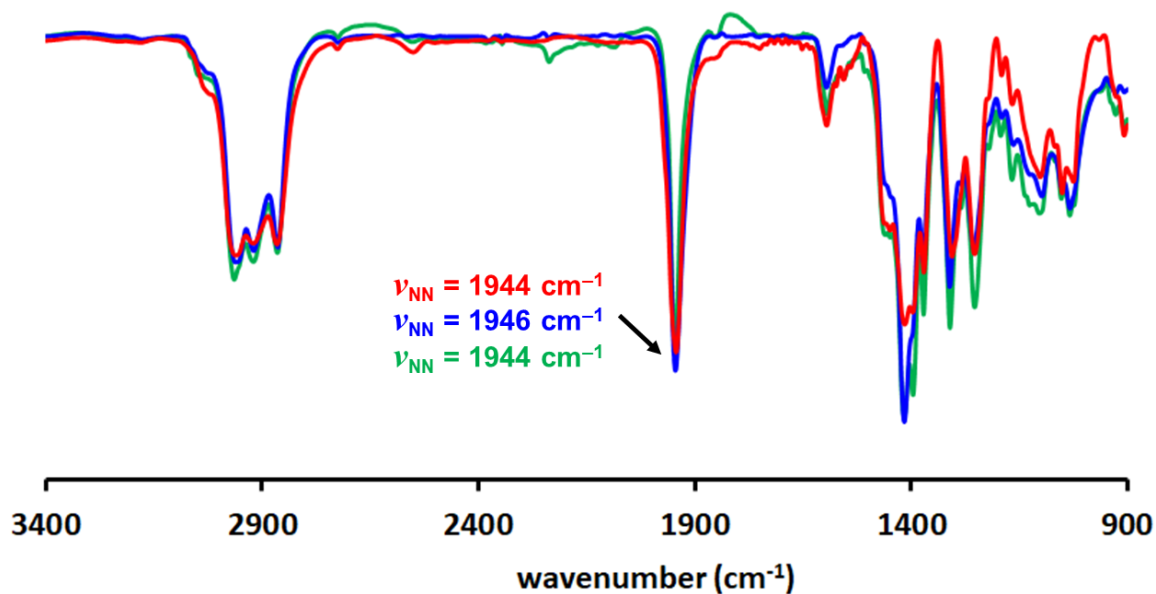


Figure S98. IR spectra of $(\text{acriPNP})\text{NiD}$ (**3-D**, red line), $(\text{acriPNP})\text{NiPh}$ (**4-Ph**, blue line) and $(\text{acriPNP})\text{NiPh-}d_5$ (**4-C₆D₅**, green line) (KBr pellet).

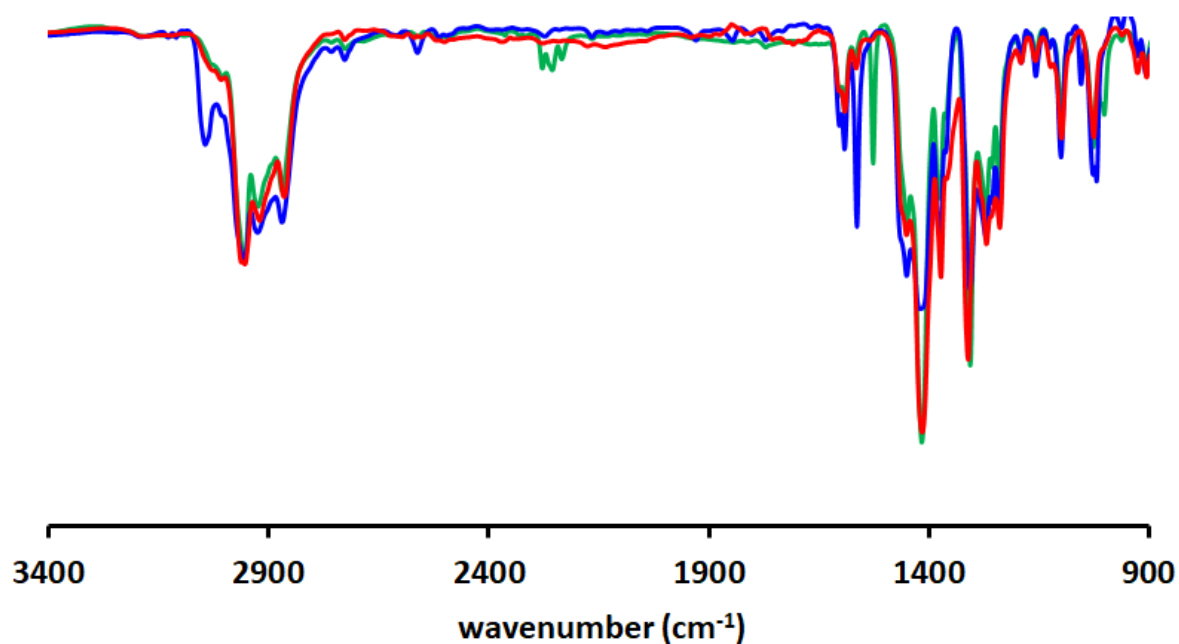


Figure S99. IR spectra of (^{acri}PNP)Ni(2-naphthyl) (**4-Naph**, red line) and (^{acri}PNP)Ni(2-anthracenyl) (**4-Anth**, blue line) (KBr pellet).

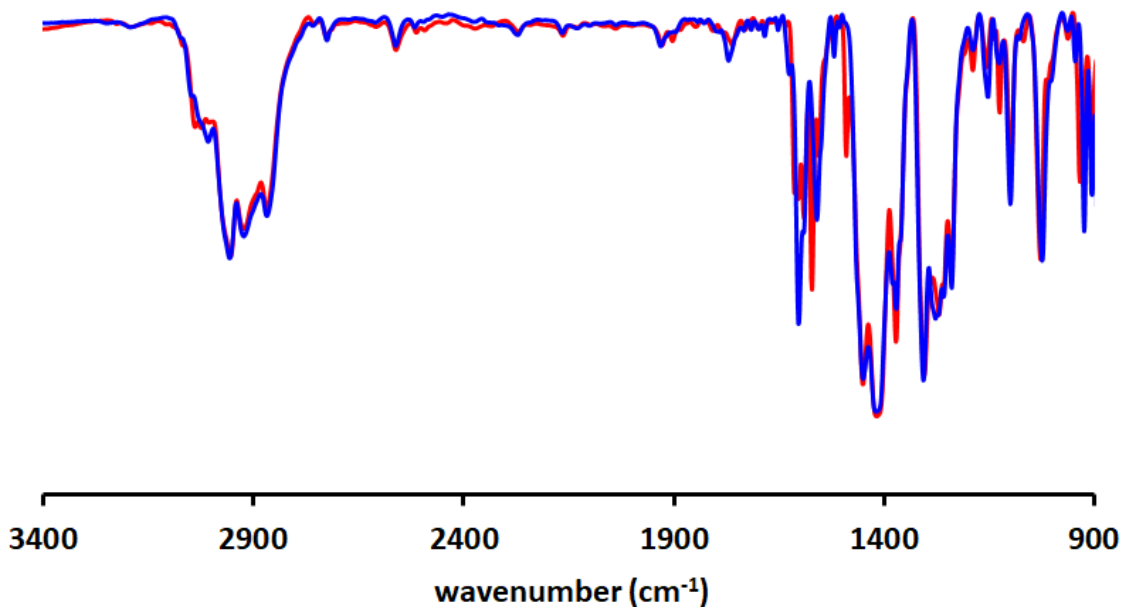


Figure S100. IR spectra of (^{acri}PNP)Ni(*o*-tolyl) (**4-*o*Tol**, red line), (^{acri}PNP)Ni(*m*-tolyl) (**4-*m*Tol**, blue line), (^{acri}PNP)Ni(*p*-tolyl) (**4-*p*Tol**, green line) and (^{acri}PNP)Ni(benzyl) (dotted black line) (KBr pellet).

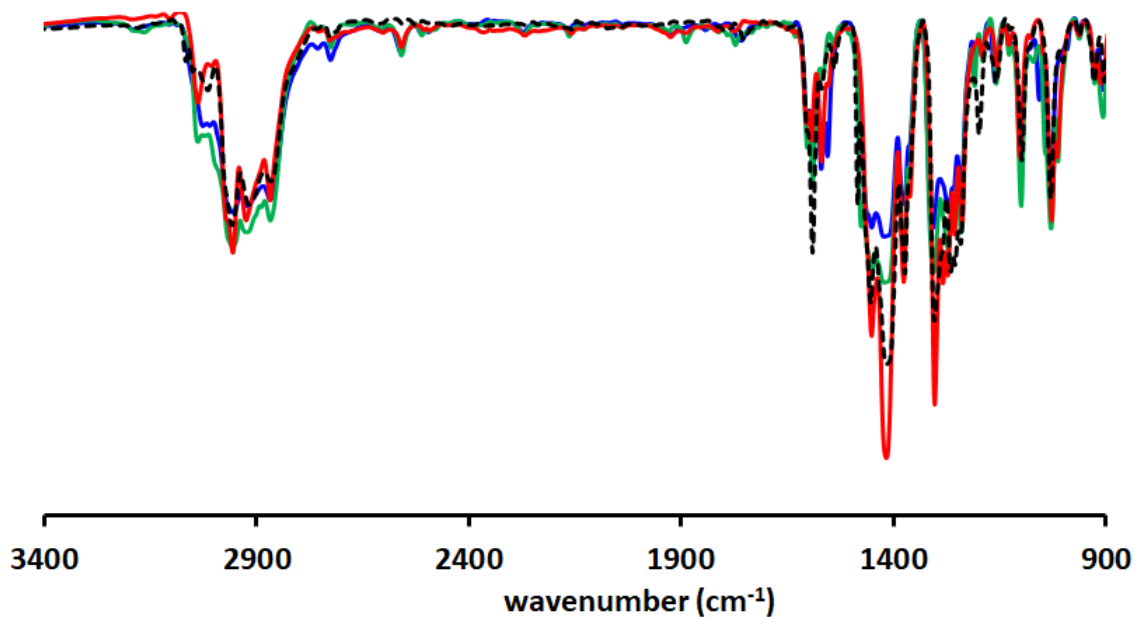


Figure S101. IR spectra of $(\text{acriPNP})\text{Ni}(\text{CH}=\text{CH}_2)$ (**5**, red) and $(\text{acriPNP})\text{NiPh}$ (**4-Ph**, blue) (top: full spectra, bottom: zoomed spectra, KBr pellet).

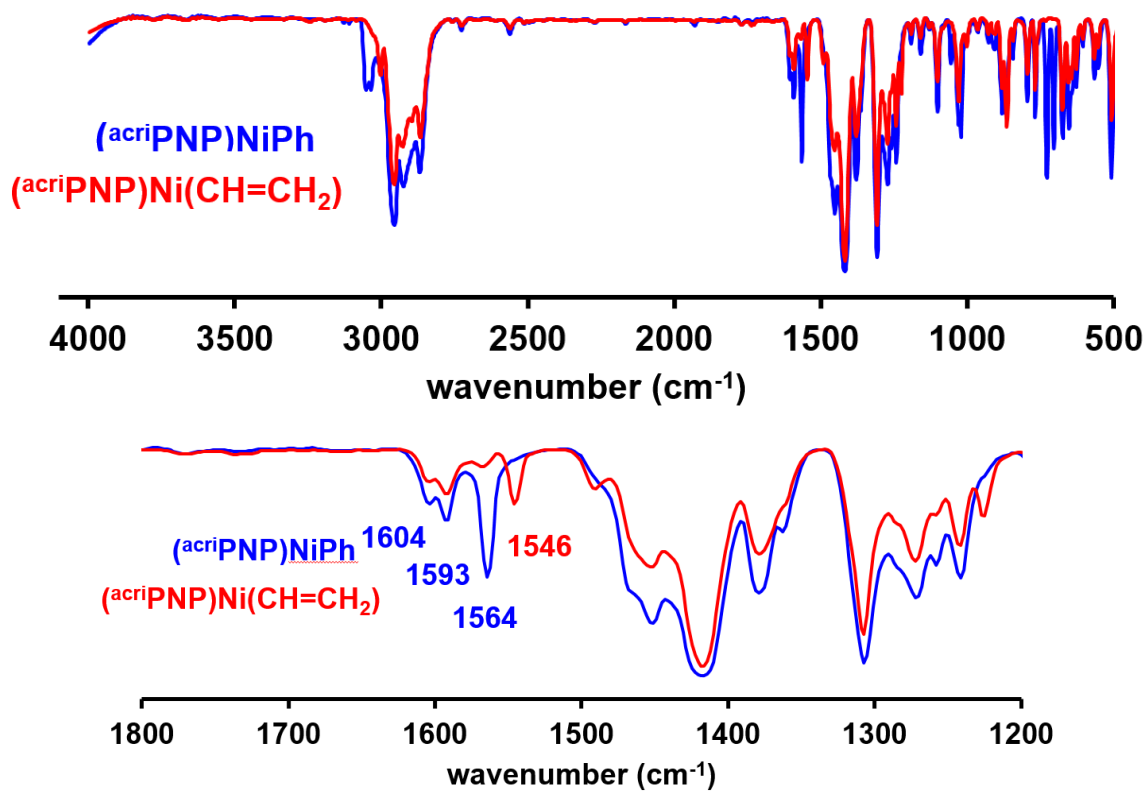


Figure S102. ESI MS of $(^{acri}PNP)Ni(CH=CH_2)$ (**5**). 0.25 mM THF solution.

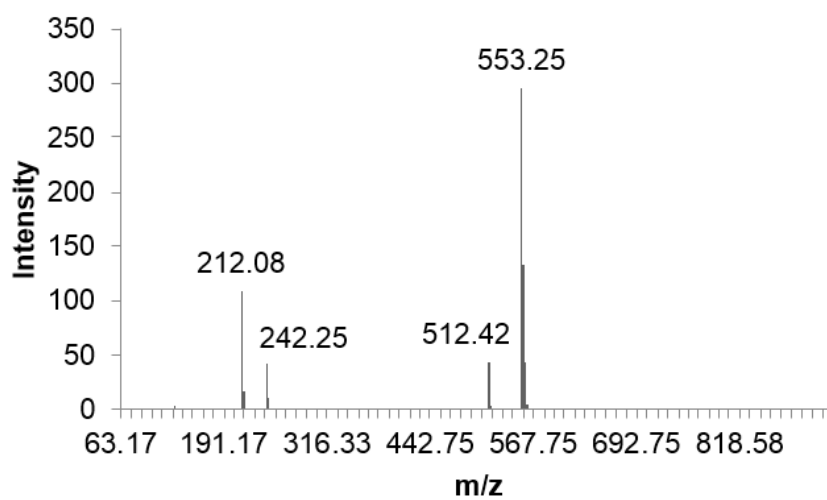
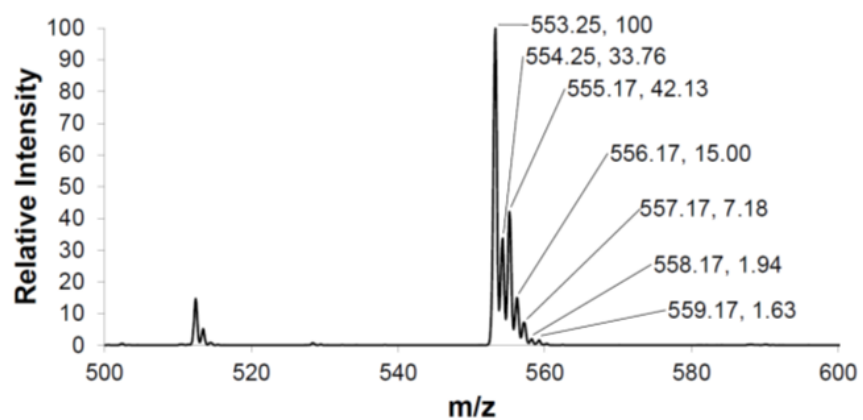


Figure S103. Cyclic voltammogram of $(^{acri}PNP)Ni \cdot C_{10}H_8$ (**1**• $C_{10}H_8$) with scan rates: 100, 200, 300, and 400 mV/s. $Ni^{II/I}$ couple at -1.10 V and $Ni^{I/0}$ couple at -2.75 V vs. Fc/Fc^+ were observed in THF with 0.3 M tetra-*n*-butylammonium hexafluorophosphate as an electrolyte.

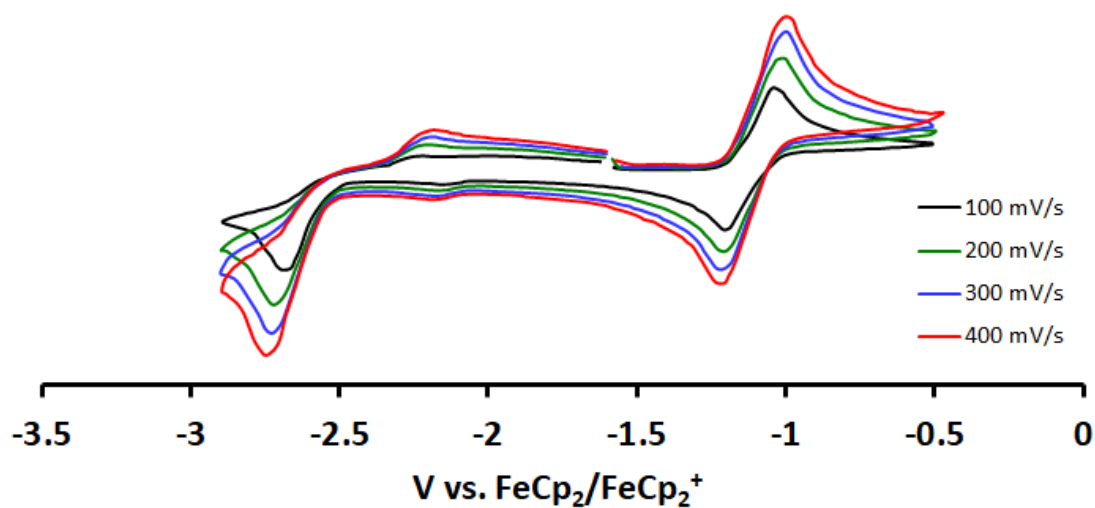


Figure S104. Cyclic voltammogram of $(^{acri}PNP)NiH$ (**3**) with scan rates: 100, 200, 300, and 400 mV/s. $Ni^{II/I}$ couple at -3.43 V vs. Fc/Fc^+ were observed in THF with 0.3 M tetra-*n*-butylammonium hexafluorophosphate as an electrolyte.

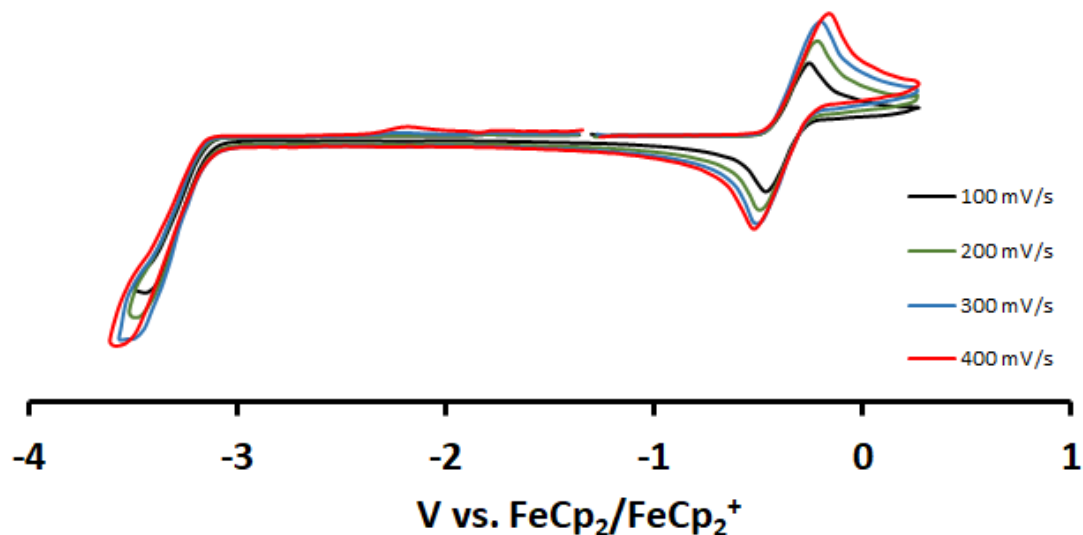


Figure S105. Cyclic voltammogram of (^{acri}PNP)NiPh (**4-Ph**) with scan rates: 100, 200, 300, and 400 mV/s. Ni^{II/I} couple at -3.11 V vs. Fc/Fc⁺ were observed in THF with 0.3 M tetra-*n*-butylammonium hexafluorophosphate as an electrolyte.

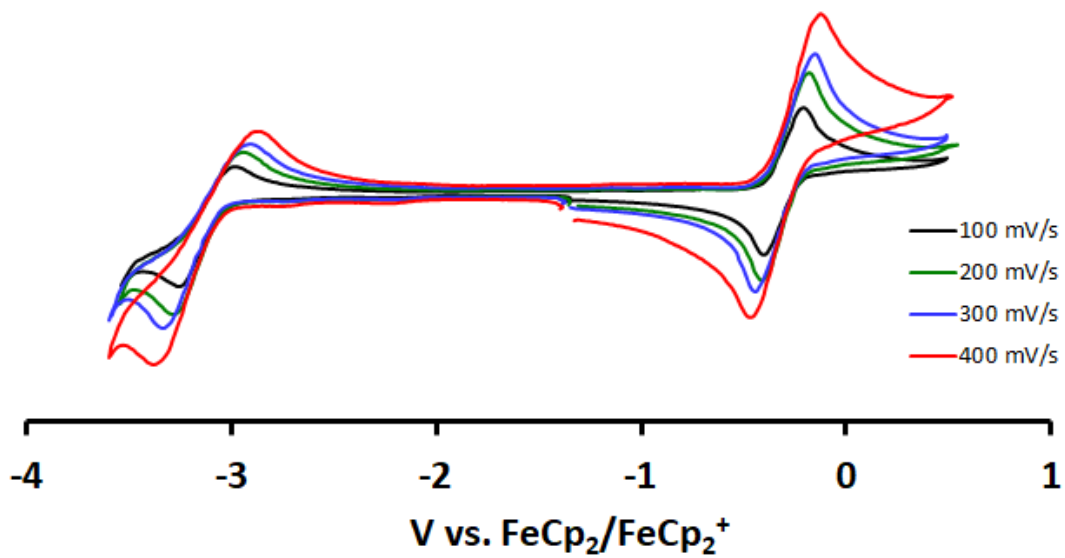


Figure S106. Top views of optimized structures for (^{acri}PNP)NiCl from DFT calculations. Hydrogen atoms are omitted for clarity.

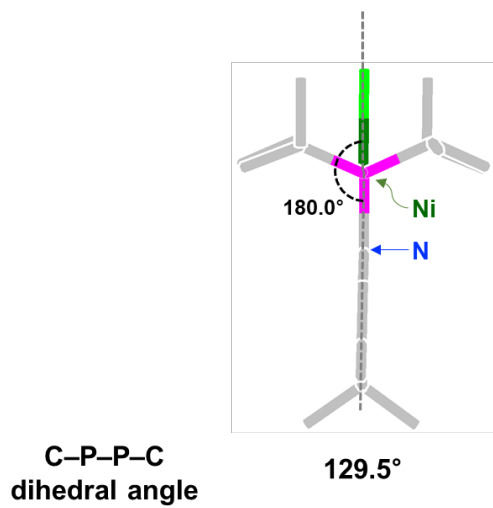


Table S11. Selected bond distances and angles for (^{acri}PNP)NiCl obtained from XRD data comparing with the calculated data based on the geometry optimization using DFT calculation (Å and °).

	calculated	crystal ¹
$d_{\text{Ni-Cl}}$	2.237	2.1767(6)
$d_{\text{Ni-N}}$	1.926	1.894(2)
$d_{\text{Ni-P}}$	2.230 2.231	2.1797(6) 2.1821(6)
$\angle\text{N-Ni-Cl}$	180.0	178.88(6)
$\angle\text{P-Ni-P}$	173.6	171.61(2)

Figure S107. Top views of optimized structures for (a) (^{acri}PNP)Ni(2-naphthyl) (**4-Naph**) and (b) (^{acri}PNP)Ni(1-naphthyl) from DFT calculations. Hydrogen atoms are omitted for clarity. The free energies of (^{acri}PNP)Ni(naphthyl) isomers are compared.

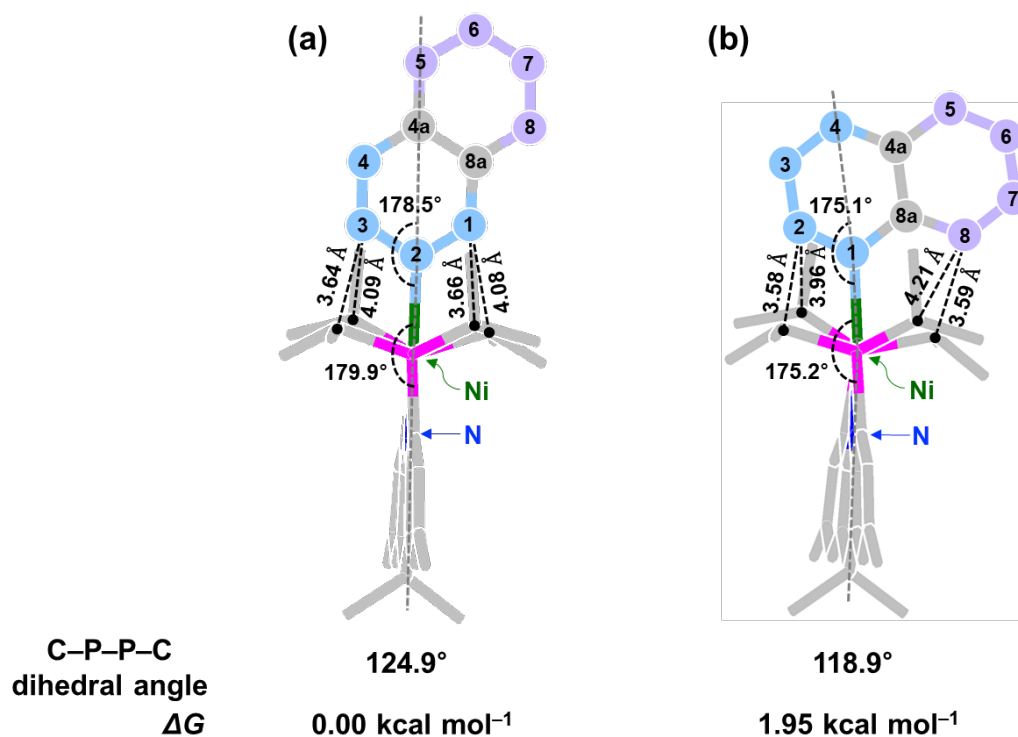


Table S12. Selected bond distances and angles for (^{acri}PNP)Ni(2-naphthyl) (**4-Naph**) and (^{acri}PNP)Ni(1-naphthyl) obtained from XRD data comparing with the calculated data based on the geometry optimization using DFT calculation (Å and °).

	(^{acri} PNP)Ni(2-naphthyl) (4-Naph)		(^{acri} PNP)Ni(1-naphthyl)
	calculated	crystal	calculated
d _{Ni-C}	1.926	1.900(2)	1.938
d _{Ni-N}	1.978	1.927(2)	1.984
d _{Ni-P}	2.230	2.1625(9)	2.245
	2.227	2.1582(8)	2.238
∠N-Ni-C	179.9	179.0(1)	175.2
∠P-Ni-P	171.7	172.09(3)	170.9

Figure S108. Top views of optimized structures for (a) $(^{acri}PNP)Ni(2\text{-anthracenyl})$ (**4-Anth**), (b) $(^{acri}PNP)Ni(1\text{-anthracenyl})$ and (c) $(^{acri}PNP)Ni(9\text{-anthracenyl})$ from DFT calculations. Hydrogen atoms are omitted for clarity. The free energies of $(^{acri}PNP)Ni(\text{anthracenyl})$ isomers are compared.

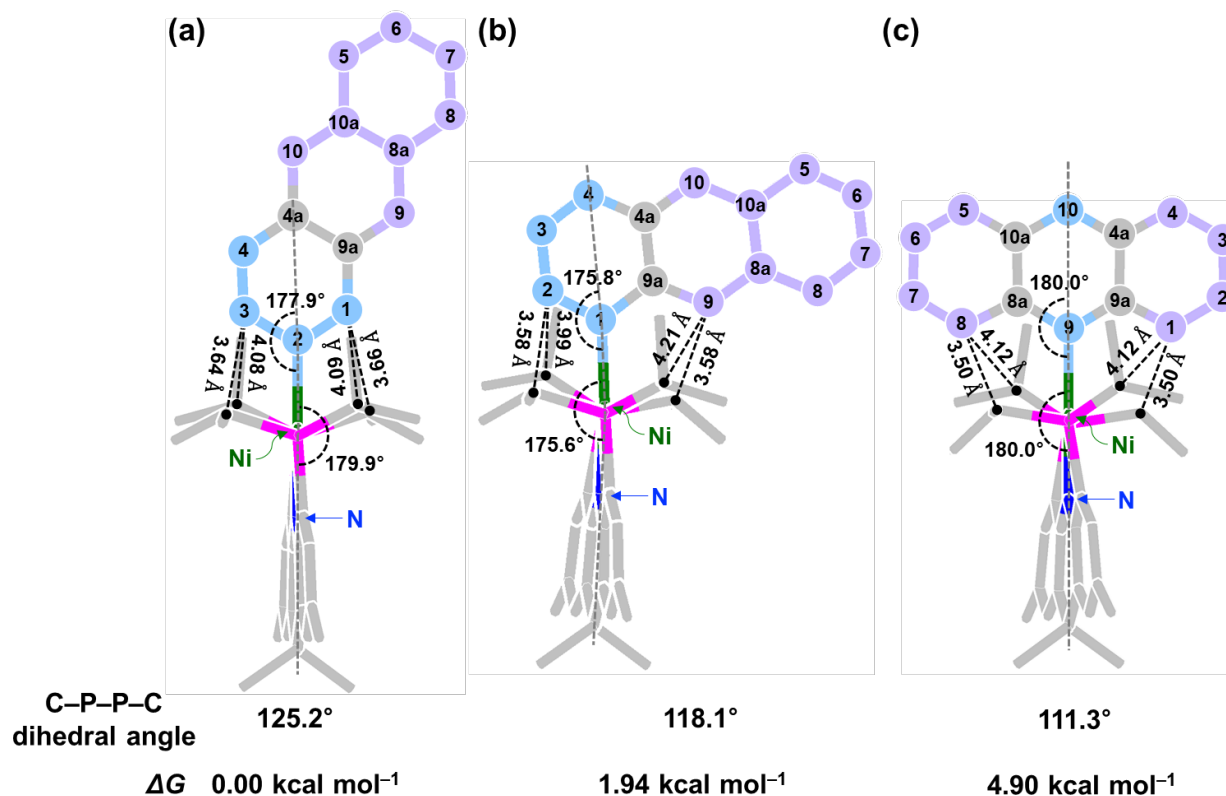


Table S13. Selected bond distances and angles for $(^{acri}PNP)Ni(2\text{-anthracenyl})$ (**4-Anth**), $(^{acri}PNP)Ni(1\text{-anthracenyl})$ and $(^{acri}PNP)Ni(9\text{-anthracenyl})$ obtained from XRD data comparing with the calculated data based on the geometry optimization using DFT calculation (\AA and $^\circ$).

	$(^{acri}PNP)Ni(2\text{-anthracenyl})$ (4-Anth)		$(^{acri}PNP)Ni(1\text{-anthracenyl})$	$(^{acri}PNP)Ni(9\text{-anthracenyl})$
	calculated	crystal	calculated	calculated
d_{Ni-C}	1.926	1.900(2)	1.936	1.947
d_{Ni-N}	1.978	1.927(2)	1.984	1.991
d_{Ni-P}	2.232	2.1625(9)	2.248	2.255
	2.228	2.1582(8)	2.234	2.255
$\angle N-Ni-C$	179.9	179.0(1)	175.6	180.0
$\angle P-Ni-P$	171.7	172.09(3)	170.8	169.7

Figure S109. Top views of optimized structures for (a) $(^{acri}PNP)Ni(p\text{-tolyl})$ (**4-*p*Tol**), (b) $(^{acri}PNP)Ni(m\text{-tolyl})$ (**4-*m*Tol**), (c) $(^{acri}PNP)Ni(o\text{-tolyl})$ (**4-*o*Tol**) and (d) $(^{acri}PNP)Ni(\text{benzyl})$ from DFT calculations. Hydrogen atoms are omitted for clarity. The free energies of $(^{acri}PNP)Ni(\text{tolyl})$ isomers and $(^{acri}PNP)Ni(\text{benzyl})$ are compared.

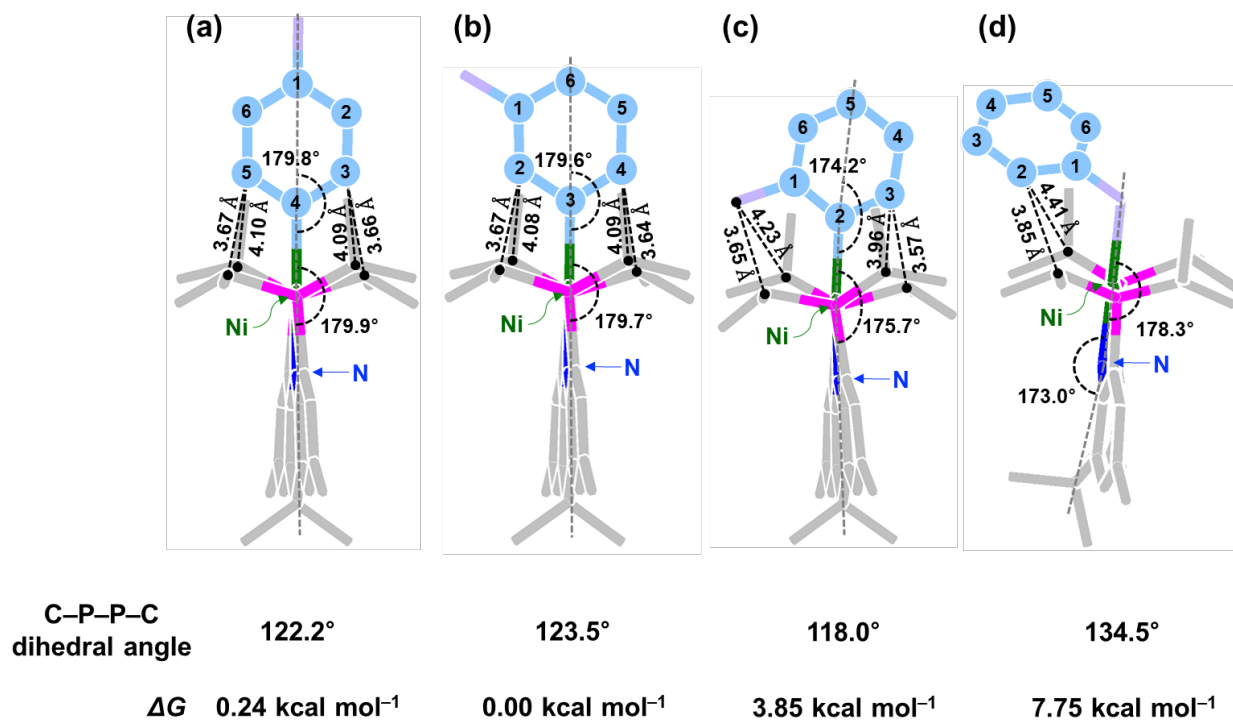
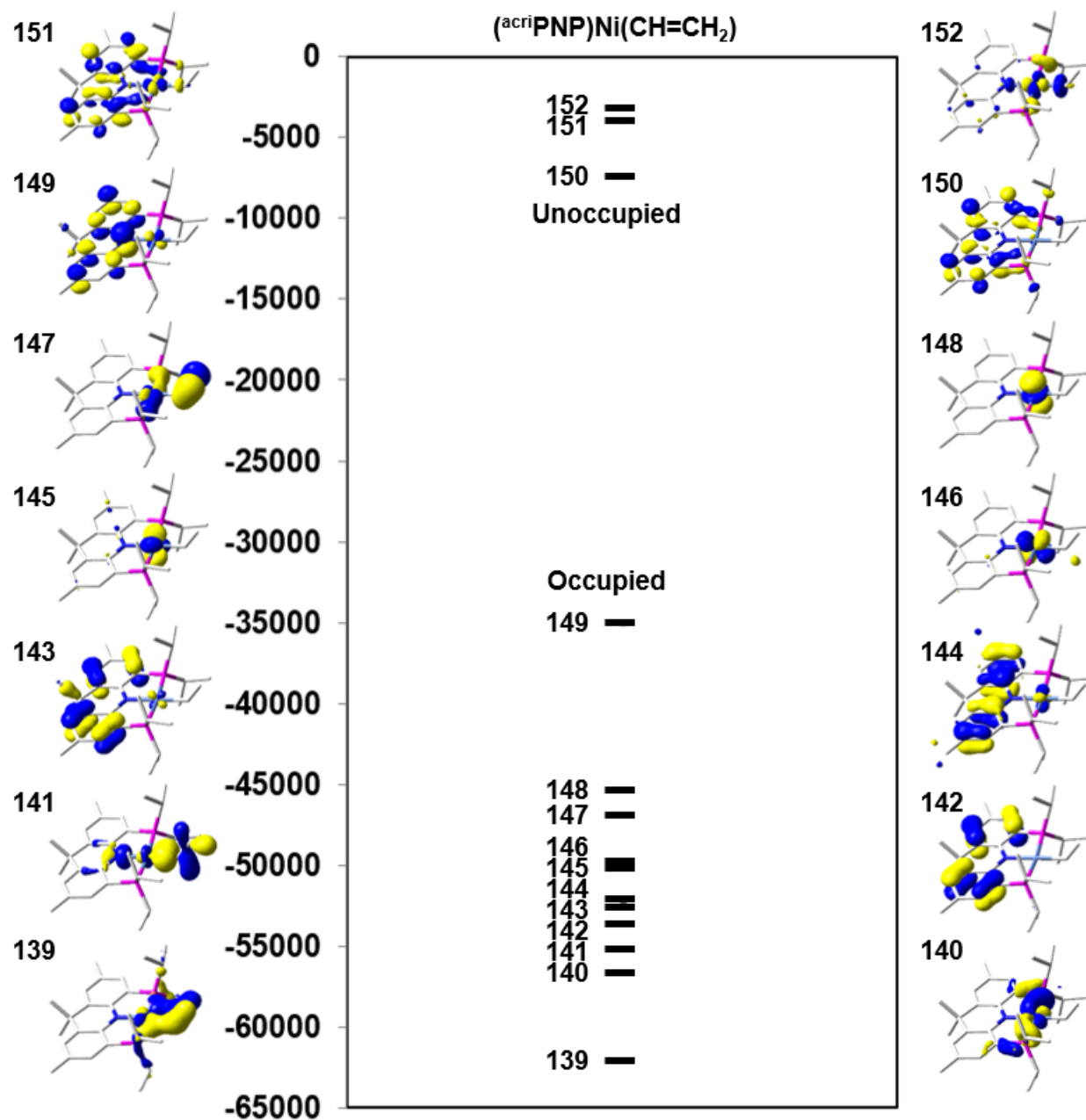


Table S14. Selected bond distances and angles for (^{acri}PNP)Ni(*p*-tolyl) (**4-*p*Tol**), (^{acri}PNP)Ni(*m*-tolyl) (**4-*m*Tol**), (^{acri}PNP)Ni(*o*-tolyl) (**4-*o*Tol**) and (^{acri}PNP)Ni(benzyl) obtained from XRD data comparing with the calculated data based on the geometry optimization using DFT calculation (Å and °).

	(^{acri} PNP)Ni(<i>p</i> -tolyl) (4-<i>p</i>Tol)		(^{acri} PNP)Ni(<i>m</i> -tolyl) (4-<i>m</i>Tol)	
	calculated	crystal	calculated	crystal
d _{Ni-C}	1.928	1.908(6)	1.927	1.9084(1)
d _{Ni-N}	1.979	1.933(5)	1.979	1.9241(1)
d _{Ni-P}	2.226	2.169(2)	2.228	2.1626(1)
	2.226	2.167(2)	2.227	2.1624(1)
∠N-Ni-C	179.9	178.5(2)	179.7	178.073(2)
∠P-Ni-P	171.7	172.26(7)	171.7	171.896(2)
	(^{acri} PNP)Ni(<i>o</i> -tolyl) (4-<i>o</i>Tol)		(^{acri} PNP)Ni(benzyl)	
	calculated	crystal	calculated	crystal
d _{Ni-C}	1.941	1.950(9)	2.001	2.008(5), 1.990(5)
d _{Ni-N}	1.989	1.934(5)	1.998	1.924(4), 1.938(4)
d _{Ni-P}	2.237	2.184(2)	2.261	2.178(2), 2.174(2)
	2.242	2.184(2)	2.236	2.213(2), 2.199(2)
∠N-Ni-C	175.7	173.2(3)	178.3	176.9(2), 173.2(2)
∠P-Ni-P	170.6	171.21(8)	166.6	165.11(6), 163.01(6)

Figure S110. Electronic structure for $(^{acri}PNP)Ni(CH=CH_2)$ (**5**) derived from the geometry optimization and frequency calculations using unrestricted B3LYP level of DFT; energies in cm^{-1} . ¹. Lobal representations correspond to the orbitals indicated by the number with 0.05 isocontours.



References

- 1 (a) C. Yoo, Y. Lee, *Angew. Chem. Int. Ed.*, 2017, **56**, 9502–9506; (b) N. A. Yakelis, R. G. Bergman, *Organometallics*, 2005, **24**, 3579–3581.
- 2 SMART, Version 5.0; data collection software; Bruker AXS, Inc., Madison, WI, USA, 1998.
- 3 SAINT, Version 5.0; data integration software; Bruker AXS, Inc., Madison, WI, USA, 1998.
- 4 G. M. Sheldrick, SADABS: program for absorption correction with the Bruker SMART system; Universität Göttingen, Göttingen, Germany, 1996.
- 5 G. M. Sheldrick, SHELXTL, Version 6.1, Bruker AXS, Inc., Madison, WI, USA, 2000.
- 6 D. Sahoo, C. Yoo, Y. Lee, *J. Am. Chem. Soc.*, 2017, **140**, 2179–2185.
- 7 M. J. Frisch, G. W. Trucks, H. B. Schlegel, G. E. Scuseria, M. A. Robb, J. R. Cheeseman, G. Scalmani, V. Barone, B. Mennucci, G. A. Petersson, H. Nakatsuji, M. Caricato, X. Li, H. P. Hratchian, A. F. Izmaylov, J. Bloino, G. Zheng, J. L. Sonnenberg, M. Hada, M. Ehara, K. Toyota, R. Fukuda, J. Hasegawa, M. Ishida, T. Nakajima, Y. Honda, O. Kitao, H. Nakai, T. Vreven, J. A. Montgomery, Jr. J. E. Peralta, F. Ogliaro, M. Bearpark, J. J. Heyd, E. Brothers, K. N. Kudin, V. N. Staroverov, T. Keith, R. Kobayashi, J. Normand, K. Raghavachari, A. Rendell, J. C. Burant, S. S. Iyengar, J. Tomasi, M. Cossi, N. Rega, J. M. Millam, M. Klene, J. E. Knox, J. B. Cross, V. Bakken, C. Adamo, J. Jaramillo, R. Gomperts, R. E. Stratmann, O. Yazyev, A. J. Austin, R. Cammi, C. Pomelli, J. W. Ochterski, R. L. Martin, K. Morokuma, V. G. Zakrzewski, G. A. Voth, P. Salvador, J. J. Dannenberg, S. Dapprich, A. D. Daniels, O. Farkas, J. B. Foresman, J. V. Ortiz, J. Cioslowski, D. J. Fox, Gaussian 09, Revision D.01; Gaussian, Inc.: Wallingford CT, 2013.
- 8 A. D. Becke, *J. Chem. Phys.*, 1993, **98**, 5648–5652.
- 9 C. Lee, W. Yang, R. G. Parr, *Phys. Rev. B*, 1988, **37**, 785–789.
- 10 S. H. Vosko, L. Wilk, M. Nusair, *Can. J. Phys.*, 1980, **58**, 1200–1211.
- 11 M. Castillo, S. Fortier, A. J. Metta-Magana, *New J. Chem.*, 2016, **40**, 1923–1926.
- 12 C. G. Screttas, M. Micha-Screttas, *J. Organomet. Chem.*, 1983, **252**, 263–265.
- 13 T. R. Hoye, A. W. Aspaas, B. M. Eklov, T. D. Ryba, *Org. Lett.*, 2005, **7**, 2205–2208.